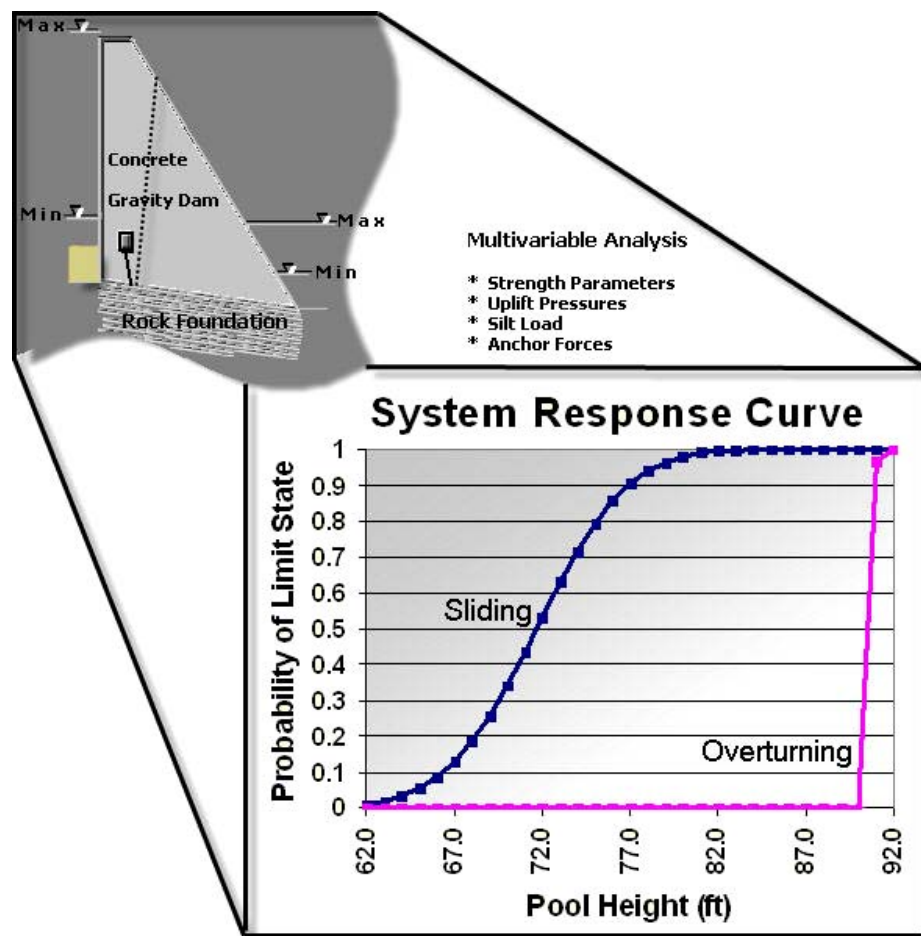Information Technology Laboratory

US Army Corps
of Engineers®
Engineer Research and
Development Center

Fragility Analysis of a Concrete Gravity Dam and Its System Response Curve Computed by the Analytical Program GDLAD_Sloping_Base

Robert M. Ebeling, Moira T. Fong, Amos Chase, Sr., and Elias Arredondo

November 2008

Fragility Analysis of a Concrete Gravity Dam and Its System Response Curve Computed by the Analytical Program GDLAD_Sloping_Base

Robert M. Ebeling, Moira T. Fong, and Elias Arredondo

Information Technology Laboratory
U.S. Army Engineer Research and Development Center
3909 Halls Ferry Road
Vicksburg, MS 39180-6199

Amos Chase, Sr.

Science Applications International Corporation
3532 Manor Drive, Suite 4
Vicksburg, MS 39180

Final report

Abstract: This research report describes the engineering formulation and corresponding software developed for expressing the computed stability results for an idealized two-dimensional cross section of a rock-founded concrete gravity dam in terms of fragility curves for the potential modes of failure (e.g., sliding, overturning). Within the U.S. Army Corps of Engineers the term *system response curve* is now being used to describe what is commonly referred to in the technical literature as the fragility curve; the term system response curve is used for the hydrologic fragility assessment of rock-founded concrete gravity dams. This report uses this new Corps terminology. Uncertainty in strength, uplift parameters, silt-induced earth pressure, and post-tensioned anchor forces are accounted for in a multivariate probabilistic stability analysis resulting in the computation of a system response curve. The PC software GDLAD_Sloping_Base (Gravity Dam Layout and Design) is used in this research and development effort to perform the computations and construct the system response curve.

The resulting engineering methodology and corresponding software are applicable to a concrete gravity dam founded on rock with a level or sloping base. GDLAD_Sloping_Base is also capable of performing a deterministic (sliding and overturning) stability evaluation.

Contents

Figures and Tables

Figures

Tables

Preface

This research report describes the engineering formulation and corresponding software developed for expressing the computed stability results for an idealized two-dimensional cross section of a rock-founded concrete gravity dam in terms of fragility curves for the potential modes of failure (e.g., sliding, overturning). Within the U.S. Army Corps of Engineers the term *system response curve* is now being used to describe what has been commonly referred to in the technical literature as the fragility curve; the term is used for the hydrologic fragility assessment of rock-founded concrete gravity dams. This report uses this new Corps terminology. Uncertainty in strength, uplift parameters, silt-induced earth pressure, and post-tensioned anchor forces are accounted for in a multivariate probabilistic stability analysis resulting in the computation of the system response curve. The PC software GDLAD_Sloping_Base (Gravity Dam Layout and Design) is used in this research and development effort to perform the computations and construct the system response curve. Funding to initiate research and software development and the engineering study was provided by Headquarters, U.S. Army Corps of Engineers (HQUSACE), as part of the Flood and Coastal Storm Damage Reduction Research and Development Program. The research was performed under the Dam Safety Focus Area, Work Unit 142082, "Simplified Probabilistic Models for Concrete Gravity Dams" for which Dr. Robert M. Ebeling, Engineering Informatics Systems Division (EISD), Information Technology Laboratory (ITL), U.S. Army Engineer Research and Development Center (ERDC), was the Principal Investigator. Additional funding was provided by the Engineering Risk and Reliability Directory of Expertise. Andy Harkness (of Pittsburgh District), Technical Manager of the Engineering Risk and Reliability Directory of Expertise supervised this R&D effort.

H. Wayne Jones, ITL, was the Dam Safety Focus Area Manager; William R. Curtis, Coastal and Hydraulics Laboratory (CHL), ERDC, was the Flood and Coastal Storm Damage Reduction Research and Development Program Manager; and Dr. Michael Sharp, Geotechnical and Structures Laboratory (GSL), ERDC, was the Water Resources Infrastructure Technical Director.

Unit Conversion Factors

Multiply	By	To Obtain
feet	0.3048	meters
pounds (mass)	0.45359237	kilograms
pounds (mass) per cubic foot	16.01846	kilograms per cubic meter

1 System Response/Fragility Curves for Concrete Gravity Dams Founded on Rock and With a Sloping Base

1.1 Introduction

The stability and safety of the U.S. Army Corps of Engineers rock-founded concrete gravity dam are discussed in Engineer Manual (EM) 1110-2-2100 (Headquarters, U.S. Army Corps of Engineers (HQUSACE) 2005) dealing with the stability of concrete structures. In this manual, the stability of the idealized two-dimensional cross section of the concrete gravity dam (Figure 1.1) is expressed in terms of a factor of safety against sliding, the base area in compression, and the stability of the rock foundation to resist a bearing failure. These computations and stability criteria are geared toward deterministic analyses. However, there is uncertainty in the parameters used in stability analyses. One example is uncertainty in the shear strength parameters for the dam-to-foundation interface as well as for the rock foundation. Another source of uncertainty is in the parameters used to define the uplift pressure distribution along the interface of the sloping dam and rock foundation. Still other sources of uncertainty are the silt-induced earth pressure and post-tensioned anchor forces, when present. One method of analysis used to formally and explicitly account for this uncertainty in the analysis is by expressing the computed stability results in terms of fragility curves for the potential modes of failure (e.g., sliding, overturning, etc.). Within the Corps the term *system response curve* is now being introduced to describe what has been commonly referred to in the technical literature as the fragility curve; the term is used for the hydrologic fragility assessment of rock-founded concrete gravity dams. This report uses this new Corps terminology.

Tekie and Ellingwood (2002), along with others, discuss the development of fragility curves used in a hydrologic fragility assessment and the computation of the probability of failure of a rock-founded gravity dam. This report describes the engineering formulation and corresponding PC-based software, named GDLAD_Sloping_Base, which is used to compute system response curves for a two-dimensional cross section of a gravity dam founded on a sloping rock base. GDLAD is an acronym for G̲ravity D̲am Layout a̲nd D̲esign.
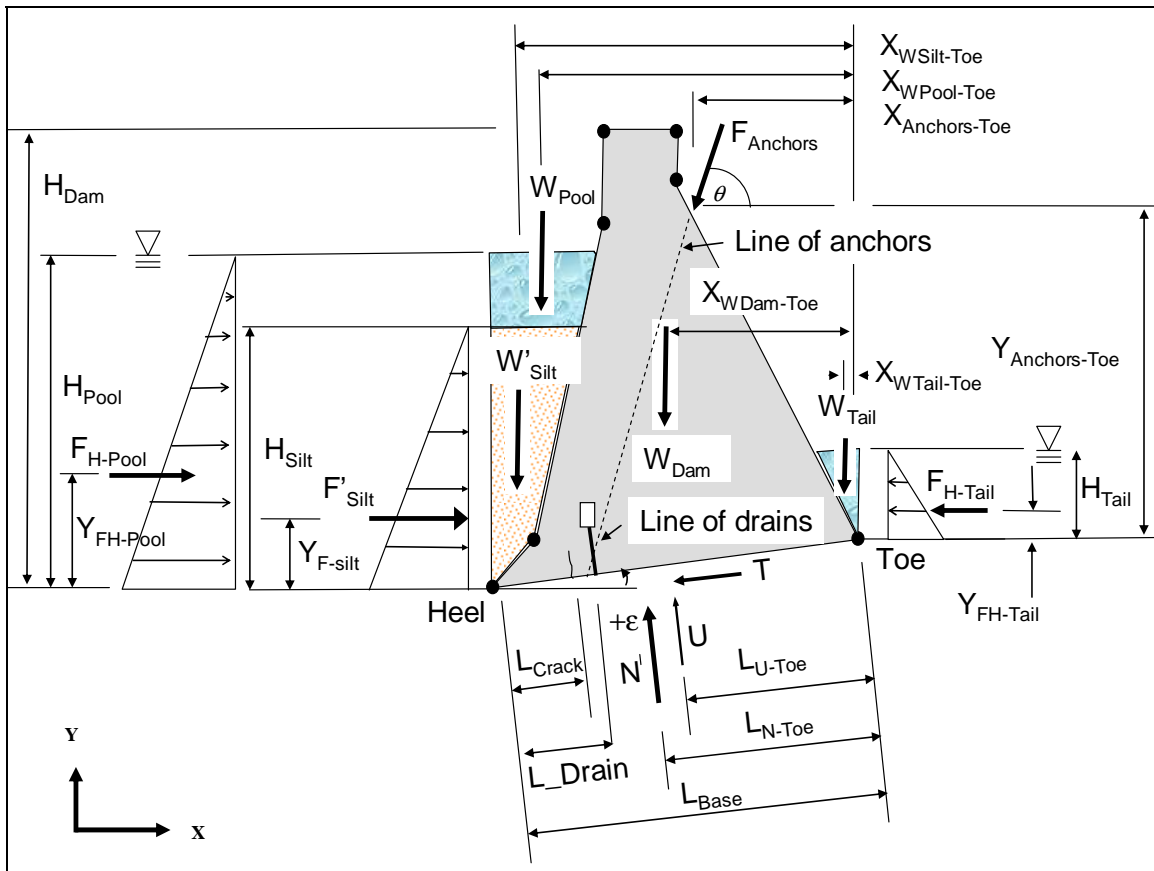
Figure 1.1. Two-dimensional free-body diagram of a gravity dam with anchors – positive base slope ε and fully submerged silt bed load.

The system response curve is used to predict the probably of dam failure, given the hydraulic hazard. Consider the example of a dam in which the sliding limit state, i.e., $FS_{slide} \leq 1.0$, is the limit state resulting in failure of the dam. Then the probability of failure, $P_{failure}$, of the dam for pools less than or equal to a specific height of pool H_{Pool}, i.e., $Pool \leq H_{Pool}$, is given by the product of

$$P_{failure} = P\left(FS_{slide} \leq 1.0 \,|\, Pool = H_{Pool}\right) \bullet P\left(Pool = H_{Pool}\right) \qquad (1.1)$$

where the first probability is from the system response curve developed using the engineering procedure and corresponding PC-based software discussed in this report and the second probability is the hydraulic hazard expressed as an annual probability. The second probability comes from a separate analysis of the hydraulic hazard for the dam, considering channel inflows and storm runoff from the watershed behind the dam.

1.2 Report contents

Chapter 2 discusses the equations of equilibrium for a rock-founded concrete gravity dam two-dimensional cross section with a sloping base, the multivariate probabilistic analysis, and the computation of system response curves. Uncertainty in strength, uplift parameters, silt-induced earth pressure and post-tensioned anchor forces are accounted for in a multivariate probabilistic stability analysis.

Chapter 3 discusses the Visual Modeler, the graphical user interface (GUI) that accepts user input, executes the FORTRAN engineering formulation discussed in Chapter 2, and displays the resultant analyses for evaluation. Example problems are provided as a guide for applying the software.

Chapter 4 summarizes the results and conclusions of this engineering formulation and corresponding PC-based software and discusses additional research needs.

Appendix A discusses the computation of cross-sectional areas, centroid, moment of inertia, and mass moment of inertia via planimeters and Green's theorem for point-by-point geometry definition.

Appendix B discusses the non-site-specific uplift pressure distribution approach, with consideration of the impact the length of cracking along the base of the dam, relative to the line of rock foundation drains, has on uplift water pressure distribution.

Appendix C describes the contents of the ASCII input data file to the FORTRAN engineering computer program portion of GDLAD_Sloping_Base. This input data file, always designated as GDLAD_Sloping_Base.in, is created by the GUI, the Visual Modeler portion of GDLAD_Sloping_Base, presented in Chapter 3.

2   Equations of Equilibrium, Multivariate Probabilistic Analysis, and System Response/Fragility Curves

2.1 Introduction

This chapter discusses the equations of equilibrium for a rock-founded concrete gravity dam two-dimensional cross section with a sloping base, the probabilistic analysis of inherent uncertainty of certain model parameters, and the computation of system response (i.e., fragility) curves.

2.2 Equations of equilibrium for rock-founded gravity dams with a sloping base

2.2.1 Free-body diagram

Consider the free-body diagram shown in Figure 2.1 of an idealized two-dimensional cross section of a concrete gravity dam founded on a sloping rock base. The case shown is $H_{Pool} < H_{Dam}$. This idealized gravity dam cross section retains a pool as well as a submerged bed load of silt. The base of the dam forms one face of the free-body diagram, with slope of the base shown at a positive angle ε from horizontal in this figure. The dam-to-rock-foundation interface forces include the effective force normal to the interface N', the resultant uplift water pressure force U, and shear force T required for equilibrium. Another face of the free-body diagram is defined by an imaginary vertical plane extending upward from the heel of the dam. The hydrostatic water pressure resultant force $F_{H\text{-}Pool}$ acts normal to this face as does the effective horizontal silt force F'_{Silt}. (Hydrostatic water pressures are assumed within the silt bed.) The last face of the free-body diagram is defined by an imaginary vertical plane extending upwards from the toe of the dam. The hydrostatic tailwater pressure resultant force $F_{H\text{-}Tail}$ acts normal to this face. The body forces from the weight of the dam W_{Dam}, the effective weight of the silt W'_{Silt}, the weight of the pool W_{Pool}, and the weight of the tailwater W_{Tail} all act on the free-body cross section as shown in this figure. The possibility of an anchor force acting on the two-dimensional free-body diagram is represented by the force $F_{Anchors}$.
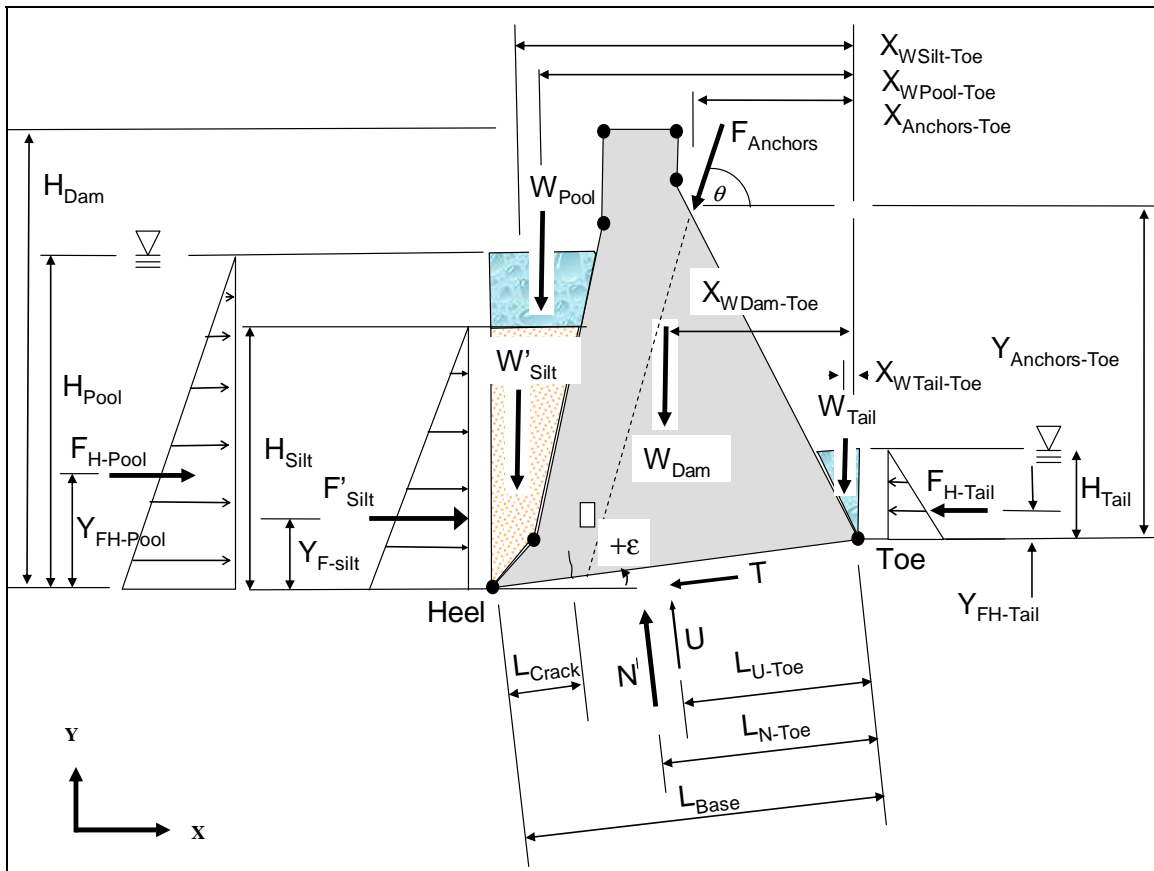
Figure 2.1. Two-dimensional free-body cross section of a gravity dam with anchors – positive base slope ε and a fully submerged silt bed load.

The Figure 2.2 free-body diagram of an idealized two-dimensional cross section of a concrete gravity dam founded on a sloping rock base is the same as that shown in Figure 2.1, with the exception that in Figure 2.2 the slope of the base is at a negative angle ε from horizontal.

The Figure 2.3 free-body diagram of an idealized two-dimensional cross section of a concrete gravity dam founded on a sloping rock base is the same as that shown in Figure 2.1, with the exception that this idealized gravity dam cross section retains a partially submerged bed load of silt versus the fully submerged silt. Hydrostatic water pressures are assumed within the silt bed.
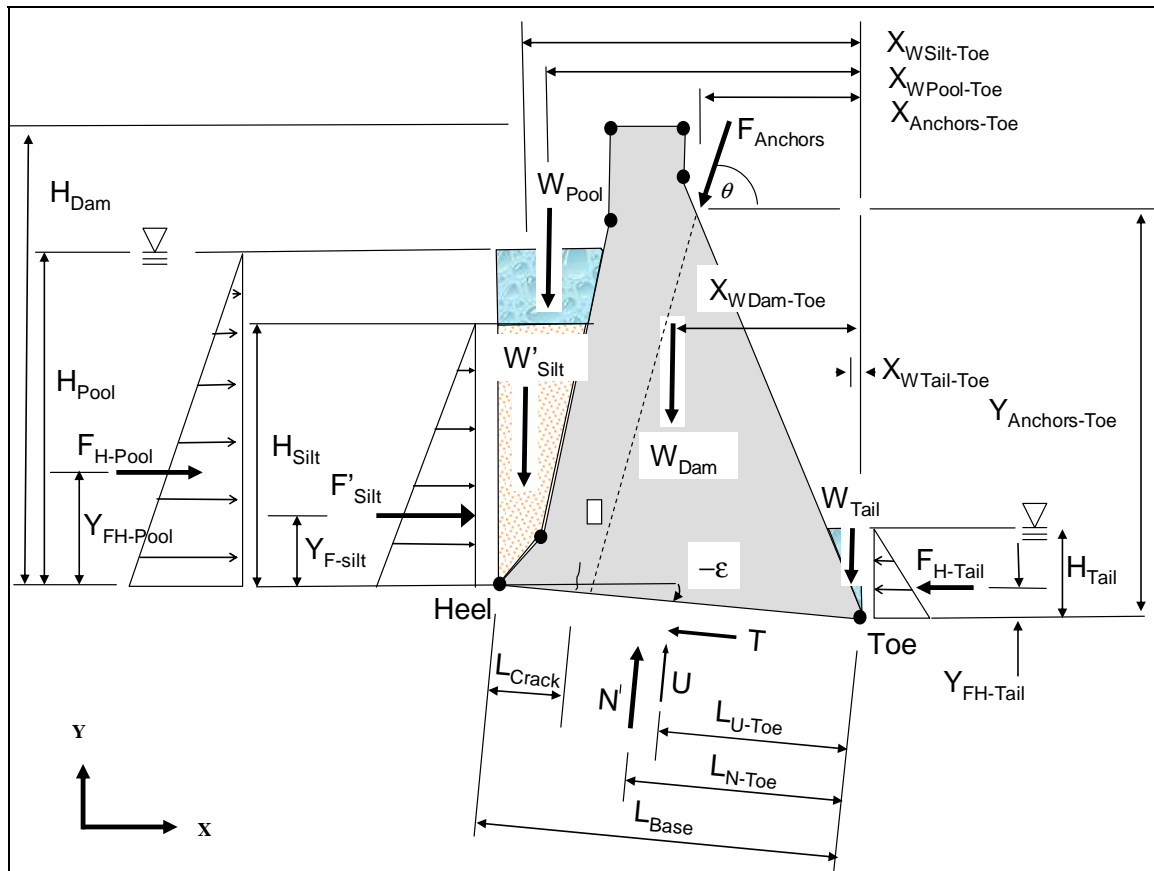
Figure 2.2. Two-dimensional free-body cross section of a gravity dam with anchors – negative base slope ε and a fully submerged silt bed load.

2.2.2 Forces acting on the free-body diagram

$F_{H\text{-}Pool}$ is the horizontal resultant water pressure force that the pool exerts on the dam; F'_{Silt} is the horizontal resultant effective earth pressure force that the silt exerts on the dam (assuming hydrostatic pore water pressures within the silt); T is the shear force required for equilibrium of forces acting on the free-body diagram of the idealized two-dimensional gravity dam cross section; N' is the effective resultant force of the rigid base acting normal to the base of the dam; U is the resultant water pressure force acting normal to the base of the dam; $F_{H\text{-}Tail}$ is the horizontal resultant water pressure force that the tailwater exerts on the dam; and $F_{Anchors}$ is the resultant force exerted on the dam (per unit length along the axis of the dam) from a group of anchors post-tensioned into rock. The orientation of the anchors is at an angle θ from horizontal.
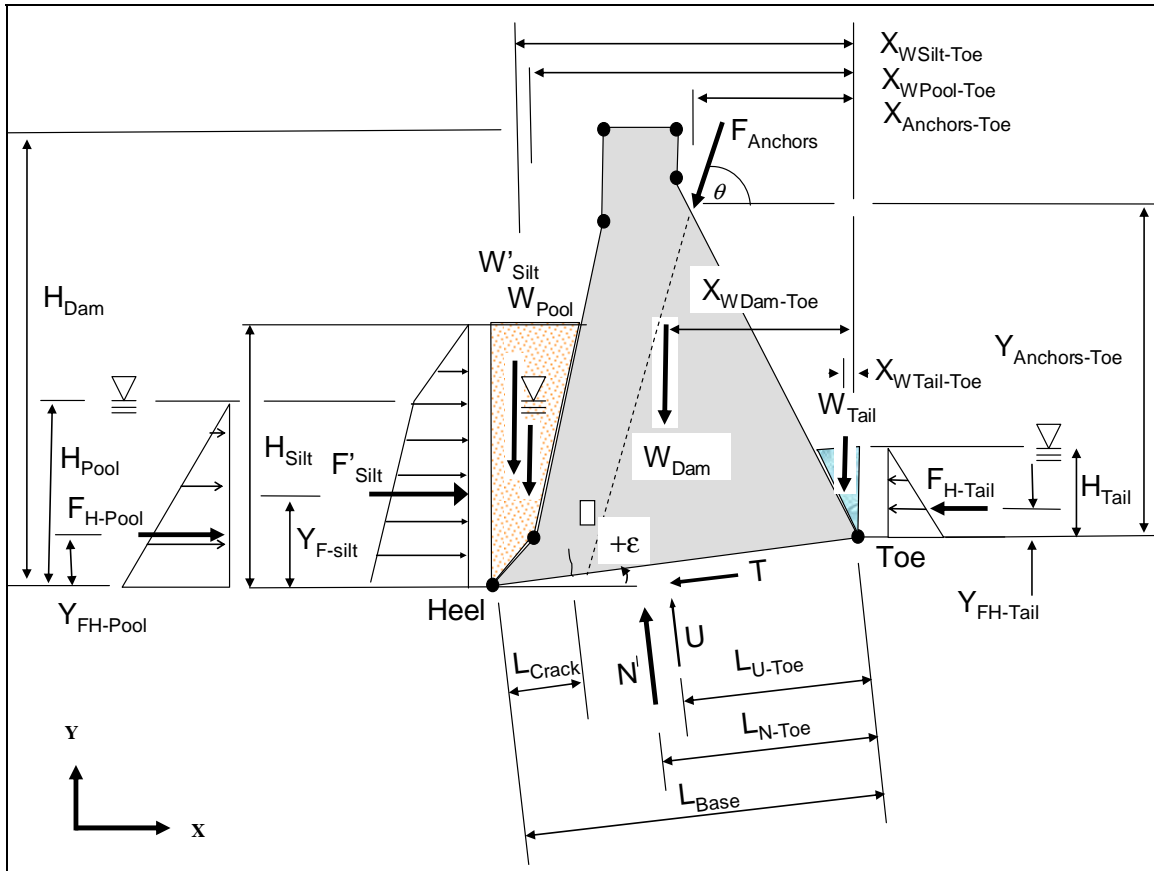
Figure 2.3. Two-dimensional free-body cross section of a gravity dam with anchors – positive base slope ε and a partially submerged silt bed load.

In the cases of $H_{Pool} < H_{Dam}$ in Figures 2.1 to 2.3, the force $F_{H\text{-}Pool}$ is

$$F_{H-Pool} = \frac{1}{2} \bullet \gamma_{Water} \bullet \left(H_{Pool}\right)^2 \qquad (2.1)$$

with a position of $Y_{FH\text{-}Pool}$ given by

$$Y_{FH-Pool} = \frac{1}{3} \bullet H_{Pool} \qquad (2.2)$$

In the Figure 2.4 case of $H_{Pool} > H_{Dam}$, the force $F_{H\text{-}Pool}$ is

$$F_{H-Pool} = \frac{1}{2} \bullet H_{Dam} \bullet \left[\gamma_{Water} \bullet \left(H_{Pool} - H_{Dam}\right) + \gamma_{Water} \bullet \left(H_{Pool}\right)\right] \qquad (2.3)$$
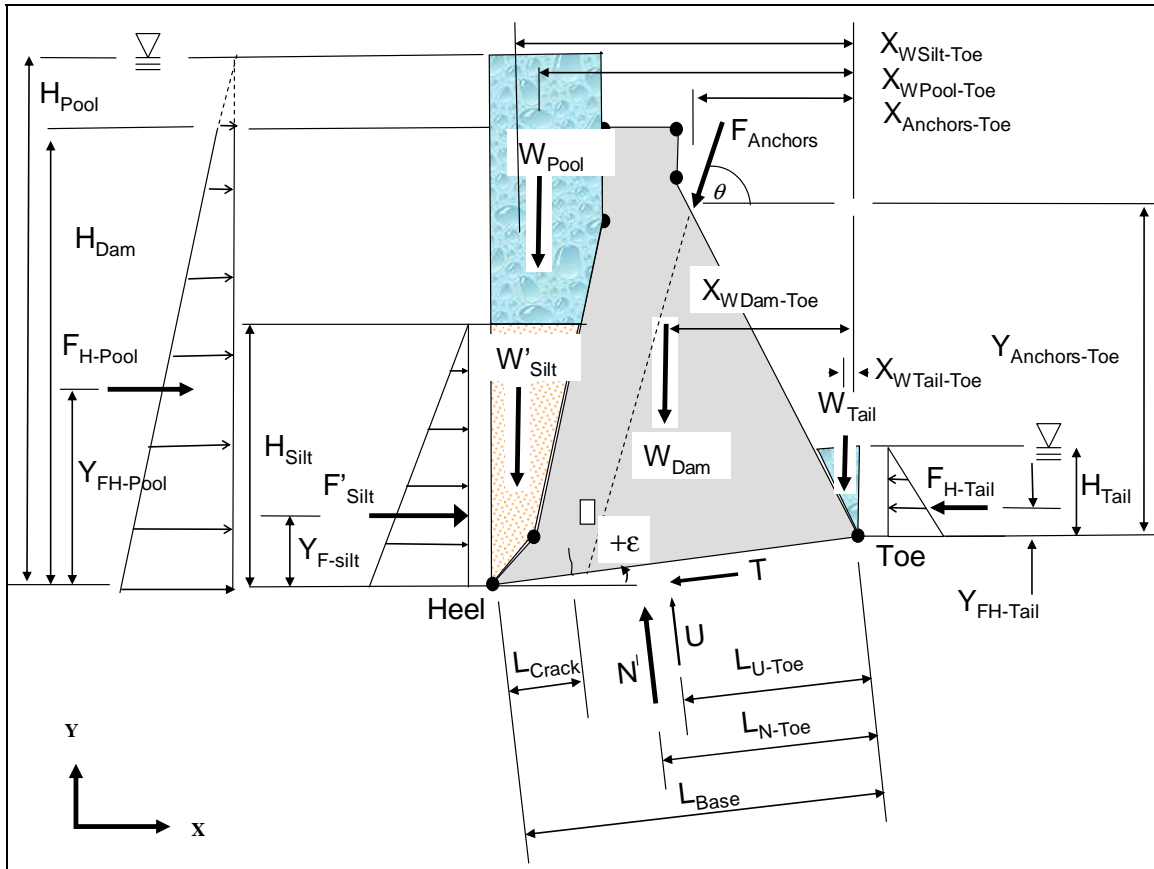
Figure 2.4. Two-dimensional free-body cross section of a gravity dam with $H_{Pool} > H_{Dam}$ – positive base slope ε and a fully submerged silt bed load.

and with its position in Figure 2.4 given by

$$Y_{FH-Pool} = \frac{(H_{Dam})^2 \bullet \left[\frac{1}{3} \bullet \gamma_{Water} \bullet (H_{Pool} - H_{Dam}) + \frac{1}{6} \bullet \gamma_{Water} \bullet (H_{Pool})\right]}{F_{H-Pool}} \quad (2.4)$$

For the fully submerged silt layer of Figures 2.1, 2.2, and 2.4, the force F'_{Silt} is

$$F'_{Silt} = K_O \bullet \frac{1}{2} \bullet \left[\gamma_{Saturated} - \gamma_{Water}\right] \bullet (H_{Silt})^2 \quad (2.5)$$

assuming hydrostatic pore water pressures within the silt. K_O is the at-rest, horizontal earth pressure coefficient within the silt. This force acts at a position $Y_{FH-silt}$ of

$$Y_{F-silt} = \frac{1}{3} \bullet H_{Silt} \tag{2.6}$$

In the case of a partially submerged silt layer of Figure 2.3, the force F'_{Silt} is

$$F'_{Silt} = K_O \bullet \left\{ \begin{array}{l} \frac{1}{2} \bullet \gamma_{Moist} \bullet \left(H_{Silt} - H_{Pool} \right)^2 \\ + \gamma_{Moist} \bullet \left(H_{Silt} - H_{Pool} \right) \bullet H_{Pool} \\ + \frac{1}{2} \bullet \left[\gamma_{Saturated} - \gamma_{Water} \right] \bullet \left(H_{Pool} \right)^2 \end{array} \right\} \tag{2.7}$$

assuming hydrostatic pore water pressures within the partially submerged silt. This Figure 2.3 force acts at

$$Y_{F-silt} = \frac{\left\{ \begin{array}{l} \left[K_O \bullet \frac{1}{2} \bullet \gamma_{Moist} \bullet \left(H_{Silt} - H_{Pool} \right)^2 \right] \bullet \left(H_{Pool} + \frac{\left(H_{Silt} - H_{Pool} \right)}{3} \right) \\ + \left[K_O \bullet \gamma_{Moist} \bullet \left(H_{Silt} - H_{Pool} \right) \bullet H_{Pool} \right] \bullet \left(\frac{H_{Pool}}{2} \right) \\ + \left[K_O \bullet \frac{1}{2} \bullet \left[\gamma_{Saturated} - \gamma_{Water} \right] \bullet \left(H_{Pool} \right)^2 \right] \bullet \left(\frac{H_{Pool}}{3} \right) \end{array} \right\}}{F'_{Silt}} \tag{2.8}$$

The resultant force $F_{Anchors}$ per unit length along the axis of the dam is

$$F_{Anchors} = \frac{\sum_{i=1}^{n} \left(F_{individual \ anchor} \right)_i}{anchor \ group \ spacing} \tag{2.9}$$

for n individual anchors in each anchor group. The force F_{H-Tail} is

$$F_{H-Tail} = \frac{1}{2} \bullet \gamma_{Water} \bullet \left(H_{Tail} \right)^2 \tag{2.10}$$

with a position of $Y_{FH-Tail}$ given by

$$Y_{FH-Tail} = \frac{1}{3} \bullet H_{Tail} \tag{2.11}$$

The calculation of the body forces caused by the weight of the dam W_{Dam}, the effective weight of the silt W'_{Silt}, the weight of the pool W_{Pool}, and the weight of the tailwater W_{Tail}, and their positions are computed using the procedure described in Appendix A.

Calculation of the resultant water pressure force acting normal to the base of the dam U is described in Appendix B for the non-site-specific uplift pressure distribution approach. An alternative approach is to compute U using steady-state seepage within rock discontinuities (i.e., joints, faults and/or fissures) in a separate analytical computation (Section 3.2.6), with the user inputting values of U for each pool elevation.

2.2.3 Equation of vertical equilibrium

The summation of vertical forces acting on the Figure 2.1 gravity dam (positive ε) results in

$$N' \bullet \cos(\varepsilon) + U \bullet \cos(\varepsilon) = W_{Dam} + W_{Pool} + W'_{Silt} + W_{Tail}$$

$$+ T \bullet \sin(\varepsilon) + F_{Anchors} \bullet \sin(\theta) \qquad (2.12)$$

The forces acting upward on the free-body diagram are on the left-hand side of the equal sign and the downward-acting forces are on the right-hand side. The orientations of these vertical forces do not change in the case of the Figure 2.2 gravity dam with a negative base slope angle ε. Rearranging Equation 2.12, the resultant effective force normal to the base N' is

$$N' = \frac{\begin{bmatrix} W_{Dam} + W_{Pool} + W'_{Silt} + W_{Tail} + T \bullet \sin(\varepsilon) \\ + F_{Anchors} \bullet \sin(\theta) - U \bullet \cos(\varepsilon) \end{bmatrix}}{\cos(\varepsilon)} \qquad (2.13)$$

2.2.4 Equation of horizontal equilibrium

At the onset of sliding of the Figure 2.1 rock-founded concrete gravity dam, the horizontal driving force equals the stabilizing (i.e., restoring) force. The summation of horizontal forces acting on the gravity dam (positive ε) results in

$$F_{H-Pool} + F'_{Silt} = T \bullet \cos(\varepsilon) + N' \bullet \sin(\varepsilon) + U \bullet \sin(\varepsilon)$$

$$+ F_{H-Tail} + F_{Anchors} \bullet \cos(\theta) \quad (2.14)$$

For the positive base slope angle ε shown in Figures 2.1 and 2.3, the driving forces are on the left-hand side of the equal sign in Equation 2.14 and the resisting forces are on the right-hand side. For Figure 2.2 gravity dam with a negative base slope angle ε, the two terms $[N' \bullet \sin(\varepsilon) + U \bullet \sin(\varepsilon)]$ on the right-hand side of Equation 2.14 will be negative, reflecting the fact that they are now driving forces. Solving for the shear force along the gravity dam base required for equilibrium of the free-body diagram, T, Equation 2.14 becomes

$$T = \frac{F_{H-Pool} + F'_{Silt} - N' \bullet \sin(\varepsilon) - U \bullet \sin(\varepsilon) - F_{H-Tail} - F_{Anchors} \bullet \cos(\theta)}{\cos(\varepsilon)} \quad (2.15)$$

2.2.5 Shear force *T* along the base

Introducing Equation 2.13, Equation 2.15 becomes

$$T = \frac{\left\{ F_{H-Pool} + F'_{Silt} - \left[\dfrac{\begin{array}{c} W_{Dam} + W_{Pool} + W'_{Silt} + W_{Tail} + T \bullet \sin(\varepsilon) \\ + F_{Anchors} \bullet \sin(\theta) - U \bullet \cos(\varepsilon) \end{array}}{\cos(\varepsilon)} \right] \bullet \sin(\varepsilon) \right\} - U \bullet \sin(\varepsilon) - F_{H-Tail} - F_{Anchors} \bullet \cos(\theta)}{\cos(\varepsilon)} \quad (2.16)$$

Simplifying within the bracket, Equation 2.16 becomes

$$T = \frac{\left[\begin{array}{l} F_{H-Pool} + F'_{Silt} \\[4pt] - \dfrac{\left[W_{Dam} + W_{Pool} + W'_{Silt} + W_{Tail} + F_{Anchors} \bullet \sin(\theta) - U \bullet \cos(\varepsilon) \right]}{\cos(\varepsilon)} \bullet \sin(\varepsilon) \\[10pt] - T \bullet \tan(\varepsilon) \bullet \sin(\varepsilon) - U \bullet \sin(\varepsilon) - F_{H-Tail} - F_{Anchors} \bullet \cos(\theta) \end{array} \right]}{\cos(\varepsilon)} \quad (2.17)$$

Collecting terms on the left-hand side, Equation 2.17 becomes

$$T = \frac{\begin{bmatrix} F_{H-Pool} + F'_{Silt} \\ -\begin{bmatrix} W_{Dam} + W_{Pool} + W'_{Silt} + W_{Tail} + F_{Anchors} \bullet \sin(\theta) \\ -U \bullet \cos(\varepsilon) \end{bmatrix} \bullet \tan(\varepsilon) \\ -U \bullet \sin(\varepsilon) - F_{H-Tail} - F_{Anchors} \bullet \cos(\theta) \end{bmatrix}}{\cos(\varepsilon) + \tan(\varepsilon) \bullet \sin(\varepsilon)} \quad (2.18)$$

2.2.6 Effective force normal to the base N'

Expanding, Equation 2.13 becomes

$$N' = \frac{\begin{bmatrix} W_{Dam} + W_{Pool} + W'_{Silt} + W_{Tail} \\ +F_{Anchors} \bullet \sin(\theta) - U \bullet \cos(\varepsilon) \end{bmatrix}}{\cos(\varepsilon)} + T \bullet \tan(\varepsilon) \quad (2.19)$$

Introducing Equation 2.18, Equation 2.19 becomes

$$N' = \frac{W_{Dam} + W_{Pool} + W'_{Silt} + W_{Tail} + F_{Anchors} \bullet \sin(\theta) - U \bullet \cos(\varepsilon)}{\cos(\varepsilon)}$$

$$+ \left\{ \frac{\begin{bmatrix} F_{H-Pool} + F'_{Silt} \\ -\begin{bmatrix} W_{Dam} + W_{Pool} + W'_{Silt} + W_{Tail} \\ +F_{Anchors} \bullet \sin(\theta) - U \bullet \cos(\varepsilon) \end{bmatrix} \bullet \tan(\varepsilon) \\ -U \bullet \sin(\varepsilon) - F_{H-Tail} - F_{Anchors} \bullet \cos(\theta) \end{bmatrix}}{\cos(\varepsilon) + \tan(\varepsilon) \bullet \sin(\varepsilon)} \right\} \bullet \tan(\varepsilon) \quad (2.20)$$

Combining trigonometric terms, Equation 2.20 becomes

$$N' = \frac{W_{Dam} + W_{Pool} + W'_{Silt} + W_{Tail} + F_{Anchors} \bullet \sin(\theta) - U \bullet \cos(\varepsilon)}{\cos(\varepsilon)}$$

$$+ \left\{ \begin{array}{l} F_{H-Pool} + F'_{Silt} \\[6pt] + \left[\begin{array}{l} W_{Dam} + W_{Pool} + W'_{Silt} + W_{Tail} \\ + F_{Anchors} \bullet \sin(\theta) - U \bullet \cos(\varepsilon) \end{array} \right] \bullet \tan(\varepsilon) \\[12pt] - U \bullet \sin(\varepsilon) - F_{H-Tail} - F_{Anchors} \bullet \cos(\theta) \end{array} \right\} \bullet \sin(\varepsilon) \quad (2.21)$$

Additional combination of trigonometric terms results in

$$N' = \left(F_{H-Pool} + F'_{Silt} \right) \bullet \sin(\varepsilon)$$
$$+ \left[\begin{array}{l} W_{Dam} + W_{Pool} + W'_{Silt} + W_{Tail} \\ + F_{Anchors} \bullet \sin(\theta) - U \bullet \cos(\varepsilon) \end{array} \right] \bullet \cos(\varepsilon) \quad (2.22)$$
$$- \left[U \bullet \sin(\varepsilon) + F_{H-Tail} + F_{Anchors} \bullet \cos(\theta) \right] \bullet \sin(\varepsilon)$$

And finally, this results in

$$N' = \left(F_{H-Pool} + F'_{Silt} \right) \bullet \sin(\varepsilon)$$
$$+ \left[W_{Dam} + W_{Pool} + W'_{Silt} + W_{Tail} + F_{Anchors} \bullet \sin(\theta) \right] \bullet \cos(\varepsilon) \quad (2.23)$$
$$- \left[F_{H-Tail} + F_{Anchors} \bullet \cos(\theta) \right] \bullet \sin(\varepsilon) - U$$

2.2.7 Factor of safety against sliding along the base

At incipient sliding, the shear strength along the base for the dam-to-foundation interface becomes fully mobilized. Otherwise there is reserve capacity to resist the shear force T required for equilibrium along the sloping base in the free-body diagram of the gravity dam. The factor of safety against sliding along this interface, FS_{slide}, is defined as

$$FS_{slide} = \frac{T_{ult}}{T} \quad (2.24)$$

In Equation 2.24, T is defined by Equation 2.18 and T_{ult} is the ultimate shear resistance along the interface, computed using a Mohr-Coulomb failure criterion. In an effective stress analysis, T_{ult} is given by

$$T_{ult} = c' \bullet \left(L_{Base} - L_{Crack} \right) + N' \bullet \tan(\varphi') \quad (2.25)$$

In Equation 2.25, the effective force normal to the base N' is defined by Equation 2.23.

At the onset of sliding, T is equal to T_{ult} and FS_{slide} is equal to 1.0. L_{Base} is the length of the base as measured from the points designated as heel and toe in Figures 2.1 through 2.4, and L_{Crack} is the length of the crack, if present. When a crack is present along the base of the dam, the value of (L_{Base} - L_{Crack}) is sometimes referred to as the effective base area <u>in compression</u> and designated as $L_{effective\ base}$ in this report.

2.2.8 Equation of moment equilibrium

The equation of moment equilibrium for the Figure 2.1 forces about the toe is

$$N' \bullet L_{N-Toe} = M_{Stable} - M_{Over} \tag{2.26}$$

with the overturning (clockwise) moment M_{Over} defined as

$$M_{Over} = F_{H-Pool} \bullet \left[Y_{FH-Pool} - L_{Base} \bullet \sin(\varepsilon) \right]$$
$$+ F'_{Silt} \bullet \left[Y_{F-Silt} - L_{Base} \bullet \sin(\varepsilon) \right] + U \bullet L_{U-Toe} \tag{2.27}$$

and the stabilizing (counterclockwise) moment M_{Stable} defined by

$$M_{Stable} = W_{Dam} \bullet X_{WDam-Toe} + W_{Pool} \bullet X_{WPool-Toe} + W'_{Silt} \bullet X_{WSilt-Toe}$$
$$+ W_{Tail} \bullet X_{WTail-Toe} + F_{H-Tail} \bullet Y_{FH-Tail} \tag{2.28}$$
$$+ F_{Anchors} \bullet \cos(\theta) \bullet Y_{Anchors-Toe} + F_{Anchors} \bullet \sin(\theta) \bullet X_{Anchors-Toe}$$

Thus the position of N', the effective force normal to the Figure 2.1 base, as measured from the toe L_{N-Toe} is

$$L_{N-Toe} = \frac{\left(M_{Stable} - M_{Over} \right)}{N'} \tag{2.29}$$

with M_{Over} and M_{Stable} defined by Equations 2.27 and 2.28, respectively, and N' given by Equation 2.23.

Note that for the negative sloping gravity dam base of Figure 2.2, the angle ε is negative, resulting in a positive value for the two terms of $[L_{Base} \bullet \sin(\varepsilon)]$ in Equation 2.27.

2.2.9 Effective base area in compression $L_{effective\ base}$

The effective base area in compression may now be computed using the magnitude of the effective force normal to the base N' computed by Equation 2.23 and the position of N' along the base, as measured from the toe, $L_{N\text{-}Toe}$ computed by Equation 2.29, and assuming a linear effective base pressure distribution.

Uncracked base. If the computed effective force normal to the base N' lies within the middle third of the Figure 2.1 L_{Base}, then cracking will not occur (i.e., $L_{Crack} = 0$) and $L_{effective\ base}$ is equal to L_{Base}. The corresponding effective pressure distribution normal to the base is shown in Figure 2.5. The minimum effective base pressure q'_{min} acts normal to the base at the heel in this figure and is computed to be equal to

$$q'_{min} = \frac{N'}{L_{Base}} \bullet \left[1 - \frac{6 \bullet e}{L_{Base}} \right] \tag{2.30}$$

The maximum effective base pressure q'_{max} acting normal to the base at the toe is equal to

$$q'_{max} = \frac{N'}{L_{Base}} \bullet \left[1 + \frac{6 \bullet e}{L_{Base}} \right] \tag{2.31}$$

The lateral distance as measured from the midpoint along the base (i.e., the centerline) to the location of N' is given by

$$e = \frac{L_{Base}}{2} - L_{N-Toe} \tag{2.32}$$
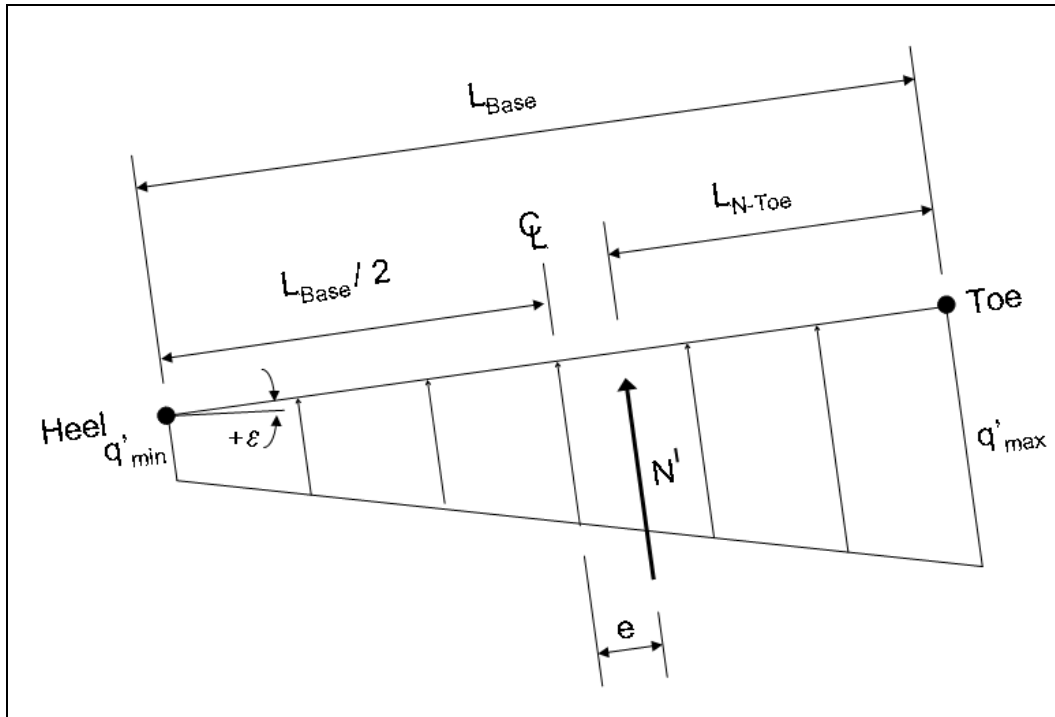
Figure 2.5. Assumed linear effective base pressure distribution with no crack.

Cracked base. If the computed effective force normal to the base N' lies outside the middle third of the Figure 2.1 L_{Base}, then cracking will occur (i.e., $L_{Crack} > 0$) and $L_{effective\ base}$ is less than L_{Base}.

When N' is outside the kern (i.e., the middle third of the base), the value for e calculated by Equation 2.32 is greater than $L_{Base}/6$. In this case

$$L_{effective\ base} = 3 \bullet L_{N-Toe} \qquad (2.33)$$

$$L_{Crack} = L_{Base} - L_{effective\ base} \qquad (2.34)$$

The corresponding effective pressure distribution normal to the base is shown in Figure 2.6. The effective normal base pressure is equal to zero between the heel and the tip of the crack, as shown in this figure.

The maximum effective base pressure acting normal to base at the toe is equal to

$$q'_{max} = \frac{N'}{L_{effective\ base}} \bullet 2 \qquad (2.35)$$
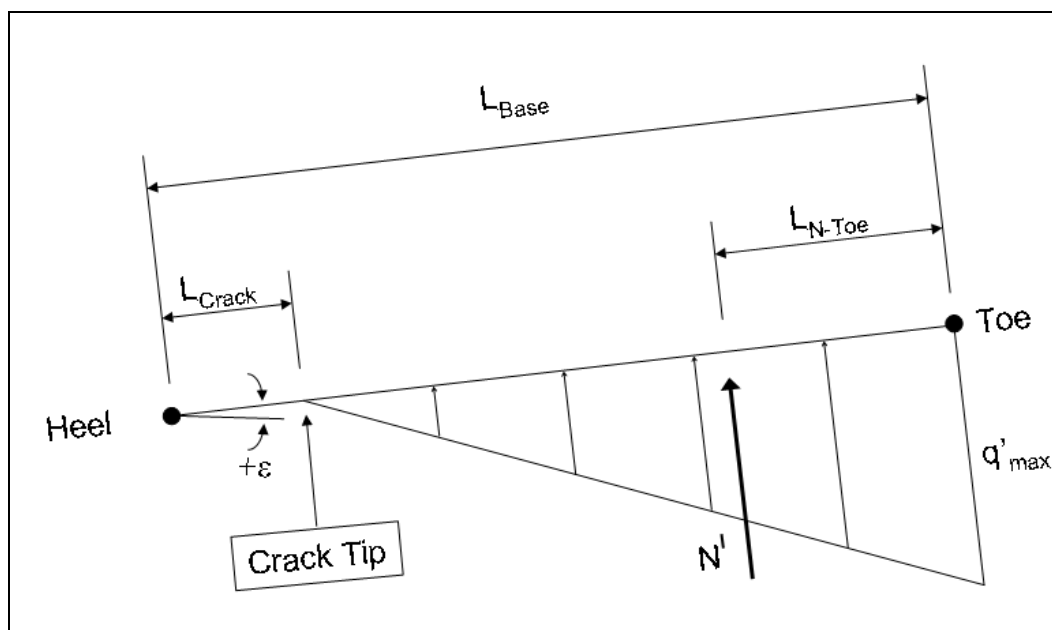
Figure 2.6. Assumed linear effective base pressure distribution with crack.

Base verged on cracking. For a dam base verged on cracking (i.e., L_{Crack} = 0), the value for e by Equation 2.32 is equal to $L_{Base}/6$. For this special case, the value for L_{N-Toe} is

$$L_{N-Toe} = \frac{L_{Base}}{3} \qquad (2.36)$$

As seen from Equations 2.33 and 2.36, the computed value for $L_{effective\ base}$ is equal to L_{Base}.

Computation of L_{Crack}. An iterative procedure is used by the PC-based GDLAD_Sloping_Base to compute the length of a crack using the equilibrium methodology outlined in this chapter of the forces acting on the Figure 2.1 idealized gravity dam cross section. The first calculation made by GDLAD_Sloping_Base assumes full contact along the base (i.e., L_{Crack} = 0) when first assigning the non-site-specific uplift pressure distribution along the sloping base of the gravity dam. This uplift pressure distribution is converted to a corresponding resultant uplift pressure force U. In the case of a non-site-specific uplift pressure distribution, the relationships given in Appendix B are used. With the value for the resultant uplift pressure force U, the equilibrium computations are made for the Figure 2.1 gravity dam cross section. At the conclusion of the initial equilibrium computation, a new value for L_{Crack} is determined (i.e., computed). Should the new crack length value differ from that used in the previous computation

(by a nominal value), a new uplift pressure distribution corresponding to this new crack length is assigned and the equilibrium computation is conducted with a new resultant uplift force U. Convergence on a value for L_{Crack} is achieved when the results for two consecutive computations are the same (or nearly the same value).

2.3 Multivariate probabilistic analysis of uncertain variables

The inherent randomness and uncertainty of some model parameters require numerical methods to obtain solutions to the resulting probabilistic problem. A numerical method such as the Latin Hypercube simulation is a sampling technique used for conducting the analysis. Latin Hypercube sampling (LHS) was selected for its efficiency and its reduction in run time compared with that of Monte Carlo simulation. When LHS is used in the multivariate case, it is important to maintain statistical independence between variables unless correlation is explicitly specified. This is necessary to preserve randomness between variables. The DakotaLHS stand-alone application from Sandia National Laboratories is the software of choice for the LHS of multiple variables.

The DakotaLHS software performs restricted pairing with rank correlation between multiple variables. With rank correlation, each variable is represented as a column vector with length corresponding to the number of samples. The values of each column are ranked by ordering all the samples in ascending order. The ranked values are then sorted such that the correlation between its values and those of every other column is as small as possible, i.e., minimum correlation or approximately zero. However, when there is established correlation between a pair or pairs of variables, correlations can be induced. This method of maintaining statistical independence among variables as well as inducing correlation between pairs of variables is known as restricted pairing and is an option available within DakotaLHS. This is the current option used for a GDLAD_Sloping_Base analysis.

For a user-specified number of simulations, DakotaLHS will generate an ASCII file that contains columns of values for all the variables that are specified by the user as random. All these random variables can be correlated, independent, or a combination of both. For variables that are correlated, a user specifies the correlation coefficient. To initiate an analysis, each variable is expressed individually with its statistical parameters, i.e., mean and standard deviation, and its distribution type. If there is

knowledge of statistical correlation between variables, these are stated with their respective correlation coefficient. Pre-testing is conducted in order to determine the number of samples or simulations needed to reproduce the original distribution that was sampled. In the multivariate case, the number of samples for an entire analysis is determined by reproducing the probability density function of the fragility curve. This is accomplished by simply increasing the number of simulations.

The variables of uncertainty for stability calculations within GDLAD_Sloping_Base are C, PHI, E, K_O, A_f, U, and $L_{U\text{-}Toe}$. These variables can also be used in a deterministic analysis or a combination of a probabilistic and deterministic analysis. Examples of model parameters and their default statistical values are given in Table 2.1 for non-site-specific uplift pressures and also in Table 2.2 for site-specific uplift pressures derived from Joint_FLOW. Table 2.1 values are used for the example problems discussed in the next chapter.

Table 2.1. Model parameters with inherent uncertainty and default statistical values for non-site-specific uplift pressures.

Parameter Name	Parameter Symbol	Mean	Standard Deviation	Distribution Type
Effective cohesion	C	100.0	25.0	Bounded Normal
Effective angle of internal friction	PHI	30.0	3.0	Bounded Normal
Non-site-specific uplift pressure (drain efficiency)	E	0.375	0.1	Bounded Normal
Horizontal earth pressure coefficient within the silt	K_O	0.39	0.0975	Bounded Normal
Allowable load per anchor, lb	A_f	35,000	3,500	Bounded Normal

Table 2.2. Model parameters with inherent uncertainty and default statistical values for site-specific uplift pressures.

Parameter Name	Parameter Symbol	Mean	Standard Deviation	Distribution Type
Effective cohesion	C	100.0	25.0	Bounded Normal
Effective angle of internal friction	PHI	30.0	3.0	Bounded Normal
Horizontal earth pressure coefficient within the silt	K_O	0.39	0.0975	Bounded Normal
Allowable load per anchor, lb	A_f	35,000	3,500	Bounded Normal
Site-specific uplift pressure (from Joint_FLOW)	U	Constant for each pool	Constant for each pool	Bounded Normal
Site-specific uplift location (from Joint_FLOW)	$L_{U\text{-}Toe}$	Constant for each pool	Constant for each pool	Bounded Normal

2.4 System response/fragility curves for rock-founded gravity dams with a sloping base

A system response curve (SRC) defines the probability of failure or the limit state of a concrete gravity dam. The SRC for sliding is constructed by taking the ratio of the accumulated sliding factors of safety that are less than or equal 1.0, i.e., failures, and the number of simulations for each pool height being analyzed. Similarly, the SRC for overturning is constructed by taking the ratio of the accumulated overturning factors of safety that are less than or equal 1.0, and the number of simulations for each pool height. As an example, Figure 2.7 shows the results of a probabilistic analysis in the form of SRCs of sliding and overturning limit states.
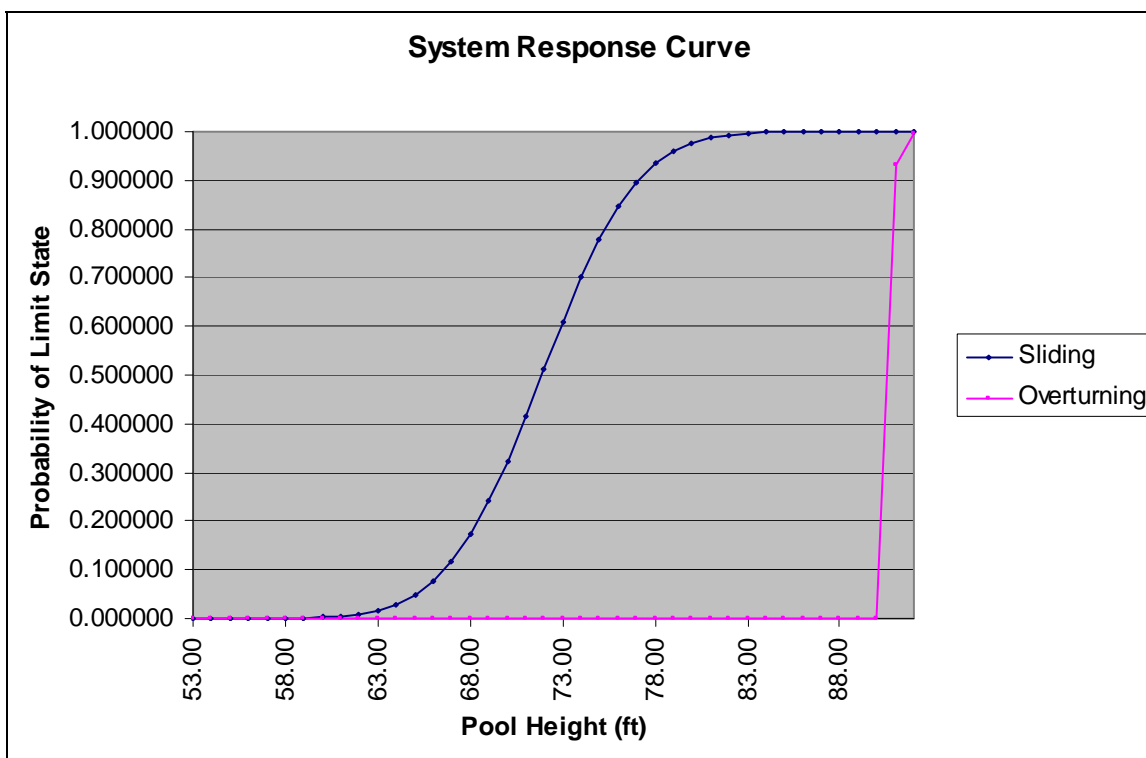
Figure 2.7. SRCs for sliding and overturning limit states.

A factor of safety is a measure of stability against sliding or overturning. For the stability analysis, the factor of safety against sliding along a planar interface is given in Equation 2.24, and the factor of safety against overturning is defined as the ratio of M_{Over} and M_{Stable}, and is expressed by Equations 2.27 and 2.28, respectively.

A probabilistic analysis considers the model parameters as random variables. The uncertain variables in the example problem are C, PHI, E, K_o, and A_f and are described in Table 2.1. These uncertain model parameters were used in the sliding stability calculations previously mentioned. A probabilistic analysis also requires a large number of samples or simulations. For the example of 40 pools, the computations of a minimum of 40,000 simulations of five random variables were evaluated to determine the factor of safety that is less than or equal to 1.0 for each pool height. Thus, 40 probabilistic analyses were performed with each defining a point on the SRCs of Figure 2.7.

3 The Visual Modeler – GDLAD_Sloping_Base for Excel

3.1 Introduction

This chapter provides guidance on the details and execution of GDLAD_Sloping_Base for Excel, which are referred to in this report as the Visual Modeler. Visual Modeler offers a pre- and post-processing friendly environment where it accepts data necessary to perform a GDLAD_Sloping_Base analysis (by executing the FORTRAN engineering formulation discussed in Chapter 2) and displays results in both tabular and graphical form. Discussions on how to perform and interpret the results of an analysis are also presented.

3.2 Visual Modeler

GDLAD_Sloping_Base is a program that is used to compute SRCs for a two-dimensional cross section of a concrete gravity dam founded on a sloping rock base. Visual Modeler provides a user interface for input to GDLAD_Sloping_Base as well as a post-processing environment for the results obtained from the analysis. This chapter is intended to give the user an understanding of creating, executing, and interpreting a GDLAD_Sloping_Base analysis.

Input data (ASCII) to GDLAD_Sloping_Base FORTRAN falls into 7 categories or groups as described in Appendix C, whereas Visual Modeler contains 11 worksheets with the first 6 accepting user input and the other 5 worksheets providing results from a GDLAD_Sloping_Base execution, which is initiated from the Analysis worksheet. The following is a list of the 11 worksheets contained within Visual Modeler:

- XYCoords
- Plot
- Pools
- Silt
- Anchors
- Analysis
- SRC
- PDF

- Deterministic
- Input Summary
- Stats

3.2.1 XYCoords worksheet

Information on the geometry of the concrete gravity dam with sloping base, the gallery within the dam, the maximum pool and maximum tail-water elevations, and specified dimension units are the relevant data entered in this worksheet, illustrated in Figure 3.1. These data are also described within Groups 1 and 2 of Appendix C as input to GDLAD_Sloping_Base.

The table of data in Figure 3.1 lists the x- and y-coordinates of the concrete gravity dam cross section with a maximum of 35 points allowable to describe the monolith. These x- and y-values are required to be entered in a clockwise direction, starting at the heel, cells B7 and B8, and working upward and to the right towards the toe (i.e., the last input data point). All other pertinent data can be entered into the input boxes highlighted in yellow within the templates, defined as follows:

- $X_{W\text{-}Gallery}$ – the distance from the toe of the dam to the center of the gallery
- $Y_{B\text{-}Gallery}$ – the height from the toe of the dam to the base of the gallery
- L_{Drain} – the distance from the heel of the dam to the bottom of the line of drains that intersect the sloping base, as measured along the base.
- *Dome* – when selected the radius is ½ $B_{Gallery}$, otherwise the radius is zero
- $H_{Gallery}$ – the height of the gallery
- $B_{Gallery}$ – the width of the gallery
- Max Pool Elevation
- Max Tailwater Elevation
- Unit Length – Units available are foot, inch, meter, centimeter, and millimeter

If all values need to be reset to the default, the **Assign Default Values** button will accomplish this task. When the user is satisfied with the input data, the **Graph** button can be selected in order to see the outline of the created dam. Selection of the **Graph** button will automatically transfer the screen to the Plot worksheet.
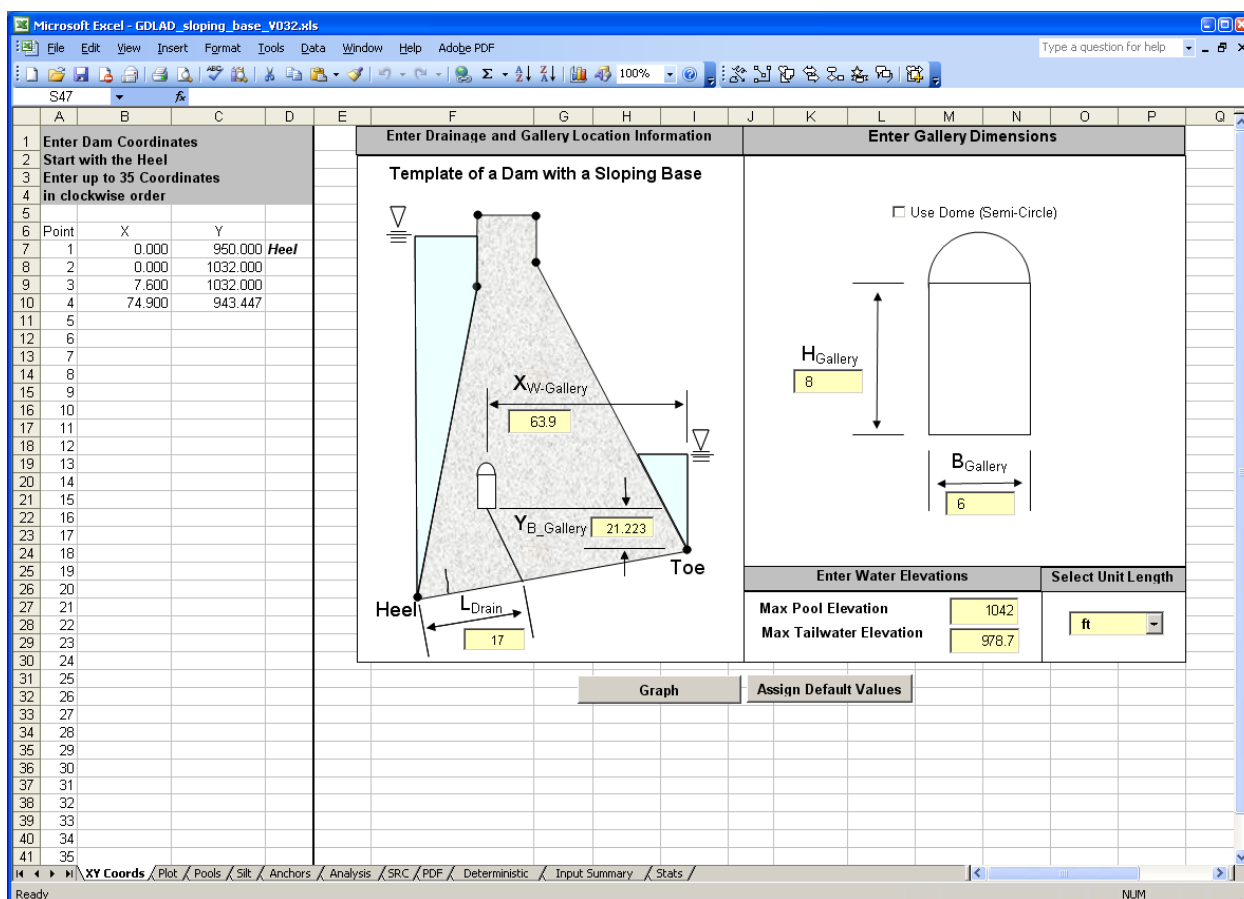
Figure 3.1. Geometry features of the concrete gravity dam presented in the XYCoords worksheet.

3.2.2 Plot worksheet

The results shown in Figure 3.2 have been calculated from user input data provided within the XYCoords worksheet. The Plot worksheet is purely for information purposes. The x- and y-coordinates of all geometries are provided in column form, and the graphical output can be visualized as the areas and locations of centers of gravity. The **Refresh** button can be selected if the user needs to repopulate and redraw the data within this worksheet.

3.2.3 Pools worksheet

The Pools worksheet is used for entering the minimum and maximum pool heights, the increment to use for generating the intermediate pool heights, and the tailwater heights as illustrated in Figure 3.3. These parameters can be entered into the boxes highlighted in yellow. Dimensions and increment units are assigned from the **Select Unit Lengths** drop-down box
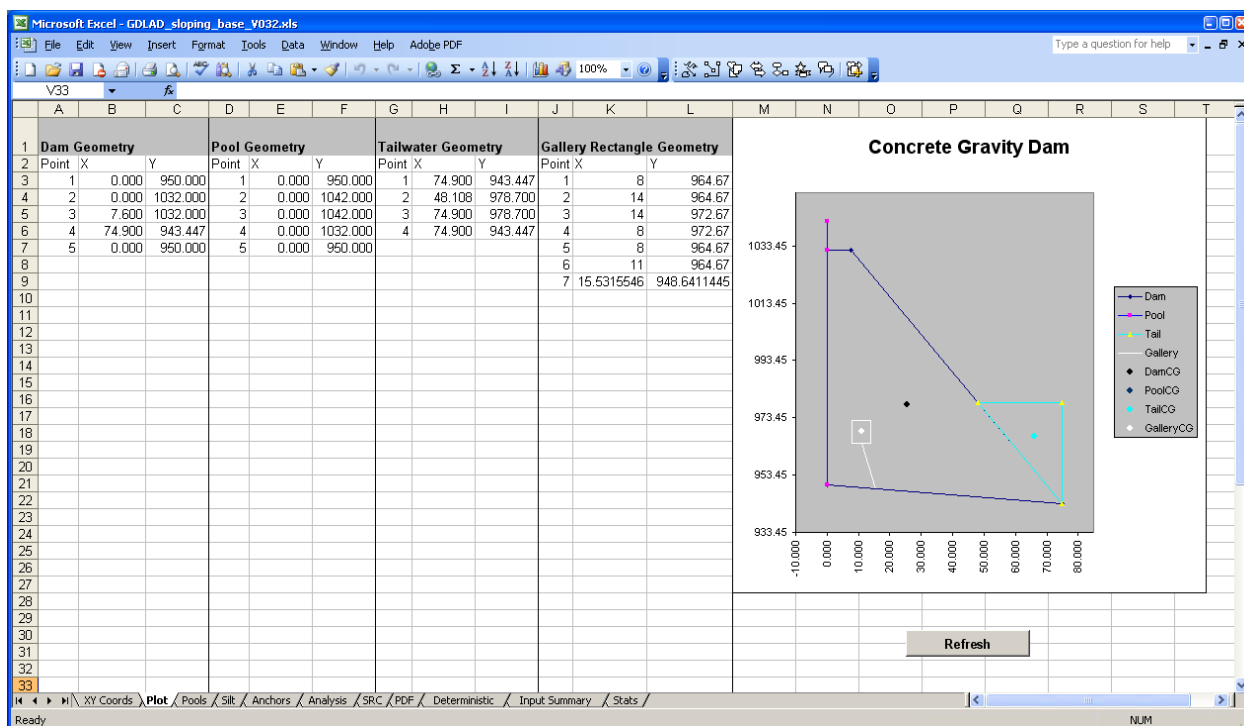
Figure 3.2. Plot worksheet providing geometric results in tabular form and overall graph of user-provided input.

within the XYCoords worksheet. The following parameters are available for user input:

- $H_{PoolMax}$ – the maximum pool height (as measured from the heel)
- $H_{PoolMin}$ – the minimum pool height (as measured from the heel)
- Increment – increment between pool heights
- Options for Variable or Constant Tailwater Height
  1. Minimum Constant Tailwater Height with
  2. Corresponding Limiting Pool Height (as measured from the toe)
  3. Maximum Constant Tailwater Height with
  4. Corresponding Limiting Pool Height (as measured from the toe)
  5. Constant Tailwater Height (as measured from the toe)

The user can select a Constant Tailwater Height for all pool levels; then only item 5 in the lower data box shown in Figure 3.3 will be accepted and items 1–4 shown in the middle data box in Figure 3.3 will be dimmed out and not available for data entry. Similarly, if the Variable Tailwater Height option is selected, only items 1 and 2, i.e., Minimum and Maximum Constant Tailwater Height and their Corresponding Limiting Pool Heights, will be defined. The Minimum and Maximum Constant Tailwater Heights are associated with corresponding lower and upper pool heights.
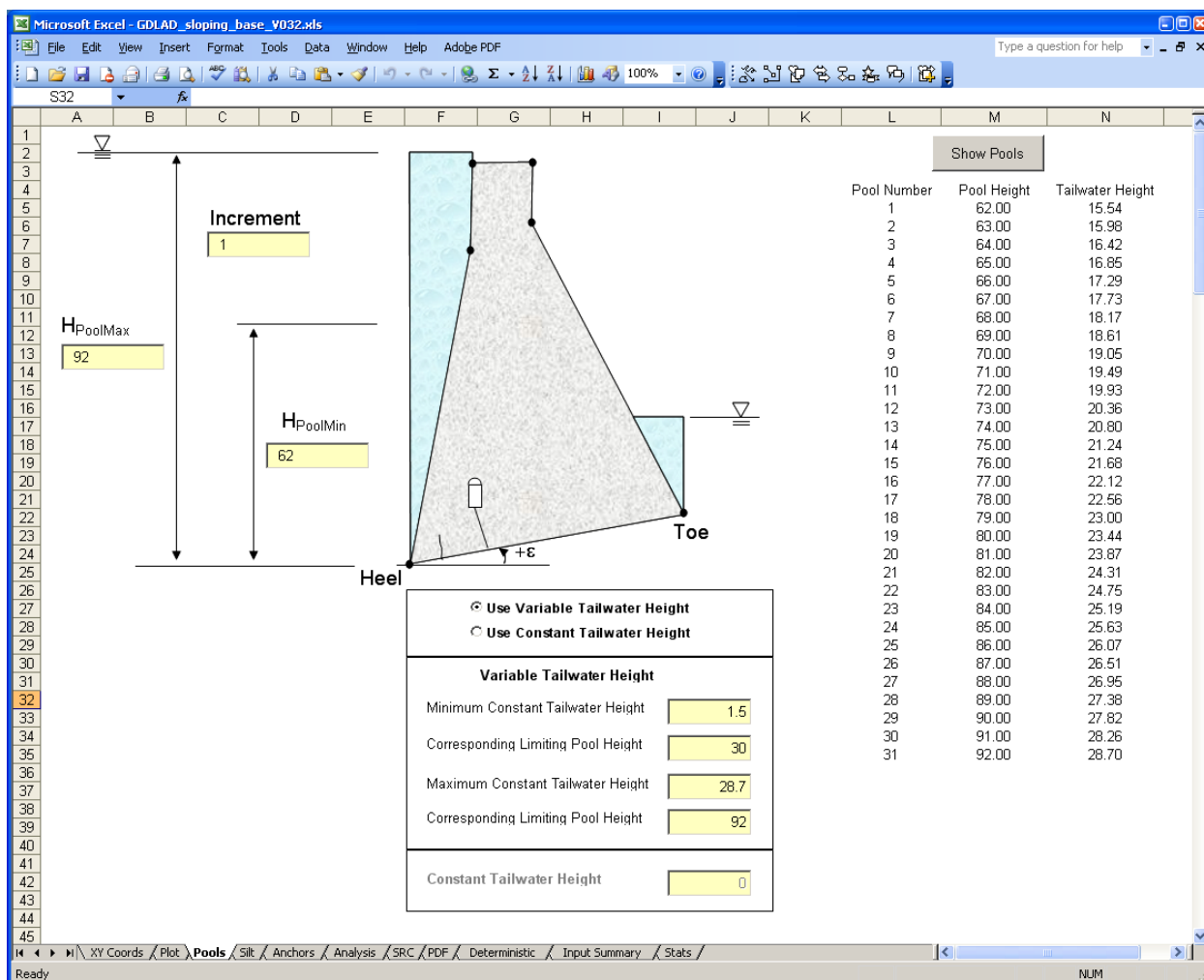
Figure 3.3. The Pools worksheet, which provides information of the heights of the pool and tailwater.

When the pool height is less than or equal to the specified limiting lower pool height, the Minimum Constant Tailwater Height value is used. When the pool height is greater than or equal to the specified limiting upper height, the Maximum Constant Tailwater Height value is used. However, if the pool height is in between the lower and upper limiting pool values, the tailwater height is calculated by linearly interpolating between the minimum and maximum values.

To preview all pool heights calculated from the minimum and maximum values entered, select the **Show Pools** button. These pool and tailwater heights are described within Group 7 of Appendix C and provided as ASCII input to GDLAD_Sloping_Base (FORTRAN). The pool heights will also be displayed in the SRC worksheet after the analysis is completed.

If the analysis is for a single pool, $H_{PoolMax}$ and $H_{PoolMin}$ should be equal, a Constant Tailwater Height entered, and only one pool height displayed when the **Show Pools** button is selected.

3.2.4 Silt worksheet

The Silt worksheet describes the silt characteristics when silt pressures in the pool are significant and will be added to the horizontal force acting on the two-dimensional cross section of the concrete gravity dam as shown in Figure 3.4. (Note that the weight of silt is also included in the stability analysis; refer to Figures 2.1 through 2.4.) Specific data within this worksheet are provided as input to GDLAD_Sloping_Base FORTRAN and described within ASCII Group 4 data input of Appendix C. Silt parameters can be entered into the boxes highlighted in yellow. The following silt parameters are available for user input:

- γ_{Moist} – the moist unit weight of the silt in pounds per cubic foot
- $\gamma_{Saturated}$ – the saturated unit weight of the silt in pounds per cubic foot
- H_{Silt} – the vertical distance from the heel to the top of the silt
- K_o – the at rest lateral pressure coefficient
    - Mean
    - Standard Deviation
    - Probability Distribution Type

EM 1110-2-2100 (HQUSACE 2005) states that horizontal silt pressure is assumed to be equivalent to that of a fluid weighing 85 pcf.[1] It also states that vertical silt pressure is determined as if silt were a soil having a wet density of 120 pcf. This results in a K_o value of 0.39, which is provided as the default. If variable K_o is uncertain, a standard deviation and probability distribution type will be expected from the user. However, if K_o is a constant and not considered random, then **Standard Deviation** should be set to zero and the distribution type will be ignored.

For a K_o distribution, a mean of 0.39 and standard deviation of 0.0975 are the default values when using Bounded Normal and Log Normal distributions. When using Uniform distribution, a minimum of 0.29 and maximum of 0.49 are the default values. The **Assign Default Values** button is available to allow the user to select preset values as input.

---

[1] A table of factors for converting non-SI units of measure to SI units is found on page ix.
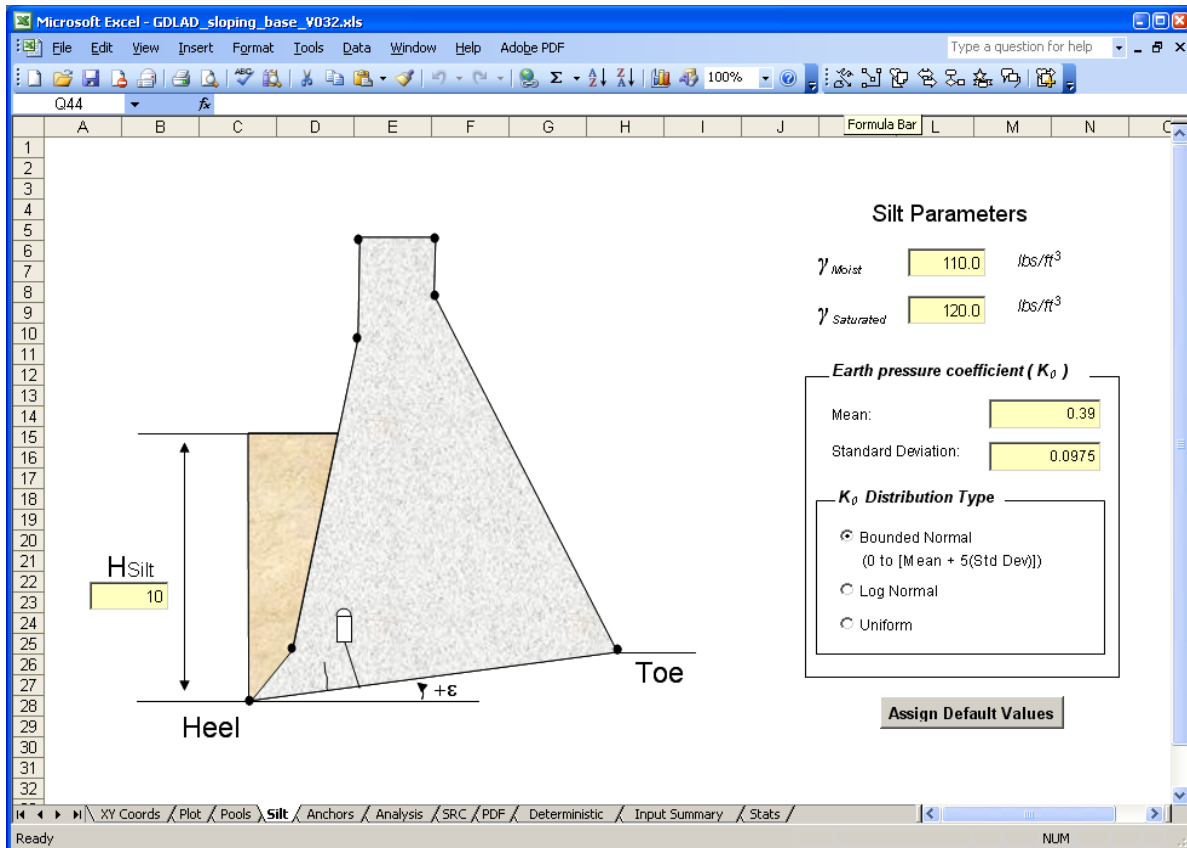
Figure 3.4. The Silt worksheet, which provides graphical presentations of silt and its parameters.

3.2.5 Anchors worksheet

The Anchors worksheet describes the anchorage features when anchor force is considered for improving sliding (or overturning) stability of the gravity dam (Figure 3.5). Specific data within this worksheet are provided as input to GDLAD_Sloping_Base and described within Group 3 of Appendix C. Relative data concerning post-tensioned anchors can be entered into the boxes highlighted in yellow. All units are assigned from the **Select Unit Lengths** box within the XYCoords worksheet. The first five input variables are defined as follows:

- Number of Anchors per Group
- Spacing of Anchor Groups
- $Y_{Anchors-Toe}$ – the vertical distance from the toe to the center of the Anchor Group
- $X_{Anchors-Toe}$ – the horizontal distance from the toe to the center of the Anchor Group
- Angle (θ) – the angle between the horizontal x-axis and the line of anchors in degrees
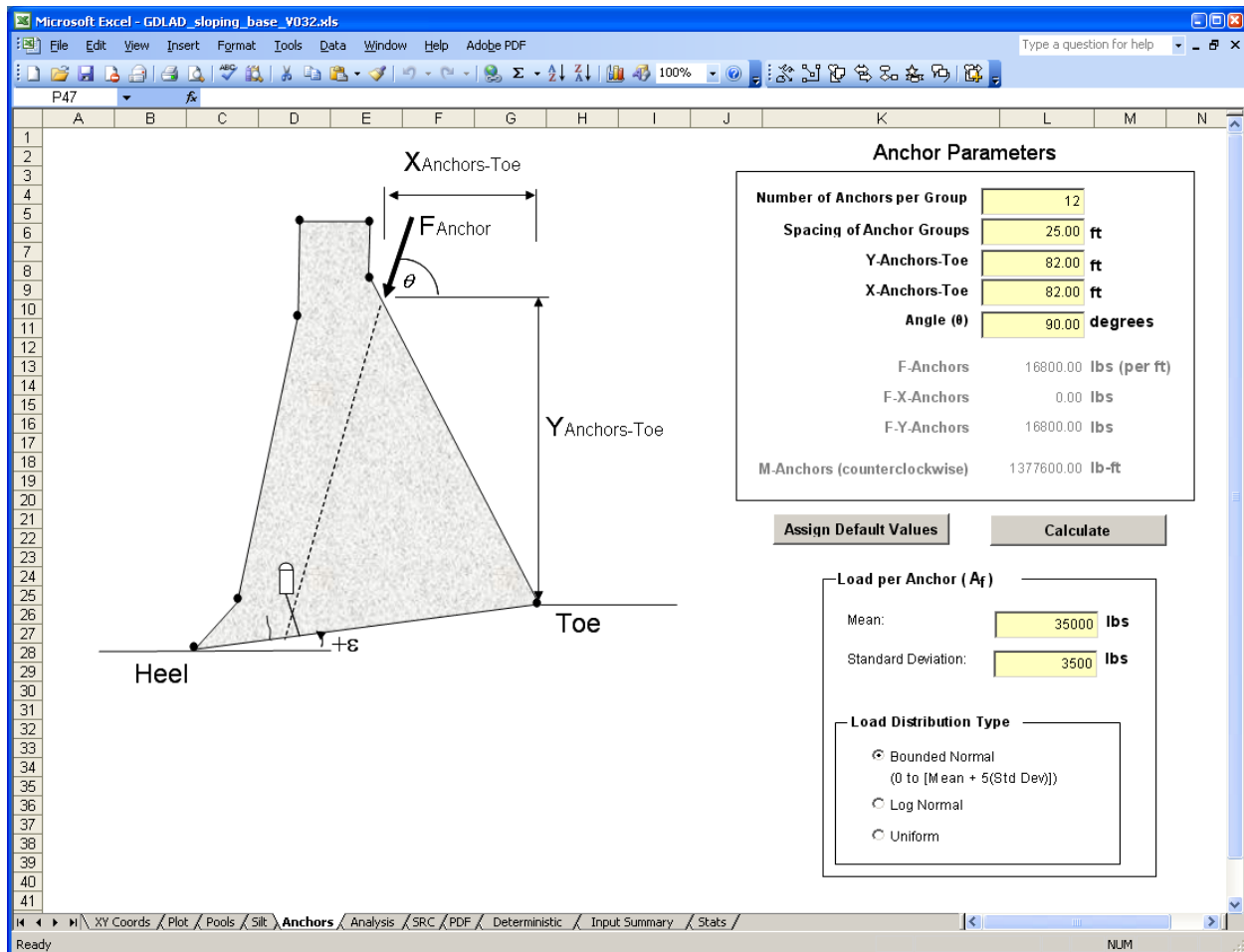
Figure 3.5. The Anchors worksheet, which provides graphical presentation of anchor positions relative to the concrete gravity dam and additional information relating to these post-tensioned anchors.

The next three input values provide information regarding the uncertainty in the allowable load per anchor A_f and thereby anchor force.

- Mean
- Standard Deviation
- Probability Distribution Type

If the variable load per anchor A_f is considered deterministic, a constant or the mean for the anchor load should be entered and the standard deviation set to zero. Distribution type will be ignored if the variable is deterministic. If the anchor load is random, then the mean, standard deviation, and distribution type must be provided.

The **Calculate** button is optional and can be selected in order to preview the resultant, horizontal, and vertical anchor forces and moment about the

toe due to the anchor forces. For an anchor force distribution, a mean load per anchor of 35,000 lb and standard deviation of 3,500 lb are the default values when using bounded normal and log normal distributions. The default values for a uniform distribution are a minimum of 31,500 lb and maximum of 38,500 lb. The **Assign Default Values** button is available to allow for preset values as input.

3.2.6 Analysis worksheet

The Analysis worksheet (Figure 3.6) allows the selection of a probabilistic or entirely deterministic analysis. This is the last user input worksheet with the ability to launch the simulation. The variables are categorized as follows:

- *Analysis Type* – If the analysis type is deterministic, constant or mean values of all random variables will be accepted and the standard deviation of these variables set to zero. If the analysis type is probabilistic, the mean and standard deviation will be required together with a selection of one out of three distribution types – bounded normal, log normal, and uniform.

Figure 3.6. Analysis worksheet, which provides for the selection of the type of analysis under consideration and for user input of statistical information for the variables.

- *Number of Simulations* – The Number of Simulations variable specifies the number of observations required to reproduce the probability density function (PDF) of the SRC. The default value is 40,000. (Note: The computed PDF can be sensitive to this value.)
- *Event Tree* – The Event Tree variable specifies the number of branches to display for the event tree. The number of branches must be an integer greater than or equal to 3 and less than or equal to 12. The default value is 12.
- *Shear Strength Parameters* – These options specify the mean and standard deviation values to use in the generation of the random effective cohesion (C) parameter and effective angle of friction (PHI) parameter for bounded normal and log normal distributions. For a Uniform distribution, the minimum and maximum values are entered instead.

  1. For effective C distribution, a mean of 100 and standard deviation of 25 are the default values when using bounded normal and log normal distributions. The default values for uniform distribution are a minimum of 70 and maximum of 130.
  2. For effective PHI distribution, a mean of 30 and standard deviation of 3 are the default values when using bounded normal and log normal distributions. The default values for uniform distribution are a minimum of 20 and maximum of 40.
  3. In the **Correlated Variables** section, the user specifies whether or not there is correlation between the C and PHI values. The default value is "Yes". The correlation coefficient r is in the range $-1 \le r \le +1$. The default value is -0.7.

- *Uplift Pressures* – Uplift pressures play an important role in the sliding and overturning stability of the concrete gravity dam. Two options are available that can describe this phenomenon: the non-site-specific uplift pressures (described extensively in Appendix B) and the site-specific uplift pressures (provided by the program Joint_FLOW). The description of Joint_FLOW is beyond the scope of this report; it will be presented in the report on GDLAD_Foundation.

  1. A non-site-specific approach to describe the uplift pressure normal to the sloping dam-rock foundation interface is the drain efficiency (E). The values entered in the **Mean** value field will be used as a constant in a deterministic analysis. For a probabilistic analysis, the

mean, standard deviation, and distribution type are required. Three distribution types are available for E: Bounded Normal, Bounded Log Normal, and Uniform. The default type is Bounded Normal. A Bounded Normal distribution is a normal distribution that is sampled only between two specific values (0 and 1 in this case). A Bounded Log Normal distribution is a Log Normal distribution that is also sampled between two specified values (0 and 1).

2. For a site-specific uplift pressure condition (using Joint_FLOW), a pre-processing step that necessitates the execution of Joint_FLOW externally is required. The option **View Data File** lists the pool and tailwater heights, the mean and standard deviations of both the uplift pressures and locations of the uplift pressures, and their correlation coefficient. These values are used in conjunction with the Distribution Types available for user selection. Three Distribution Types are available for the uplift pressure and its resultant location - Bounded Normal, Bounded Log Normal, and Uniform. The default type is Bounded Normal.

3. Values described in this worksheet are presented in Groups 5, 6, and 7 of Appendix C and provided as input to GDLAD_Sloping_Base.

- *Run Analysis* – For a probabilistic analysis, Visual Modeler will call DakotaLHS.exe to generate the number of observations for all random variables. For each pool height, DakotaLHS.exe will generate a file containing these variables for the number of observations specified in the **Number of Simulations** option. These files are named LHS_XX_O.OUT where XX represents the corresponding pool height. The message in Figure 3.7 is displayed when Visual Modeler is generating the probabilistic data (Figure 3.8) for DakotaLHS sampling for each pool height.
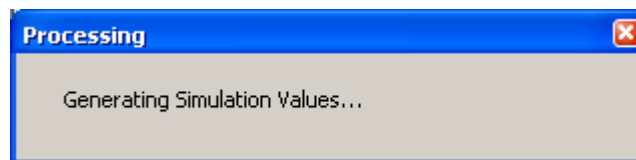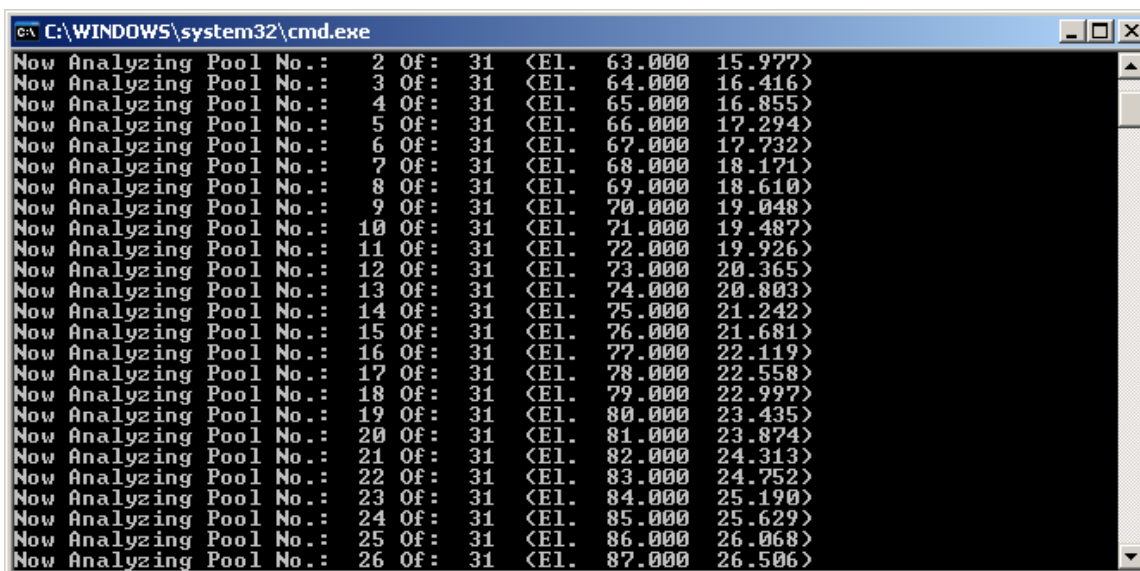
Figure 3.7. Message produced during simulation.

The previous message will not be displayed for a deterministic analysis. While the stability analyses are being performed by GDLAD_Sloping_Base FORTRAN, the screen in Figure 3.8 is displayed so that the user can see the progress of the calculations:

Figure 3.8. Screen displayed while the probabilistic analysis is performed.

When the analysis is complete, the SRC will be displayed automatically within the SRC worksheet.

3.2.7 SRC worksheet

GDLAD_Sloping_Base generates the SRC of the sliding limit state. A second SRC is generated for the overturning limit state.

Each point on the Figure 3.9 graph represents the fraction of the stability analyses resulting in the sliding factor of safety being less than or equal to 1.0.

Inspection of the plot of the SRC for the sliding limit state (Figure 3.9) shows that around pool height 72 ft, there is a 0.50 (50 percent) probability of a sliding factor of safety less than or equal to 1.0. At pool height 83 ft, there is a nearly 100 percent probability of a sliding limit state occurring; i.e., a sliding factor less than or equal to 1.0.

The SRC for the overturning limit state is also plotted in Figure 3.9. As can be seen, non-zero probabilities of overturning limit state did not occur until much higher pool heights, around the pool height of 91 ft.
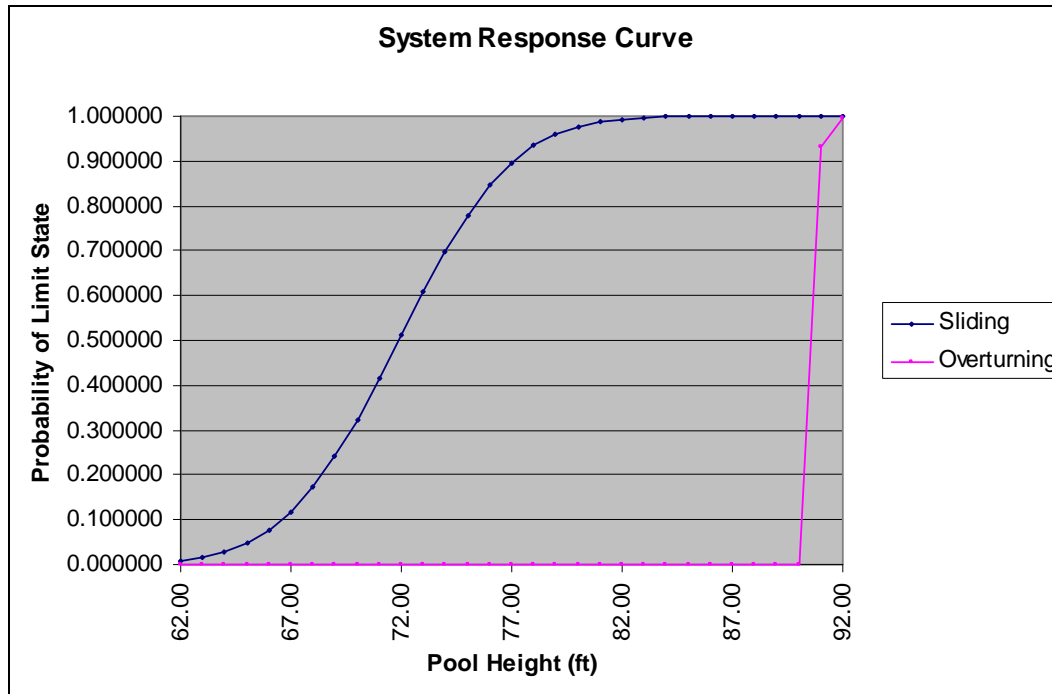
Figure 3.9. The SRC worksheet displaying the SRCs.

3.2.8 PDF worksheet

Figure 3.10, showing the PDF curve, was generated by numerically differentiating the SRC. The total area under the PDF curve is 1.0. This means that the total probability of the limit state, for all simulations at all pool heights, is 1.0.

If the area under the graph is divided into segments, the area under each segment can be calculated. Each of these areas can then be a branch of an event tree as shown in Figure 3.11.

For the calculation of the event tree with 12 branches, the PDF is divided into 10 equal segments plus two additional segments at the tails on the left and right portions of the graph. The pool height range can be seen to be 62 to 90 ft. Dividing this range into 10 segments resulted in a range for each segment of $(90 − 62)/10 = 2.8$ ft.

The tails (0 to 62 ft and 90 ft to infinity) are assigned a probability of 0.0 since there are no data in these ranges. For the middle 10 segments, the area under each segment is numerically derived from the points on the PDF. The area under each segment represents the total probability of reaching the limit state in this pool range.
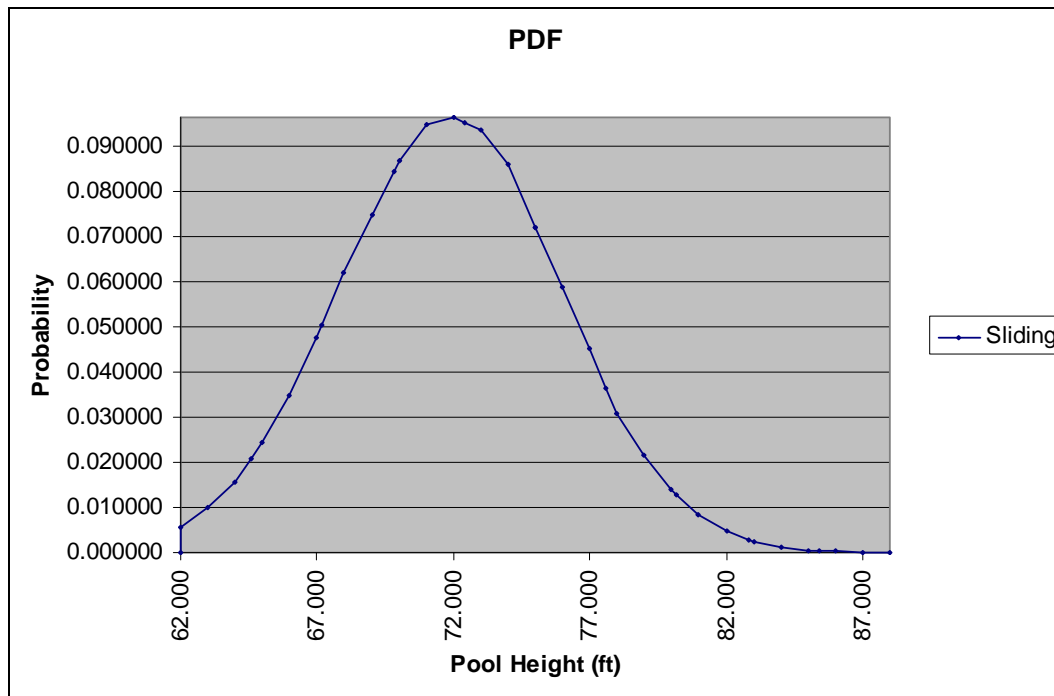
Figure 3.10. The PDF worksheet displaying the PDF curve.

Event Tree		
Pool Range		
Low Pool	High Pool	Probability
0.00	62.00	0.000000
62.00	64.80	0.036530
64.80	67.60	0.107557
67.60	70.40	0.209737
70.40	73.20	0.268227
73.20	76.00	0.217643
76.00	78.80	0.113395
78.80	81.60	0.037378
81.60	84.40	0.008158
84.40	87.20	0.001259
87.20	90.00	0.000115
90.00	infinity	0.000000
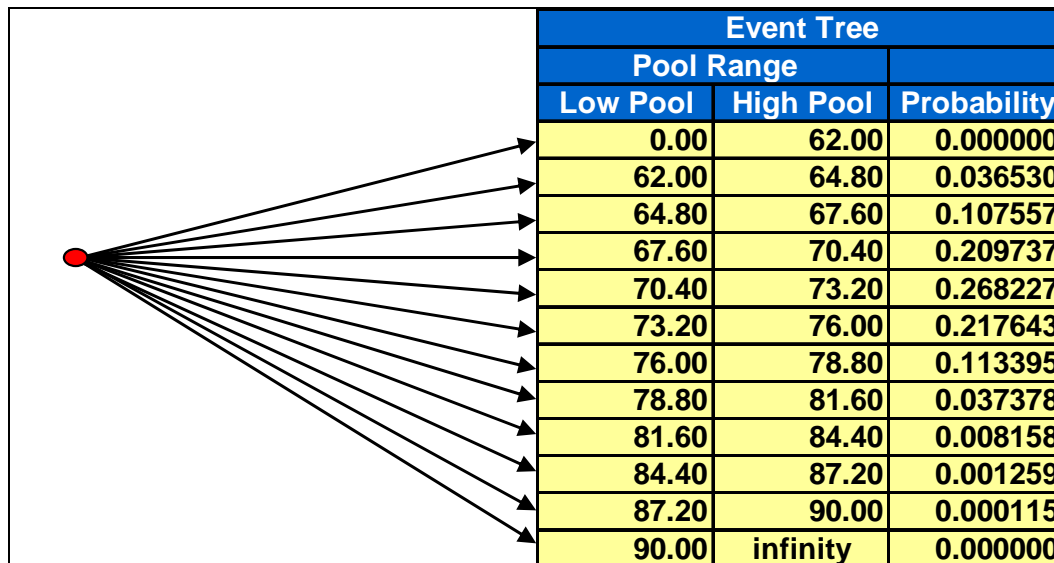
Figure 3.11. The event tree with twelve branches as displayed in the PDF worksheet.

The data used for plotting the SRC and PDF graphs are stored in two ASCII output files named CDF.OUT (the SRC is the fragility curve and is a conditional cumulative distribution function, CDF) and PDF.OUT, respectively. These files are saved in the same location as the Visual Modeler.

3.2.9 Deterministic worksheet

The Deterministic worksheet shows the values for a single deterministic analysis. A single deterministic analysis can be conducted by entering the same value for the minimum and maximum pool heights and a constant tailwater height in the Pools worksheet as well as entering zeroes for the values of standard deviations for C, PHI, and E in the Analysis worksheet; A_f in the Anchors worksheet; and K_o in the Silt worksheet. All standard deviation values are automatically set to zero if the analysis type is deterministic. After a simulation run, the Deterministic worksheet will automatically be presented to the user.

3.2.10 Input Summary worksheet

The Input Summary worksheet shows the values that were selected in the **Probabilistic Analysis** section (Figure 3.6).

3.2.11 Stats worksheet

The Stats worksheet shows program statistics including the elapsed time and the total number of analyses performed.

Two examples in the following sections demonstrate the process.

3.3 Example 1 – Concrete gravity dam with silt loading

For this example, GDLAD_Sloping_Base will analyze the sliding stability of the concrete gravity dam under the influence of silt pressures.

3.3.1 Geometry of the concrete gravity dam

The example shows the geometry describing the concrete gravity dam with an upstream face that is vertical as illustrated in Figure 3.12. All elevations are shown in inch-pound units with the length unit as feet.
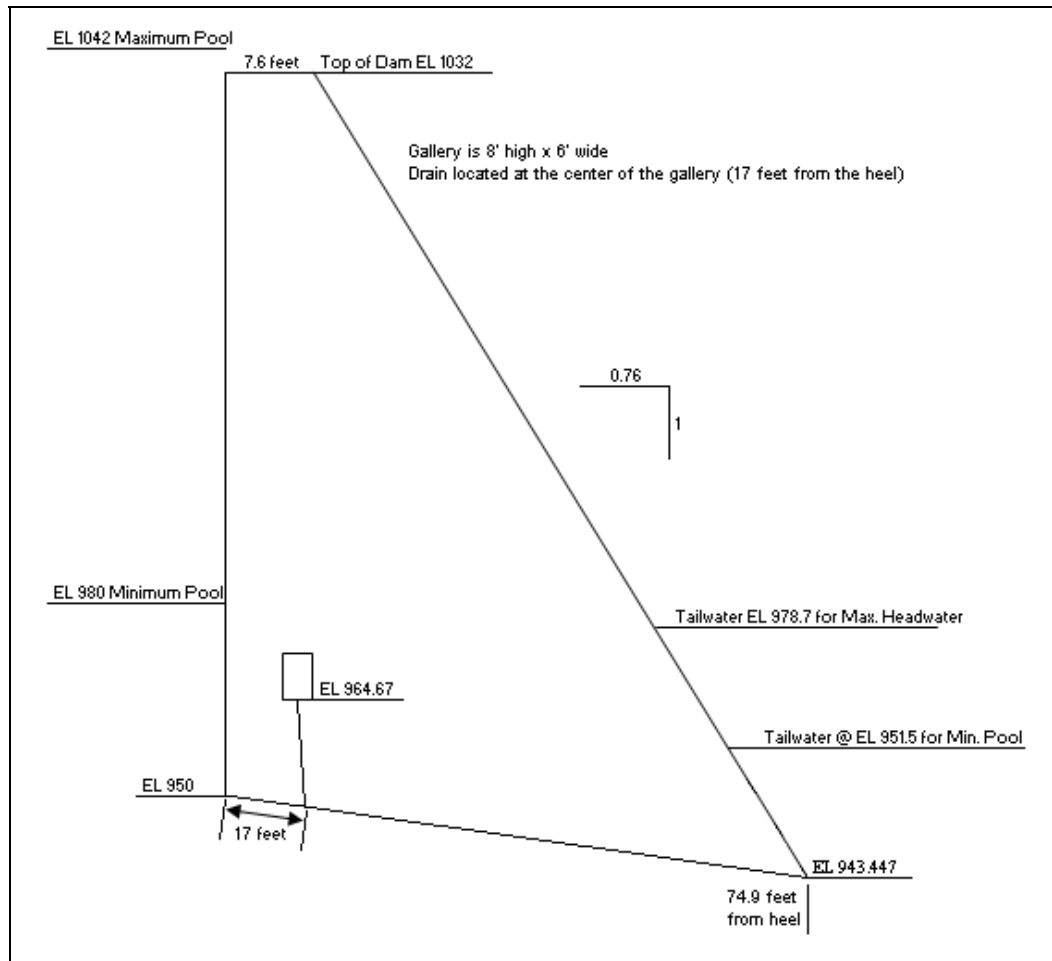
Figure 3.12. Geometry of a concrete gravity dam.

3.3.2 XYCoords worksheet

The first step is to enter the x- and y-coordinates that define the geometry of the dam. These values can easily be entered by selecting the XYCoords worksheet. Starting at the heel (lower left corner) of the dam cross section enter the x- and y-coordinates (0.0, 950.0 at cells B7, C7) of the heel. Continuing clockwise, the coordinates of the next point at the upper left corner of the dam should be x = 0.0, y = 1032.0 (cells B8, C8), the third point at x = 7.6, y = 1032.0 (cells B9, C8), and the fourth and last point located at the toe, x = 74.9, y = 943.447 (cells B10, C10). These coordinates, the parameters relative to the gallery, the line of drains, the maximum pool and tailwater elevations, and the unit length specifications are entered into the XYCoords worksheet as shown in Figure 3.13, such that

- $X_{W\text{-}Gallery}$ = 63.9
- $Y_{B\text{-}Gallery}$ = 21.223

- L_{Drain} = 17
- $R_{Gallery}$ = 0
- $H_{Gallery}$ = 8
- $B_{Gallery}$ = 6
- Max Pool Elevation   = 1042
- Max Tailwater Elevation   = 978.7
- Unit Length   = ft
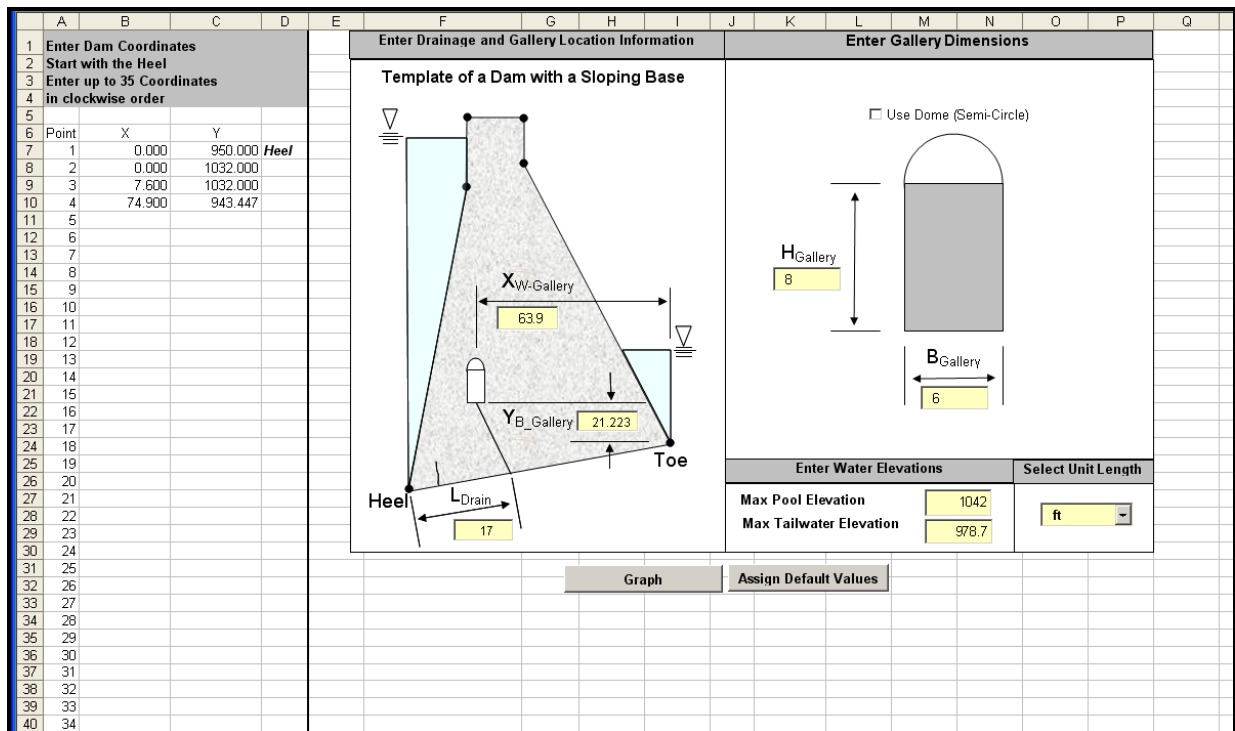
Figure 3.13. Data entered in the XYCoords worksheet for example 1.

The next step is to select the **Graph** button to view the cross-sectional areas and moments of inertia of the concrete gravity dam, the pool, the tailwater, and the gallery. Selection of this button will automatically display the Plot worksheet.

3.3.3 Plot worksheet

The ability to view the cross-sectional areas as well as the centroids as defined in the XYCoords worksheet of all geometries is displayed in the Plot worksheet. In addition to the graphical representation of these geometries, the x- and y-coordinates are also presented in tabular form (Figure 3.14).
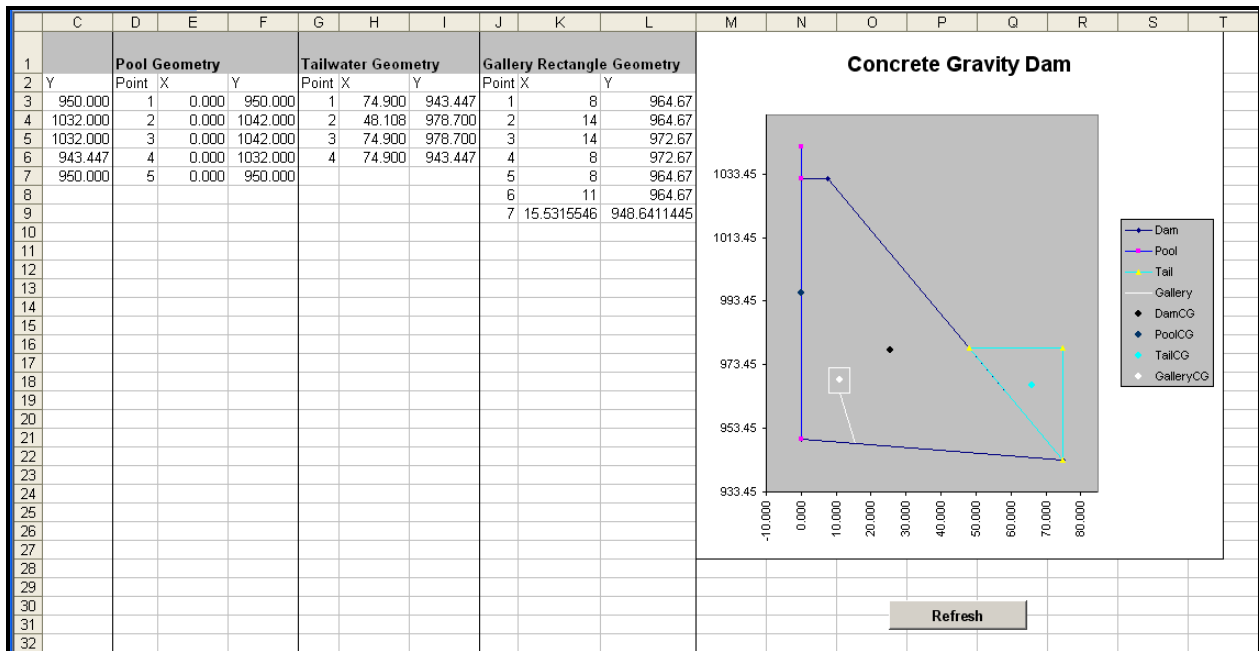
Figure 3.14. Data entered in the Plot worksheet for example 1.

3.3.4 Pools worksheet

The Pools worksheet requires the user to provide pool and tailwater heights from the given pool and tailwater elevations as described in Figure 3.12. For the minimum pool elevation of 980 ft and a maximum pool elevation of 1,042 ft, the pool heights can be measured relative to the heel of the dam (950 ft). This procedure is also used for calculating the heights of the tailwater relative to the toe. The following values are provided as input to the Pools worksheet:

- $H_{PoolMax}$ = 92
- $H_{PoolMin}$ = 30
- Increment = 1
- Variable Tailwater Height
  1. Minimum Constant Tailwater Height = 1.5
     Corresponding Limiting Pool Height = 30
  2. Maximum Constant Tailwater Height = 28.7
     Corresponding Limiting Pool Height = 92

Note: Because the Variable Tailwater Height option was selected, the Constant Tailwater Height will be dimmed out and not available for user input. It is good practice to select the **Show Pools** button at this point; this shows the variability of the pools and the number of pools that will be

evaluated for this analysis. Figure 3.15 shows the input provided and a partial printout of the pool and tailwater heights. The total number of pools for example 1 is 63.
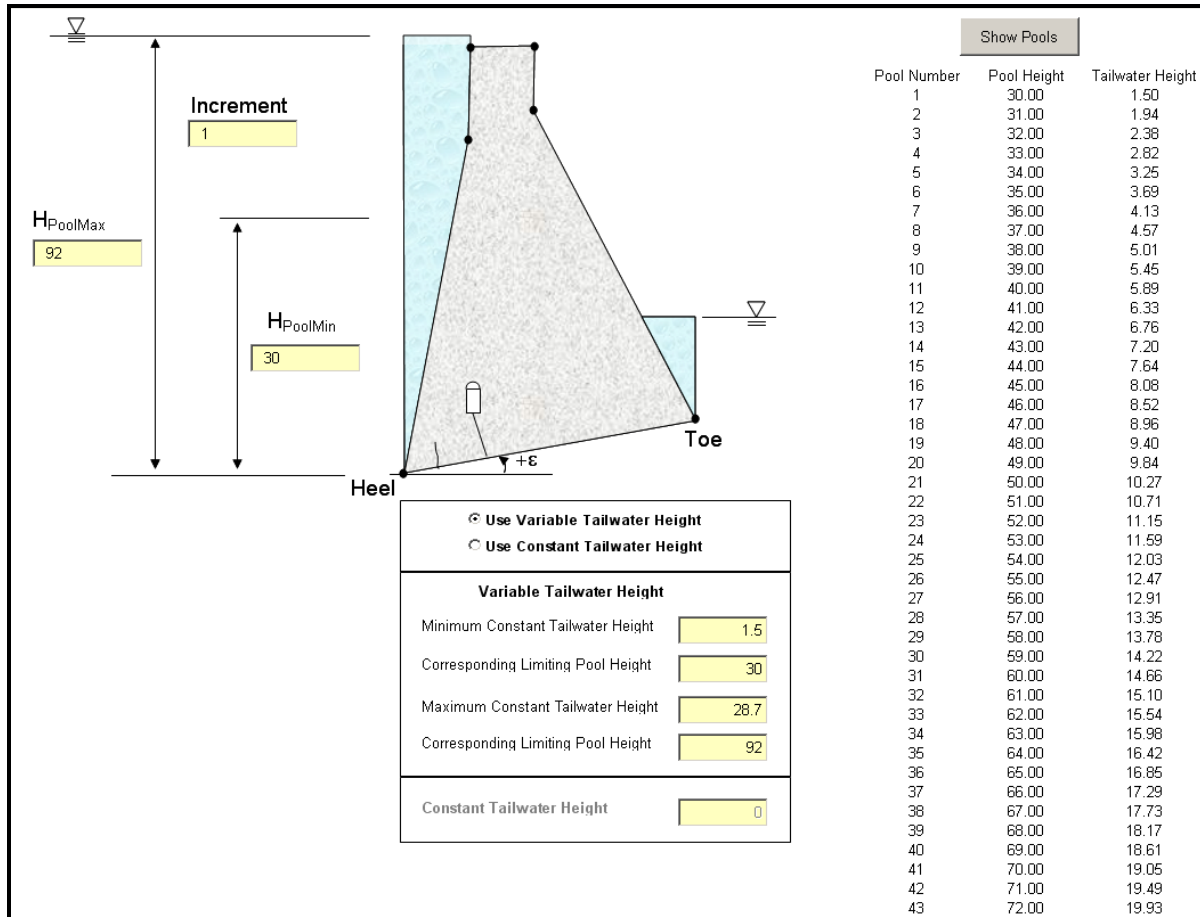
Figure 3.15. Data entered in the Pools worksheet for example 1.

3.3.5 Silt worksheet

For example 1, the height of silt will be set at 10 ft, and the defaults for the other parameters will be accepted. These input data can be seen in Figure 3.16 as follows.

- γ_{Moist} = 110.0
- $\gamma_{Saturated}$ = 120.0
- H_{Silt} = 10
- K_o (Mean)   = 0.39
- Standard Deviation   = 0.0975
- Probability Distribution Type = Bounded Normal
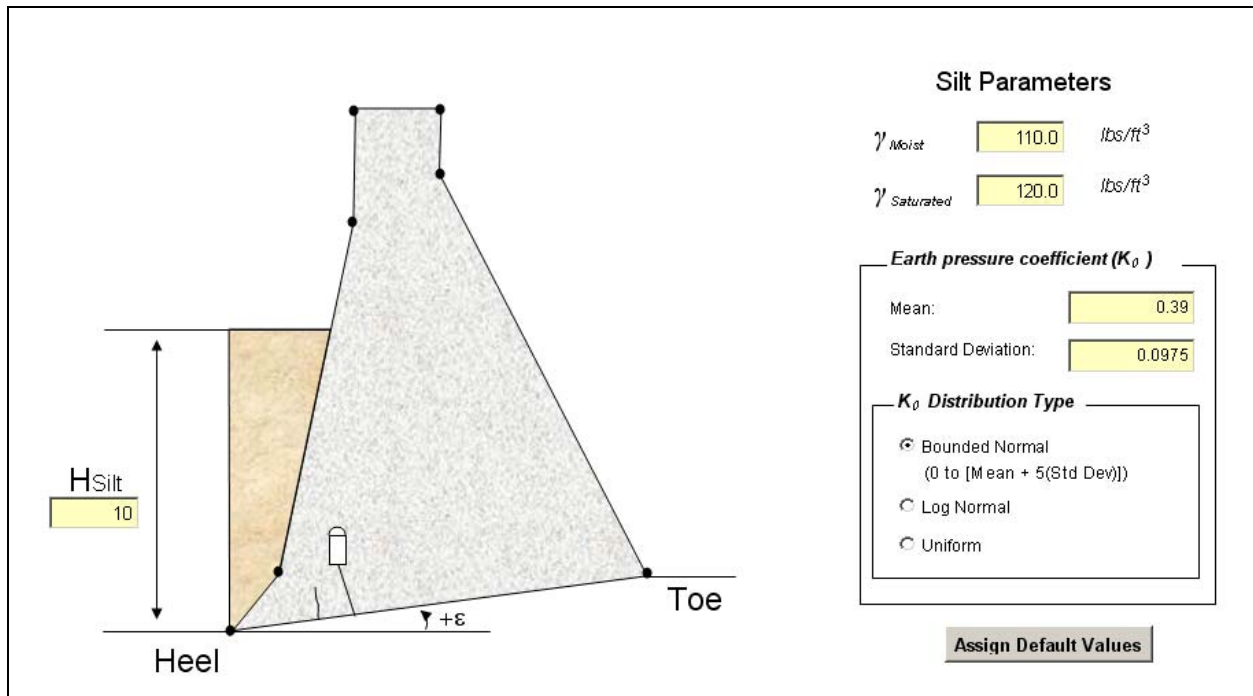
Figure 3.16. Data entered in the Silt worksheet for example 1.

3.3.6 Anchors worksheet

Because no anchor force is available for this example, the mean and standard deviation values will be set to 0.0.

3.3.7 Analysis worksheet

The analysis type for example 1 is probabilistic, and values for all relevant parameters are provided as follows and shown in Figure 3.17.

- Analysis Type   = Probabilistic
- Number of Simulations   = 40,000
- Event Tree   = 12
- Shear Strength Parameters
  1. C
     - Mean   = 100.0
     - Standard Deviation   = 25.0
  2. PHI
     - Mean   = 30.0
     - Standard Deviation   = 3.0
  3. C and PHI Distribution type = Bounded Normal
  4. Correlated Variables   = Yes
     - Correlation Coefficient   = -0.7

Figure 3.17. Data entered in the Analysis worksheet for example 1.

- Uplift Pressures   = Non-site-specific
  - Mean   = 0.375
  - Standard Deviation   = 0.1
  - E Distribution Type   = Bounded Normal

The program is now ready to perform an analysis. Select the **Run Analysis** button. A message will appear "Generating Simulation Values...." to let the user know that the simulation is underway. This process will take a minute or two, depending on the number of pools being evaluated and the speed of the computer. The next display will show the stability analysis being performed by GDLAD_Sloping_Base for each pool. Upon completion, the output shown in Figure 3.18 is presented. This shows the data within the SRC worksheet.

3.3.8 SRC and PDF worksheets providing results for example 1

The data in Figure 3.18 show the SRC and a partial listing of the data for each pool height. According to these data, sliding does not occur until a pool height of 53 ft. Also notice the PDF and the event tree presented in the PDF worksheet, both shown in Figure 3.19. Since sliding did not occur until a height of 53 ft, the data within the Event Tree show several zero probabilities. Also, since sliding did not occur until a height of 53 ft, i.e., the important information lies above pool heights of 53 ft, the analysis will need to be rerun by first setting the minimum pool height to 53 ft.

Pool Height	Sliding	Overturning	Largest
30.00	0.000000	0.000000	0.000000
31.00	0.000000	0.000000	0.000000
32.00	0.000000	0.000000	0.000000
33.00	0.000000	0.000000	0.000000
34.00	0.000000	0.000000	0.000000
35.00	0.000000	0.000000	0.000000
36.00	0.000000	0.000000	0.000000
37.00	0.000000	0.000000	0.000000
38.00	0.000000	0.000000	0.000000
39.00	0.000000	0.000000	0.000000
40.00	0.000000	0.000000	0.000000
41.00	0.000000	0.000000	0.000000
42.00	0.000000	0.000000	0.000000
43.00	0.000000	0.000000	0.000000
44.00	0.000000	0.000000	0.000000
45.00	0.000000	0.000000	0.000000
46.00	0.000000	0.000000	0.000000
47.00	0.000000	0.000000	0.000000
48.00	0.000000	0.000000	0.000000
49.00	0.000000	0.000000	0.000000
50.00	0.000000	0.000000	0.000000
51.00	0.000000	0.000000	0.000000
52.00	0.000000	0.000000	0.000000
53.00	0.000050	0.000000	0.000050
54.00	0.000050	0.000000	0.000050
55.00	0.000050	0.000000	0.000050
56.00	0.000250	0.000000	0.000250
57.00	0.000350	0.000000	0.000350
58.00	0.000750	0.000000	0.000750
59.00	0.001450	0.000000	0.001450
60.00	0.002850	0.000000	0.002850

Figure 3.18. Output for the SRC worksheet for example 1.

3.3.9 Rerun analysis of example 1 for minimum pool height of 53 ft

The rerun analysis is easily accomplished by first going to the Pools work-sheet and changing the minimum pool height variable $H_{PoolMin}$ to 53 ft (Figure 3.20). Selecting the **Show Pools** button will show a new listing of 40 pools, starting at the new pool height of 53.0 ft and ending at 92.0 ft.

Next, return to the Analysis worksheet and select **Run Analysis** one more time. **Results** of the SRC are presented in Figure 3.21, and the PDF and the event tree are shown in Figure 3.22.

From the SRC in Figure 3.21, at about a pool height of 72 ft, there is a 50 percent probability of sliding limit state occurring. At the pool height of approximately 83 ft, there is 100 percent probability of a sliding limit state occurring.

The first non-zero probability of an overturning limit state does not occur in this example until a pool height of 91.0 ft. So the sliding limit state defines the SRC for this dam.

The Event Tree corresponding to the PDF is presented in the PDF work-sheet, both shown in Figure 3.22 for example 1.
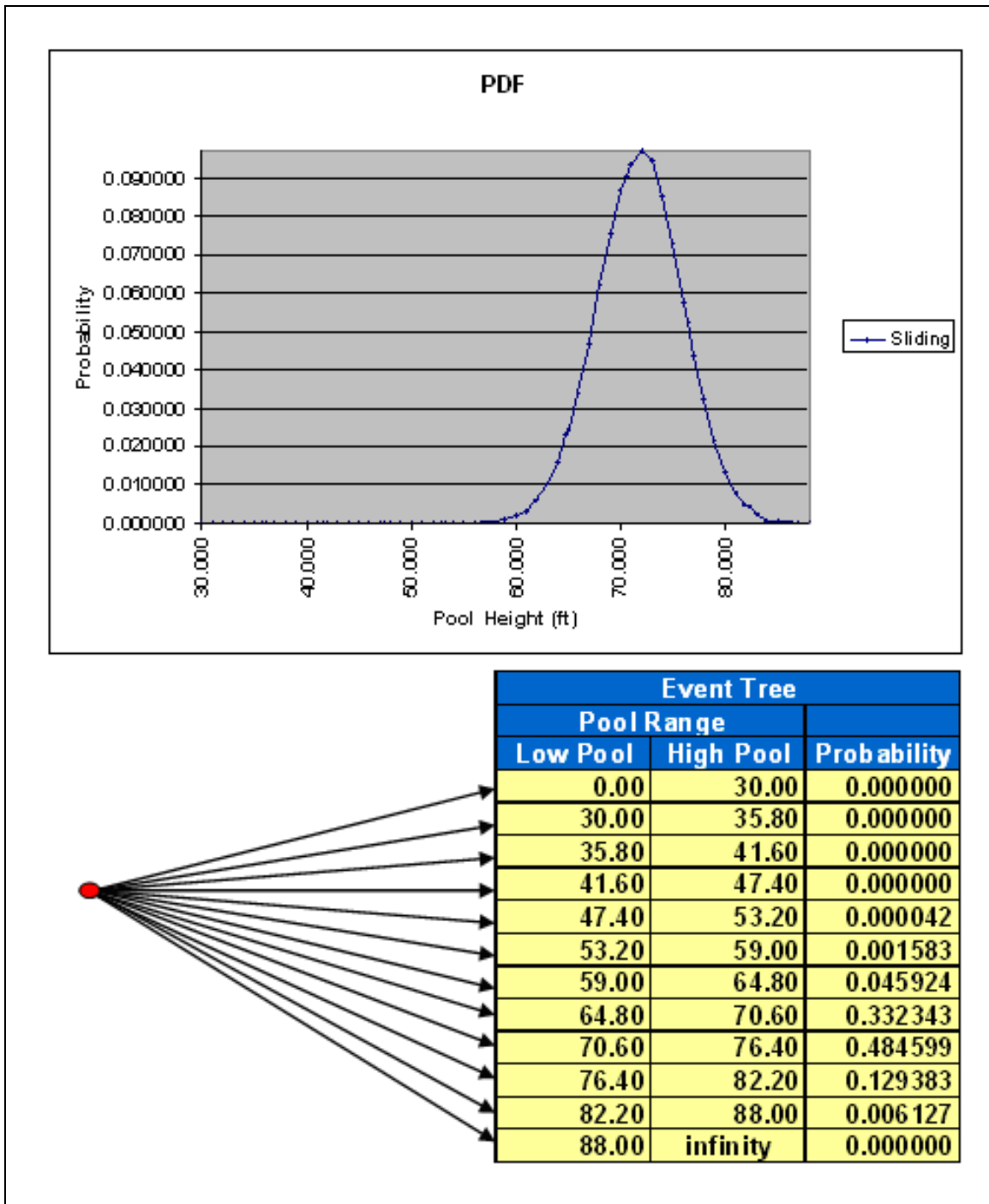
Figure 3.19. Data contained within the PDF worksheet for example 1.

Show Pools

Increment

1

$H_{PoolMax}$

92

$H_{PoolMin}$

53

Toe

Heel

+ε

○ Use Variable Tailwater Height
○ Use Constant Tailwater Height

Variable Tailwater Height

Minimum Constant Tailwater Height	1.5
Corresponding Limiting Pool Height	30
Maximum Constant Tailwater Height	28.7
Corresponding Limiting Pool Height	92
Constant Tailwater Height	0

Pool Number	Pool Height	Tailwater Height
1	53.00	11.59
2	54.00	12.03
3	55.00	12.47
4	56.00	12.91
5	57.00	13.35
6	58.00	13.78
7	59.00	14.22
8	60.00	14.66
9	61.00	15.10
10	62.00	15.54
11	63.00	15.98
12	64.00	16.42
13	65.00	16.85
14	66.00	17.29
15	67.00	17.73
16	68.00	18.17
17	69.00	18.61
18	70.00	19.05
19	71.00	19.49
20	72.00	19.93
21	73.00	20.36
22	74.00	20.80
23	75.00	21.24
24	76.00	21.68
25	77.00	22.12
26	78.00	22.56
27	79.00	23.00
28	80.00	23.44
29	81.00	23.87
30	82.00	24.31
31	83.00	24.75
32	84.00	25.19
33	85.00	25.63
34	86.00	26.07
35	87.00	26.51
36	88.00	26.95
37	89.00	27.38
38	90.00	27.82
39	91.00	28.26
40	92.00	28.70

Figure 3.20. Data entered in the Pools worksheet with modified minimum pool height for example 1.

3.4 Example 2 – Concrete gravity dam with silt loading and anchor force

For this example, GDLAD_Sloping_Base will analyze the sliding stability of the concrete gravity dam under the influence of silt pressures, as in example 1; however, this example considers the addition of post-tensioned (PT) anchors. With this in mind, refer to sections 3.3.1 thru 3.3.5 and 3.3.7 for examples of data entry to the XYCoords, Plot, Pools, Silt, and Analysis worksheets.

3.4.1 Anchors worksheet

For example 2, the mean working anchor force will be set to 35,000 lb and the standard deviation to 3,500 lb and the defaults for the other parameters will be accepted. The following data can be seen in Figure 3.23:
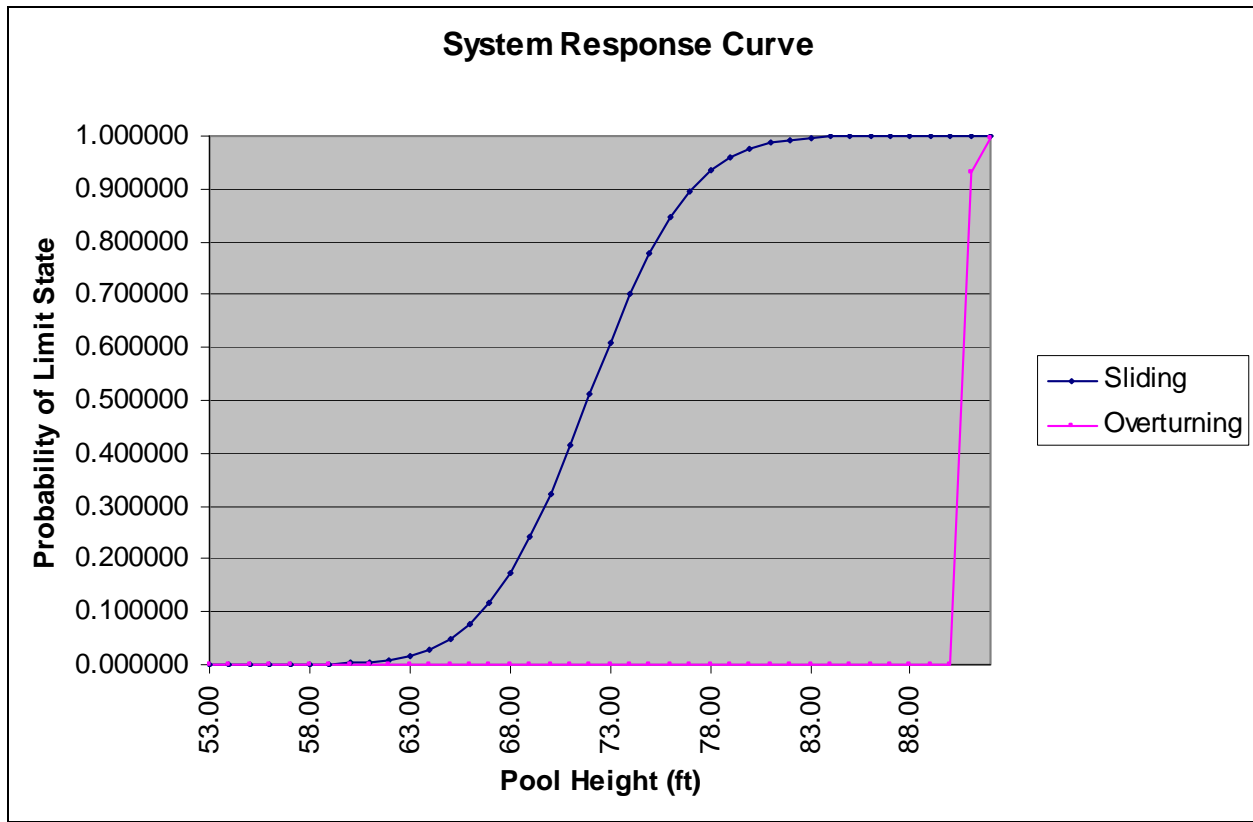
Figure 3.21. Results of the SRC worksheet with modified minimum pool height of 53 ft for example 1.

- Number of Anchors per Group = 12
- Spacing of Anchor Groups = 25
- $Y_{Anchors\text{-}Toe}$ = 82
- $X_{Anchors\text{-}Toe}$ = 82
- Angle (θ) = 90
- A_f *(Mean)* – Load per Anchor = 35,000
- Standard Deviation = 3,500
- Probability Distribution Type = Bounded Normal

The **Calculate** button can be selected at this time to preview the resultant, horizontal, and vertical anchor forces and moment caused by the anchor forces.

Example 2 will now be run on the Analysis worksheet. Note: changes have been made to the Anchors worksheet only. The minimum pool height is 53 ft with a total of 40 pool heights (see section 3.3.8).
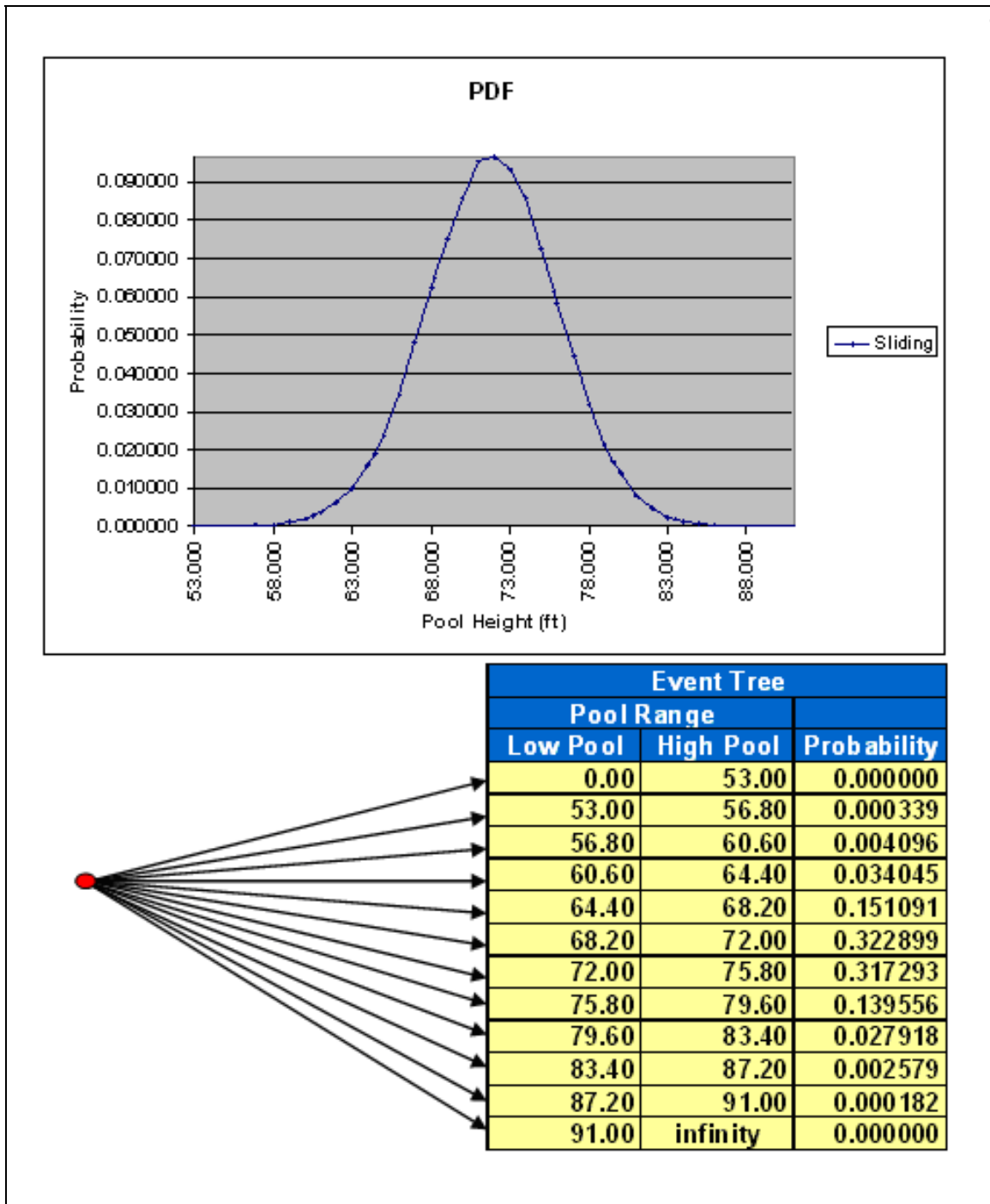
Figure 3.22. Results of the PDF worksheet with modified minimum pool height of 53 ft for example 1.
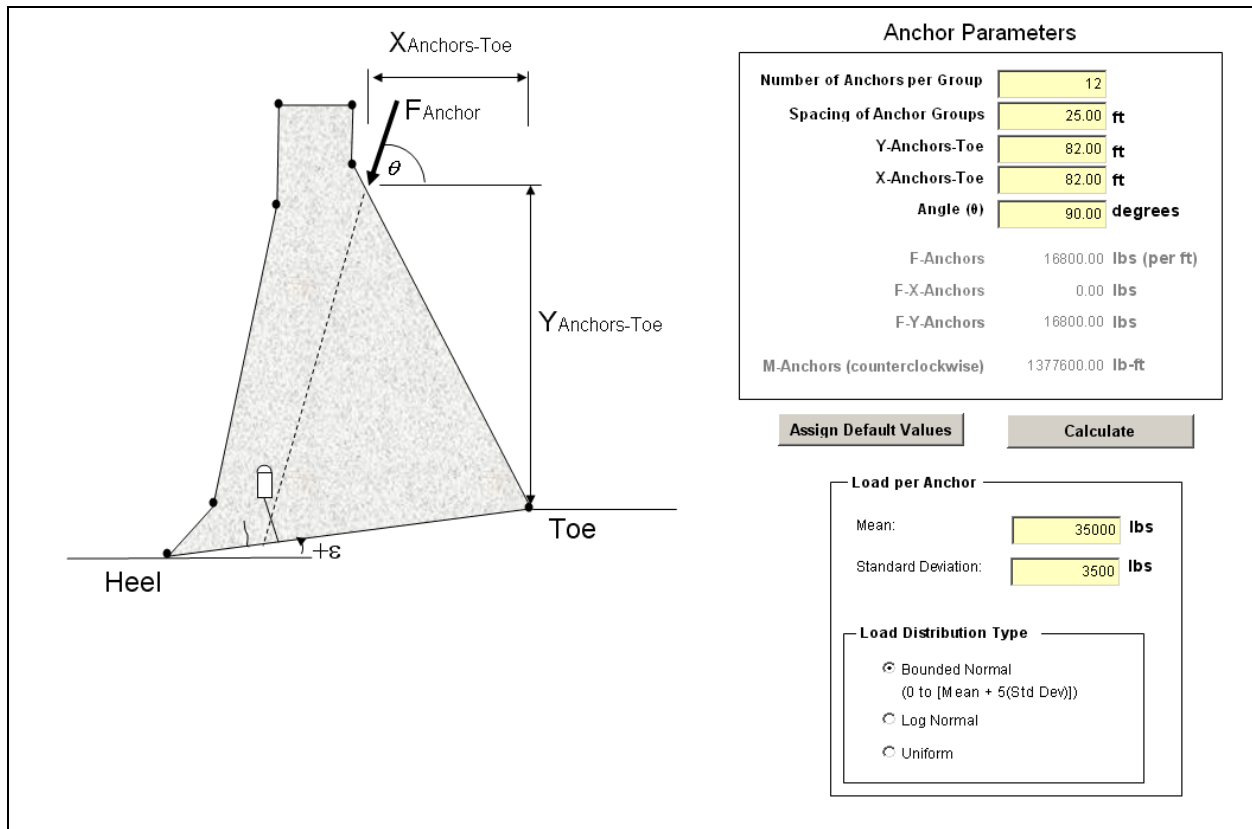
Figure 3.23. Results of the Anchors worksheet for example 2.

3.4.2 SRC, PDF, and event tree results for example 2

From the SRCs in Figure 3.24, at about a pool height of 72 ft, there is a 37 percent probability of a sliding limit state. At the pool height of approximately 85 ft, there is 100 percent probability of a sliding limit state.

Note that overturning stability was also evaluated for these pool elevations, but with the addition of the PT anchors, there is zero probability of overturning as shown in Figure 3.24 for this concrete gravity dam cross-section example problem.

The PDF and the event tree are presented in the PDF worksheet, both shown in Figure 3.25 for this second example.

System Response Curve
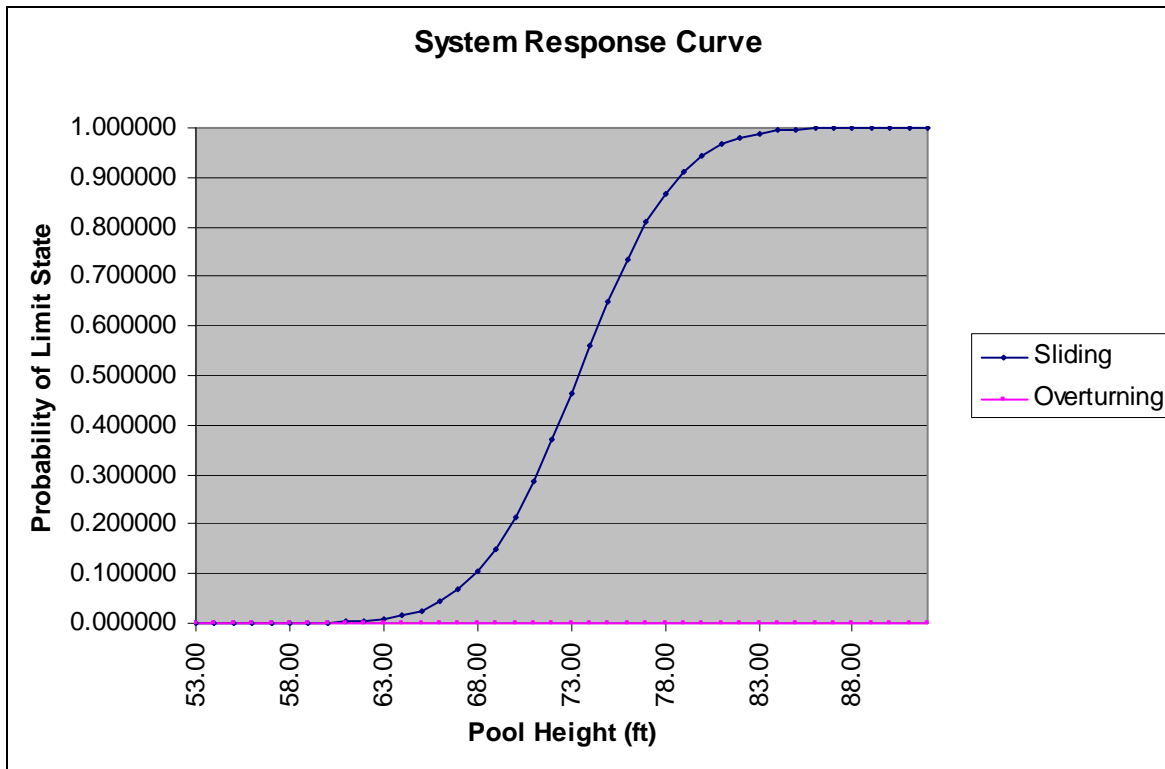
Figure 3.24. SRCs for example 2.

3.5 Comparison of SRCs from examples 1 and 2

This section shows a comparison of two SRCs derived from the previous two examples described in sections 3.3 and 3.4. As can be seen from Figure 3.26, at a pool height of 72 ft, the probability of the sliding limit state decreased from 51 percent to 37 percent with the addition of PT anchors.
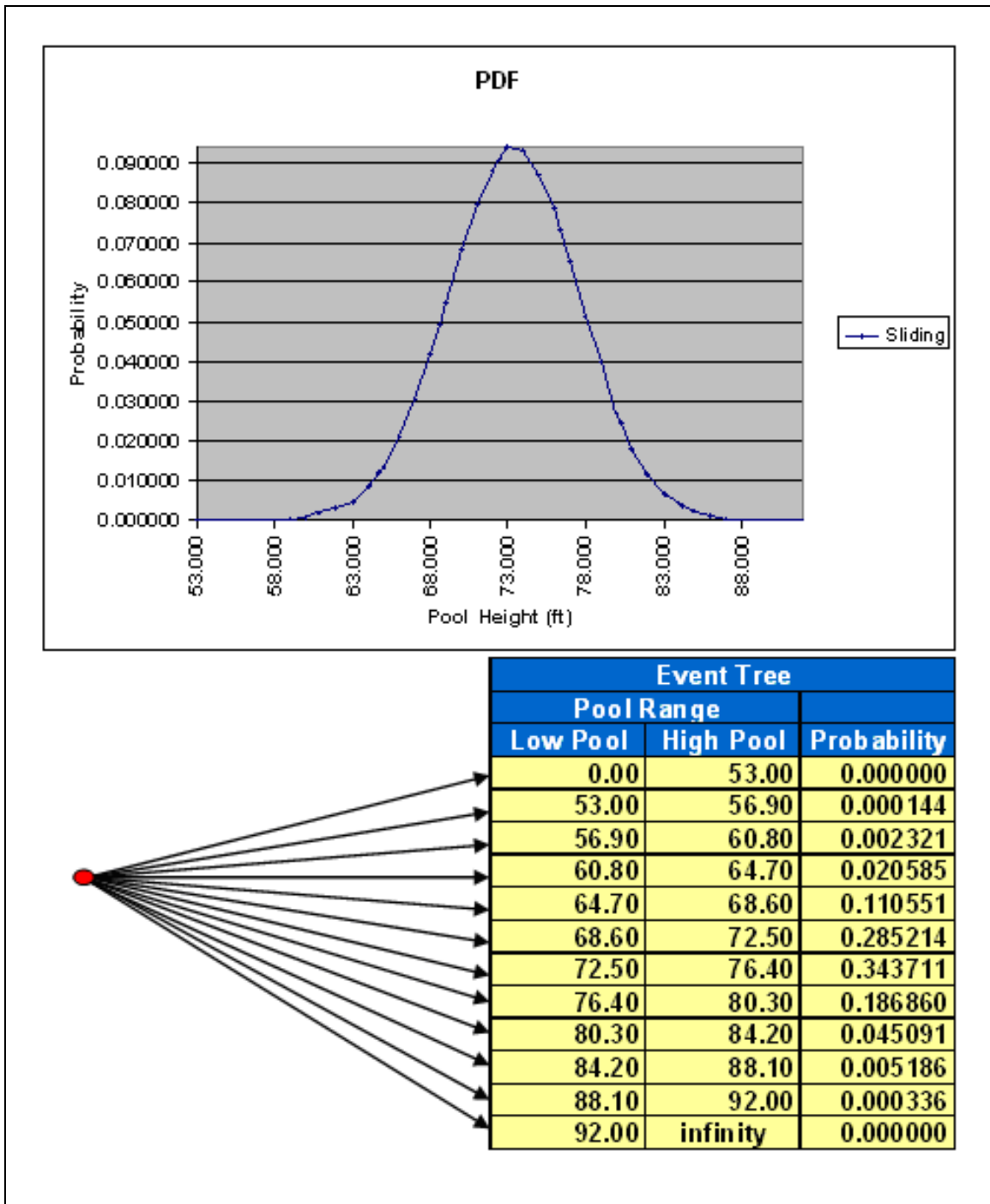
Figure 3.25. PDF curve for example 2.
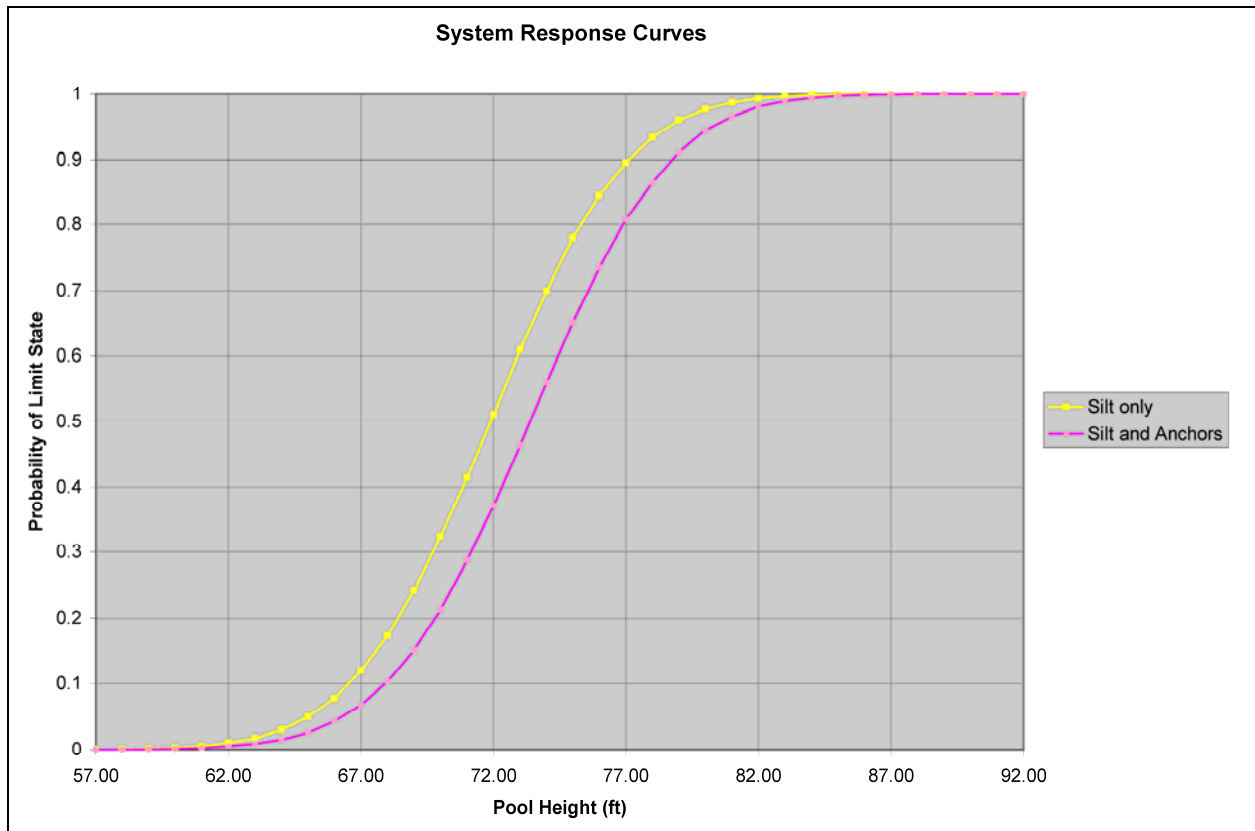
Figure 3.26. SRCs for examples 1 and 2.

4   Summary, Conclusions, and Recommendations

4.1 Summary and conclusions

This report describes one method of a probabilistic analysis used to formally and explicitly account for the uncertainty in the analysis by expressing the computed stability results in terms of fragility curves for the potential modes of failure (e.g., sliding, overturning, etc.). Within the U.S. Army Corps of Engineers the term *system response curve* (SRC) is now being introduced to describe what is commonly referred to in the technical literature as the fragility curve; the term is used for the hydrologic fragility assessment of rock-founded concrete gravity dams.

This report also describes the engineering formulation and corresponding PC-based software, named GDLAD_Sloping_Base, which is used to compute SRCs for a two-dimensional cross section of a gravity dam founded on a sloping rock base. GDLAD is an acronym for Gravity Dam Layout and Design.

The SRC is used to predict the probably of dam failure, given the hydraulic hazard. Consider the example of a dam in which the sliding limit state, i.e., $FS_{slide} \leq 1.0$, is the limit state resulting in failure of the dam. Then the probability of failure $P_{failure}$ of the dam for pools less than or equal to a specific H_{Pool}, height of pool, i.e., Pool $\leq H_{Pool}$, is expressed by the product terms

$$P_{failure} = P\left(FS_{slide} \leq 1.0 \mid Pool = H_{Pool}\right) \bullet P\left(Pool = H_{Pool}\right) \quad \text{(bis 1.1)}$$

where the first probability term is derived from the SRC developed using the engineering procedure and corresponding PC-based software discussed in this report and the second probability term is the hydraulic hazard expressed as an annual probability. The second probability term comes from a separate analysis of the hydraulic hazard for the dam, considering channel inflows and storm runoff from the watershed behind the dam.

4.2 Recommendations for updates and future research

Current unit capabilities are for inch-pound units with force expressed in pounds and lengths expressed in feet or inches. A future update would be to expand GDLAD_Sloping_Base to SI units.

One recommendation for future research would be to expand the limit states for which SRCs are computed to the evaluation of the probability of a rock bearing capacity failure. Another recommendation for future research is to expand the general formulation described in this report to gravity dams founded within rock.

References

Beer, F. P., E. R. Johnston, Jr., E. R. Eisenberg, W. E. Clausen, and G. H. Staab. 2004. *Vector mechanics for engineers: Statics and dynamics*, 7th Edition. New York: McGraw-Hill.

Bourke, P. 1988. Calculating the area and centroid of a polygon. 7 Mar 2008. http://local.wasp.uwa.edu.au/~pbourke/geometry/polyarea/.

Ebeling, R. M., L. K. Nuss, F. T. Tracy, and B. Brand. 2000. *Evaluation and comparison of stability analysis and uplift criteria for concrete gravity dams by three federal agencies*. ERDC/ITL TR-00-1. Vicksburg, MS: U.S. Army Engineer Research and Development Center.

Headquarters, U.S. Army Corps of Engineers.1995. *Gravity dam design*. EM-1110-2-2200. Washington, DC.

_____. 2005. Stability analysis of concrete structures. EM-1110-2-2100. Washington, DC.

Iman, R. L., and W. J. Conover. 1982. A distribution-free approach to inducing rank correlation among input variables. *Communications in Statistics* B11(3):311–334.

Li, Y.-M., and J. Zhang. 1997. Centroid, area, and moments of inertia for laminas. Accessed 14 Mar 2008, http://www.infogoaround.org/JBook/Inertia.html.

Press, W. H., S. A. Teukolsky, W. T. Vetterling, and B. P. Flannery. 1996. *Numerical recipes in FORTRAN 90: The art of parallel scientific computing*. 2nd ed. New York: Cambridge University Press.

Tekie, P. B., and B. R. Ellingwood. 2002. *Fragility analysis of concrete gravity dams*. ERDC/ITL TR-02-6. Vicksburg, MS: U.S. Army Engineer Research and Development Center.

Wikipedia. 2008. Second moment of area. Wikimedia Foundation, Inc. Accessed 4 Mar 2008. http://en.wikipedia.org/wiki/Second_moment_of_area.

Appendix A: Area, Centroid, Moment of Inertia, and Mass Moment of Inertia

A.1 Applying Green's theorem to a composite closed curve

Determining the areas of irregular objects is a common and important problem in engineering applications. This section describes the basic algorithm implemented in GDLAD_Sloping_Base. The algorithm is based on the more general Green's theorem and works for a simple closed curve that does not intersect itself. It is used in GDLAD_Sloping_Base for determining the areas of the gross dam cross section, pool water, silt region, and tailwater. Basic geometric shapes of a rectangle or a rectangle and a half-circle are used to define the gallery. The net area of the dam is the gross dam area less the area of the gallery.

Consider the problem of measuring the area of the composite polygon in Figure A1. This polygon represents the gross dam cross-sectional area and includes the area of the gallery.

For the given concrete gravity dam geometry, the six point coordinates identifying the composition of the dam are defined in a clockwise manner in the global coordinate system when specified as input to GDLAD_Sloping_Base (see example in Chapter 3). The first point specified is at the heel and the last point specified is at the toe. However, for the algorithms used in this appendix a new "local coordinate system" and a new point reference numbering order are specified. In this local coordinate system, the points start at the toe and are specified in a counterclockwise manner around the geometry of the dam.

The global X- and Y-coordinates are temporarily shifted to a "local coordinate system" contained within the first quadrant by subtracting the Min-X value from all X-coordinates and by subtracting the Min-Y value from all Y-coordinates for application of the Green's theorem area computations. This coordinate shift and counterclockwise point locations are shown in Figure A2. Upon completion of these computations, the calculated resultant parameters are translated back to the global X- and Y-coordinates system by adding Min-X and Min-Y, respectively. Note that in this appendix, the equations refer to points defined in this "local" coordinate system.
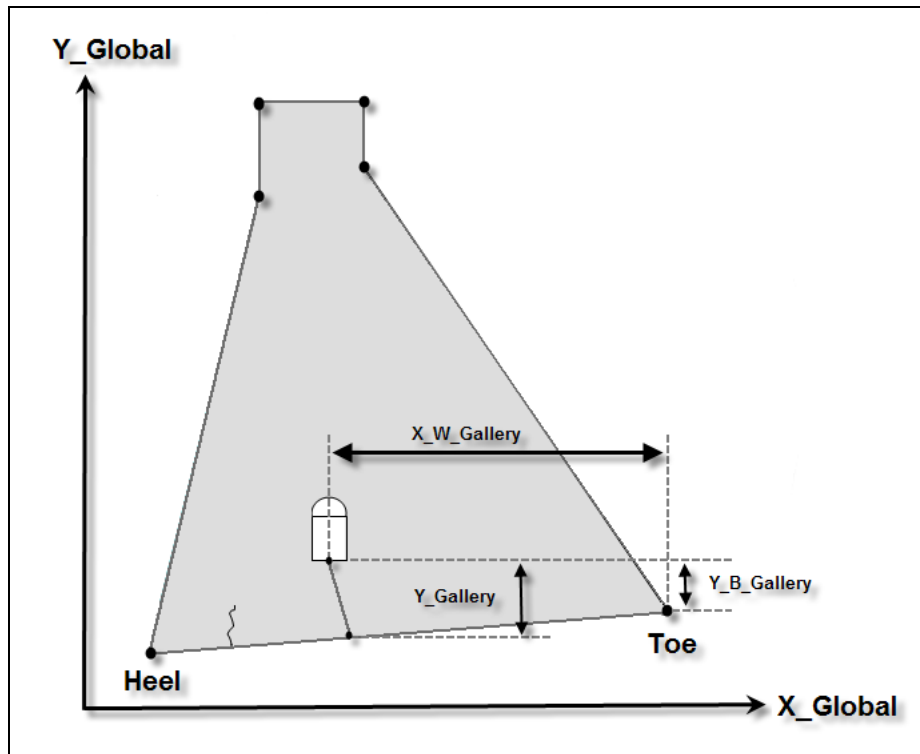
Figure A1. A concrete gravity dam geometry defined by six points in the global coordinate system.
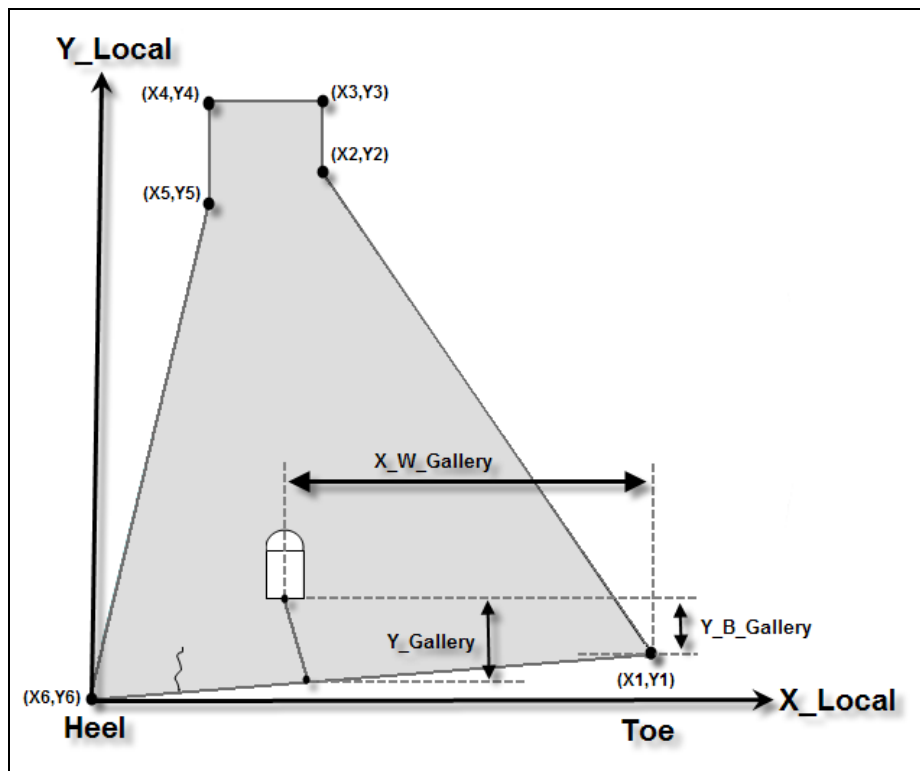
Figure A2. A concrete gravity dam geometry defined by six points in a counterclockwise manner in the local coordinate system.

It can be shown that the area of a solid polygon can be determined by dividing the polygon into trapezoids. The gross area (total area of the dam, which includes the area occupied by the gallery) can then be expressed as the sum of the areas of the trapezoids as

$$A_d = \frac{1}{2}\sum_{i=1}^{n}\left[\left(Y_{i+1} + Y_i\right) \bullet \left(X_{i+1} - X_i\right)\right] \tag{A1}$$

With further algebraic simplification, the gross area of the dam A_d can be defined as one-half the summation of the difference of two product terms for each polygon (Bourke 1988)[1]

$$A_d = \frac{1}{2}\sum_{i=1}^{n}\left(X_i Y_{i+1} - X_{i+1} Y_i\right) \tag{A2}$$

Equation A2 is used in GDLAD_Sloping_Base to compute the gross dam cross-sectional area. For the dam shown in Figure A2 (local coordinate system), n is equal to 6 and the (i) and (i + 1) points are specified in the following in counterclockwise order: 1, 2, 3, 4, 5, 6, and 1.

A.1.1 The centroid of dam (center of mass)

The position of the centroid of the gross dam in the local coordinate system, assuming the polygon is made of concrete having a uniform density (Bourke 1988), is given by

$$C_{x\_d} = \frac{1}{6A_d}\sum_{i=1}^{n}\left[\left(X_i + X_{i+1}\right) \bullet \left(X_i Y_{i+1} - X_{i+1} Y_i\right)\right] \tag{A3}$$

$$C_{y\_d} = \frac{1}{6A_d}\sum_{i=1}^{n}\left[\left(Y_i + Y_{i+1}\right) \bullet \left(X_i Y_{i+1} - X_{i+1} Y_i\right)\right] \tag{A4}$$

where A_d is computed using Equation A2.

For the dam shown in Figure A2 (local coordinate system), n is equal to 6 and the (i) and (i + 1) points are specified (counterclockwise) in the following order: 1, 2, 3, 4, 5, 6, and 1.

---

[1] References cited in this appendix are listed in the References section at the end of the main text.

A.1.2 The moment of inertia of the gross dam (second moment of area)

The x- and y-moments of inertia (i.e., second moment of area) about the x- and y-axis, respectively, of the gross dam area are defined (*Wikipedia 2008*) as follows:

$$I_{x\_d} = \frac{1}{12}\sum_{i=1}^{n}\left[\left(Y_i^2 + Y_{i+1}Y_i + Y_{i+1}^2\right)\bullet\left(X_iY_{i+1} - X_{i+1}Y_i\right)\right] \tag{A5}$$

$$I_{y\_d} = \frac{1}{12}\sum_{i=1}^{n}\left[\left(X_i^2 + X_{i+1}X_i + X_{i+1}^2\right)\bullet\left(X_iY_{i+1} - X_{i+1}Y_i\right)\right] \tag{A6}$$

For the dam shown in Figure A2 (local coordinate system), n is equal to 6 and the (i) and ($i + 1$) points are specified (counterclockwise) in the following order; 1, 2, 3, 4, 5, 6, and 1. Note that these two second moments of inertia or moments of area are computed about the local x- and y-axes, respectively, of Figure A2.

The moments of inertia about the centroid of the gross dam can be computed from the parallel axis theorem and Equations A5 and A6

$$I_{x\_d\_cg} = I_{x\_d} - A_d \bullet \left(C_{y\_d}\right)^2 \tag{A7}$$

$$I_{y\_d\_cg} = I_{y\_d} - A_d \bullet \left(C_{x\_d}\right)^2 \tag{A8}$$

Applying the parallel axis theorem a second time, the moment of inertia of the gross dam about the toe of the dam can be determined. The x- and y-components are calculated in Equations A9 and A10:

$$I_{xx\_d} = I_{x\_d\_cg} + A_d \bullet \left(ytoe_{local} - C_{y\_d}\right)^2 \tag{A9}$$

$$I_{yy\_d} = I_{y\_d\_cg} + A_d \bullet \left(xtoe_{local} - C_{x\_d}\right)^2 \tag{A10}$$

where A_d is computed using Equation A2, $xtoe_{local}$ is x-component at the toe of the dam in local coordinates, and $ytoe_{local}$ is y-component at the toe of the dam in local coordinates.

The expressions of Equations A2 through A6 were compared to alternate numerical algorithms (Li and Zhang 1997) for verification of results.

A.2 The component areas of the gallery

The gallery is made up of two objects, a rectangle and a semicircle (Figure A3). The area, centroid, and moments of inertia will be calculated for both separately.
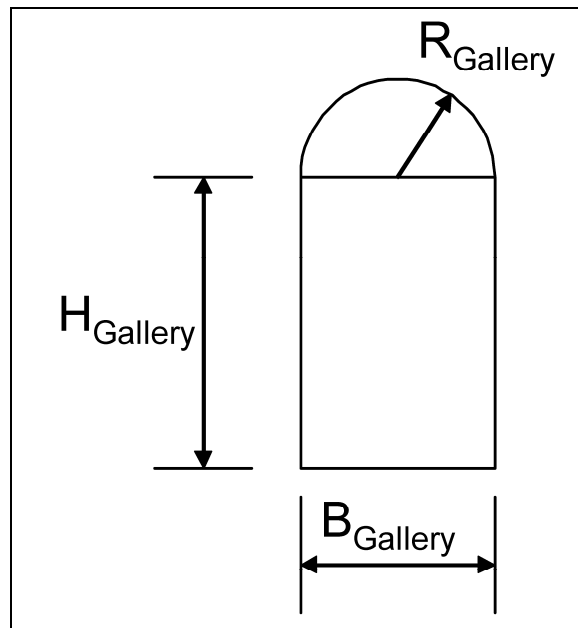
Figure A3. The gallery of the concrete gravity dam.

The equations for the individual areas can be found in various mathematic texts as

$$A_r = H\_Gallery \bullet B\_Gallery \qquad (A11)$$

$$A_{sc} = \frac{\pi \bullet R\_Gallery^2}{2} \qquad (A12)$$

where:

$$
\begin{aligned}
A_r &= \text{area of the rectangle} \\
H\_Gallery &= \text{height of rectangle} \\
B\_Gallery &= \text{base of rectangle} \\
A_{sc} &= \text{area of the semicircle} \\
R\_Gallery &= \text{radius of semicircle.}
\end{aligned}
$$

Should the gallery be rectangular, the radius of the gallery is set equal to zero in GDLAD_Sloping_Base. The area of the gallery ($A_{gallery}$) is the sum of the area of the rectangle and the area of a semicircle, and the weight of the gallery ($W_{gallery}$) is the product of the area and its unit weight ($\gamma_{concrete}$).

$$A_{gallery} = A_r + A_{sc} \tag{A13}$$

$$W_{gallery} = A_{gallery} \bullet \gamma_{concrete} \tag{A14}$$

Since in actuality the gallery is hollow, this weight of gallery is used in a later section to compute the net weight of the dam (gross weight of dam less the weight of gallery by Equation A14).

A.2.1 The centroid of the gallery (center of mass)

The centroid of the gallery is obtained by first finding the centroids of the rectangle and semicircle separately. The centroids for the two shapes can be readily obtained from vector mechanics texts, including Beer et al. (2004).

The centroid for the rectangle in the local coordinate system is expressed as

$$C_{x\_r} = xtoe_{local} - X\_W\_Gallery \tag{A15}$$

$$C_{y\_r} = ytoe_{local} + Y\_B\_Gallery + \frac{H\_Gallery}{2} \tag{A16}$$

The centroid for the semicircle in the local coordinate system can also be expressed as

$$C_{x\_sc} = xtoe_{local} - X\_W\_Gallery \tag{A17}$$

$$C_{y\_sc} = ytoe_{local} + Y\_B\_Gallery + H\_Gallery \tag{A18}$$

$$+ \frac{4 \bullet R\_Gallery}{3\pi}$$

with variables for Equations A15 through A18 described as

$$
\begin{aligned}
xtoe_{local} &= \text{local x-coordinate of the toe (=X1 in Figure A2)} \\
X\_W\_Gallery &= \text{x-distance to center of gallery from toe} \\
ytoe_{local} &= \text{local y-coordinate of the toe (=Y1 in Figure A2)} \\
Y\_B\_Gallery &= \text{y-distance from base of gallery to y-coordinate of the} \\
&\quad\ \ \text{toe} \\
H\_Gallery &= \text{height of rectangle} \\
R\_Gallery &= \text{radius of semicircle.}
\end{aligned}
$$

The centroid of the gallery in the local coordinate system can then be determined as follows:

$$
C_{x\_g} = \frac{\left(C_{x\_r} \bullet A_r\right) + \left(C_{x\_sc} \bullet A_{sc}\right)}{A_{gallery}} \tag{A19}
$$

$$
C_{y\_g} = \frac{\left(C_{y\_r} \bullet A_r\right) + \left(C_{y\_sc} \bullet A_{sc}\right)}{A_{gallery}} \tag{A20}
$$

A.2.2 The moment of inertia of the gallery (second moment of area)

The moment of inertia about each centroid (rectangle and semicircle) can be shown as discussed in the following paragraphs:

The moment of inertia for the rectangle about the rectangle's centroid is expressed as

$$
I_{x\_r} = \frac{B\_Gallery \bullet H\_Gallery^3}{12} \tag{A21}
$$

$$
I_{y\_r} = \frac{B\_Gallery^3 \bullet H\_Gallery}{12} \tag{A22}
$$

The moment of inertia for the semicircle about its centroid is expressed as

$$
I_{x\_sc} = \left[\frac{\left(9\pi^2\right) - 64}{72\pi}\right] R\_Gallery^4 \tag{A23}
$$

$$I_{y\_sc} = \frac{\pi \bullet R\_Gallery^4}{8} \tag{A24}$$

where:

$B\_Gallery$ = base of the rectangle
$H\_Gallery$ = height of the rectangle
$R\_Gallery$ = radius of the semicircle.

The moment of inertia of the individual rectangle and semicircle of the gallery about the toe of the dam can be computed from the parallel axis theorem. The x- and y-moments of inertia are defined for both the rectangle and semicircle in local coordinates as follows:

- The moment of inertia of the rectangular portion of the gallery is computed as

$$I_{xx\_r} = I_{x\_r} + A_r \bullet \left(ytoe_{local} - C_{y\_r} \right)^2 \tag{A25}$$

$$I_{yy\_r} = I_{y\_r} + A_r \bullet \left(xtoe_{local} - C_{x\_r} \right)^2 \tag{A26}$$

- The moment of inertia of the semicircle part of the gallery is computed as

$$I_{xx\_sc} = I_{x\_sc} + A_{sc} \bullet \left(ytoe_{local} - C_{y\_sc} \right)^2 \tag{A27}$$

$$I_{yy\_sc} = I_{y\_sc} + A_{sc} \bullet \left(xtoe_{local} - C_{x\_sc} \right)^2 \tag{A28}$$

where:

$xtoe_{local}$ = x-component at the toe of the dam in local coordinates
$ytoe_{local}$ = y-component at the toe of the dam in local coordinates.

A.3 The net area and weight of dam

The net area A_{dam} and net weight of the dam W_{dam} is calculated, with $A_{gallery}$ determined from Equation A13 and A_d from Equation A2, as follows:

$$A_{dam} = A_d - A_{gallery} \tag{A29}$$

$$W_{dam} = A_{dam} \bullet \gamma_{concrete} \tag{A30}$$

A.3.1 The net centroid of dam

The net centroid of the dam (CG_{x_dam}, CG_{y_dam}) is then calculated and translated back to global coordinates by adding the x- and y-min offsets (section A.1) as follows:

$$CG_{x\_dam} = \left\{ \frac{C_{x\_d} \bullet A_d - \left[\left(C_{x\_r} \bullet A_r\right) + \left(C_{x\_sc} \bullet A_{sc}\right)\right]}{A_{dam}} \right\} + x\_\min \tag{A31}$$

$$CG_{y\_dam} = \left\{ \frac{C_{y\_d} \bullet A_d - \left[\left(C_{y\_r} \bullet A_r\right) + \left(C_{y\_sc} \bullet A_{sc}\right)\right]}{A_{dam}} \right\} + y\_\min \tag{A32}$$

A.3.2 The net moment of inertia and mass moment of inertia of dam about its toe

The net moment of inertia of the dam about the toe can be computed as a linear sum of the moment of inertia of the gross dam and the negative moments of inertia of both the rectangle and semicircle (since they are not solid but hollow):

$$I_{xx\_dam} = I_{xx\_d} - I_{xx\_r} - I_{xx\_sc} \tag{A33}$$

$$I_{yy\_dam} = I_{yy\_d} - I_{yy\_r} - I_{yy\_sc} \tag{A34}$$

The mass moment of inertia can then be determined as the product of the area moment of inertia and its mass density.

$$I_{xx\_dam\_mass} = I_{xx\_dam} \bullet \left(\frac{\gamma_{concrete}}{G_{constant}}\right) \tag{A35}$$

$$I_{yy\_dam\_mass} = I_{yy\_dam} \bullet \left(\frac{\gamma_{concrete}}{G_{constant}}\right) \tag{A36}$$

where:

$\gamma_{concrete}$ = unit weight of concrete

$G_{constant}$ = gravitational constant (in consistent units).

The x-distance from the centroid of the dam to the toe of the dam in global coordinates can now be determined as

$$X\_W\_DamToe = xtoe - CG_{x\_dam} \qquad \text{(A37)}$$

where *xtoe* is the x-coordinate of the toe in the global coordinate.

A.3.3 The polar moment of inertia and polar mass moment of inertia of dam about its toe

The polar moment of inertia (about the toe of the dam) is related to the x- and y-moments of inertia as their sum, such that

$$I_{p\_dam} = I_{xx\_dam} + I_{yy\_dam} \qquad \text{(A38)}$$

The polar mass moment of inertia (about the toe of the dam) is related to the x- and y-mass moments of inertia and is computed as their sum, such that

$$I_{p\_dam\_mass} = I_{xx\_dam\_mass} + I_{yy\_dam\_mass} \qquad \text{(A39)}$$

A.4 The area, weight, and centroid of pool

For a given pool elevation, the x- and y-coordinates of the entire pool area can be determined by including all points on the upstream side of the dam, starting at the heel, that have a y-coordinate less than the pool elevation. These x- and y-pool coordinates are calculated in a counterclockwise manner for computing the area of the pool (local coordinate system). The area of the pool A_p, using Equation A2, and the weight of the pool, *W_Pool*, can be determined in local coordinates as

$$A_p = \frac{1}{2}\sum_{i=1}^{n}\left(X_i Y_{i+1} - X_{i+1} Y_i\right) \qquad \text{(A40)}$$

$$W\_Pool = A_p \bullet \gamma_{water} \qquad \text{(A41)}$$

The position of the centroid of the pool can be located with the same points used to compute A_p. The centroid will be determined first using Equations A3 and A4 in local coordinates and then translated back to global coordinates by adding the offset values of x_min and y_min as listed below:

$$CG_{x\_pool} = \left\{ \frac{1}{6A_p} \sum_{i=1}^{n} \left[\left(X_i + X_{i+1}\right) \bullet \left(X_i Y_{i+1} - X_{i+1} Y_i\right) \right] \right\} + x\_\min \quad \text{(A42)}$$

and

$$CG_{y\_pool} = \left\{ \frac{1}{6A_p} \sum_{i=1}^{n} \left[\left(X_y + X_{y+1}\right) \bullet \left(X_i Y_{i+1} - X_{i+1} Y_i\right) \right] \right\} + y\_\min \quad \text{(A43)}$$

The x-distance from the centroid of the pool to the toe of the dam in global coordinates can now be determined as

$$X\_W\_Pool = xtoe - CG_{x\_pool} \quad \text{(A44)}$$

A.5 The area, weight, and centroid of the tailwater

For a given tailwater elevation, the x- and y-coordinates of the entire tailwater area can be determined by including all points on the downstream side of the dam, starting at the toe, that have a y-coordinate less than the tailwater elevation. These x- and y-tailwater coordinates are calculated in a counterclockwise manner for computing the area of the tailwater (local coordinate system). The area A_t and the weight of the tailwater W_Tail can be determined using Equation A2 in local coordinates as

$$A_t = \frac{1}{2} \sum_{i=1}^{n} \left(X_i Y_{i+1} - X_{i+1} Y_i\right) \quad \text{(A45)}$$

$$W\_Tail = A_t \bullet \gamma_{water} \quad \text{(A46)}$$

The position of the centroid of the tailwater can be located with the same points used to compute A_t. The centroid will be determined first using Equations A3 and A4 in local coordinates and then translated back to

global coordinates by adding the offset values of x_min and y_min as listed below:

$$CG_{x\_tail} = \left\{ \frac{1}{6A_t} \sum_{i=1}^{n} \left[(X_i + X_{i+1}) \bullet (X_i Y_{i+1} - X_{i+1} Y_i) \right] \right\} + x\_\min \quad \text{(A47)}$$

and

$$CG_{y\_tail} = \left\{ \frac{1}{6A_t} \sum_{i=1}^{n} \left[(X_y + X_{y+1}) \bullet (X_i Y_{i+1} - X_{i+1} Y_i) \right] \right\} + y\_\min \quad \text{(A48)}$$

The x-distance from the centroid of the tailwater to the toe of the dam in global coordinates can now be determined as

$$X\_W\_Tail = xtoe - CG_{x\_tail} \quad \text{(A49)}$$

A.6 The area and effective weight of silt

The computation of the effective weight of silt acting on the upstream, inclined face of the gravity dam can be described as one of two cases: Case I is where the silt is fully submerged, and Case II is where the silt is partially submerged with the submerged part residing below the same plane as the pool water and the remainder of the moist silt located above the pool water. In both cases a portion of the total weight of silt is already accounted for by the weight of water below the pool (see section A.4).

A.6.1 Case I. The silt is fully submerged (*H_Silt < H_Pool*)

For a given silt elevation (H_Silt), the x- and y-coordinates of the entire silt area can be determined by including all points of the upstream side of the dam, starting at the heel, that have a y-coordinate less than H_Silt. The area A_{silt} and weight W_Silt of the effective silt can be determined from Equation A2 in local coordinates as

$$A_{silt} = \frac{1}{2} \sum_{i=1}^{n} (X_i Y_{i+1} - X_{i+1} Y_i) \quad \text{(A50)}$$

$$W\_Silt = A_{silt} \bullet (\gamma_{saturated} - \gamma_{water}) \quad \text{(A51)}$$

with

A_{silt} = area of saturated silt
W_Silt = effective weight of saturated silt
$\gamma_{saturated}$ = unit weight of saturated silt
γ_{water} = unit weight of water.

The second term in Equation A51, $\left(\gamma_{saturated} - \gamma_{water}\right)$, is equal to the buoyant unit weight of silt. The sum of W_Pool by Equation A41 and W_Silt by Equation A51 equals the total weight of silt acting on the upstream, inclined face of the gravity dam when the silt is fully submerged.

A.6.2 Case II. The silt is partially submerged ($H\_Silt > H\_Pool$)

Given that the silt is partially submerged, consider two regions of silt. One region measures from the heel of the dam to the height of the pool, and the other region measures from height of the pool to the height of the silt. If the height of the silt is greater then the height of the dam, then the weights and areas will be calculated up to the height of the dam.

The area and weight computations for the submerged silt or region one (i.e., the buoyant weight portion) are designated as A_s and $W\_Silt\_Saturated$ with the maximum y-component at H_Pool (see Figure 1.1). Please note that the area of the saturated part of the silt will be equal to the area of the pool (Equation A40), such that

$$A_s = A_p \tag{A52}$$

$$W\_Silt\_Saturated = A_s \bullet \left(\gamma_{saturated} - \gamma_{water}\right) \tag{A53}$$

For the second region ($H\_Silt > H\_Pool$), all points starting at H_Pool up to H_Silt at the upstream side of the dam will be included. The area and weight of the moist silt can also be determined by Equation A2 (local coordinate system), such that

$$A_m = \frac{1}{2}\sum_{i=1}^{n}\left(X_i Y_{i+1} - X_{i+1} Y_i\right) \tag{A54}$$

$$W\_Silt\_Moist = A_m \bullet \gamma_m \tag{A55}$$

with

$$A_m = \text{area of moist silt}$$
$$W\_Silt\_Moist = \text{effective weight of moist silt}$$
$$\gamma_m = \text{unit weight of moist silt (above the pool elevation).}$$

The sum of *W_Pool* by Equation A41, *W_Silt_Saturated* by Equation A53, and *W_Silt_Moist* by Equation A55 equals the total weight of saturated and moist silt acting on the upstream, inclined face of the gravity dam when the silt is partially submerged.

A.7 The centroid of effective silt (center of mass)

The computation of the effective weight of silt acting on the upstream, inclined face of the gravity dam can be described as one of two cases: Case I is where the silt is fully submerged, and Case II is where the silt is partially submerged, with the submerged part residing below the same plane as the pool water and the remainder of the moist silt located above the pool water. Both cases were described previously in section A.6.

A.7.1 Case I. The silt is fully submerged (*H_Silt* < *H_Pool*)

For a given silt elevation (*H_Silt*), the x- and y-coordinates of the effective weight of the submerged silt can be determined by including all points on the upstream side of the dam, starting at the heel, that have a y-coordinate less than or equal to *H_Silt*. The position of the centroid of the silt can be determined with Equations A3 and A4, in local coordinates, and then translated back to global coordinates by adding the offset values of x_min and y_min, respectively:

$$CG_{x\_silt} = \left\{ \frac{1}{6A_{silt}} \sum_{i=1}^{n} \left[\left(X_i + X_{i+1} \right) \bullet \left(X_i Y_{i+1} - X_{i+1} Y_i \right) \right] \right\} + x\_\min \quad \text{(A56)}$$

and

$$CG_{y\_silt} = \left\{ \frac{1}{6A_{silt}} \sum_{i=1}^{n} \left[\left(X_y + X_{y+1} \right) \bullet \left(X_i Y_{i+1} - X_{i+1} Y_i \right) \right] \right\} + y\_\min \quad \text{(A57)}$$

where *A_silt* was evaluated previously with Equation A50.

The x-distance from the centroid of the saturated silt to the toe of the dam in global coordinates can now be determined as

$$X\_W\_Silt = xtoe - CG_{x\_silt} \tag{A58}$$

A.7.2 Case II. The silt is partially submerged (*H_Silt > H_Pool*)

Given that the silt is partially submerged, consider two regions, the part that is submerged and the moist part that is above the pool. One region measures from the heel of the dam to the height of the pool, and the other region measures from the height of the pool to the height of the silt. If the height of the silt is greater then the height of the dam, then the parameters will be calculated up to the height of the dam.

As mentioned previously in section A.6, the area of the saturated part of the effective silt will be the same as the pool. Following this train of thought, the x-component of the centroid of the saturated silt will be equal to the x-component of the centroid of the pool. From Equation A42, CG_{x_pool} was determined as

$$CG_{x\_silt\_saturated} = CG_{x\_pool} \tag{A59}$$

The x-distance from the centroid of the saturated silt below the pool to the toe of the dam in global coordinates can now be determined as

$$X\_W\_Silt\_Saturated = xtoe - CG_{x\_silt\_saturated} \tag{A60}$$

For the second region (*H_Silt > H_Pool*), all points (y-components) starting at *H_Pool* up to *H_Silt* at the upstream side of the dam were included for the computations of both the area and centroid. The centroid of the moist silt can also be determined by Equation A2 (local coordinate system) and then translated back to global coordinates by adding the offset values of x_min and y_min, respectively, such that

$$CG_{x\_silt\_moist} = \left\{ \frac{1}{6A_m} \sum_{i=1}^{n} [(X_i + X_{i+1}) \bullet (X_i Y_{i+1} - X_{i+1} Y_i)] \right\} \tag{A61}$$

$$+ x\_min$$

and

$$CG_{y\_silt\_moist} = \left\{ \frac{1}{6A_m} \sum_{i=1}^{n} \left[\left(X_y + X_{y+1} \right) \bullet \left(X_i Y_{i+1} - X_{i+1} Y_i \right) \right] \right\}$$

$$+ y\_\min$$

(A62)

where A_m was evaluated previously with Equation A54.

The x-distance from the centroid of the saturated silt to the toe of the dam in global coordinates can now be determined as

$$X\_W\_Silt\_Moist = xtoe - CG_{x\_silt\_moist}$$ (A63)

Appendix B: Non-Site-Specific Uplift Pressure Diagrams and Equations

B.1 Uplift pressure distribution

An essential feature of gravity dams is the inclusion of a line of drains, i.e., individual drains spaced at regular intervals in plan along the axis of the Figure B1 dam, that extend from the gallery into the rock foundation.[1] These drains serve the critical task of intersecting rock faults, fissures and/or joints within the rock foundation through which water flows beneath the footprint of the dam. Functioning drains play a vital role in the stability of the dam by relieving water pressures acting to uplift the dam.

One non-site-specific approach used for characterizing the magnitude of the uplift pressure as well as quantifying the role the drains play in controlling the magnitude of the uplift pressures is by use of a parameter referred to as the effectiveness of the drain E. Drain effectiveness E is expressed as a decimal fraction ranging from 0 to 1.0. A value of $E = 1.0$ corresponds to the case of the drains being fully effective, and a value of $E = 0$ corresponds to the case of the drains being fully clogged and ineffective. Figures B2 through B4 show the uplift pressure distribution for different combinations of base cracking and drain effectiveness using the non-site-specific uplift pressure distribution specified along the sloping base of a gravity-dam-to-foundation interface.

Engineer Manuals 1110-2-2200 and 1110-2-2100 (HQUSACE 1995, 2005) restrict the value of E to no greater than 50 percent ($E = 0.5$).[2] If foundation testing and flow analysis provide supporting justification, the drain effectiveness can be increased beyond 50 percent. The analysis and/or design documentation must contain supporting data to justify the E value used.

---

[1] Note that the weights of the dam, pool, and tailwater are not shown in Figure B1. Please refer to Figure 1.1 for the free-body diagram containing all forces, including these weights. Additionally, no silt loading is shown in Figure B1.

[2] References cited in this appendix are listed in the References section at the end of the main text.
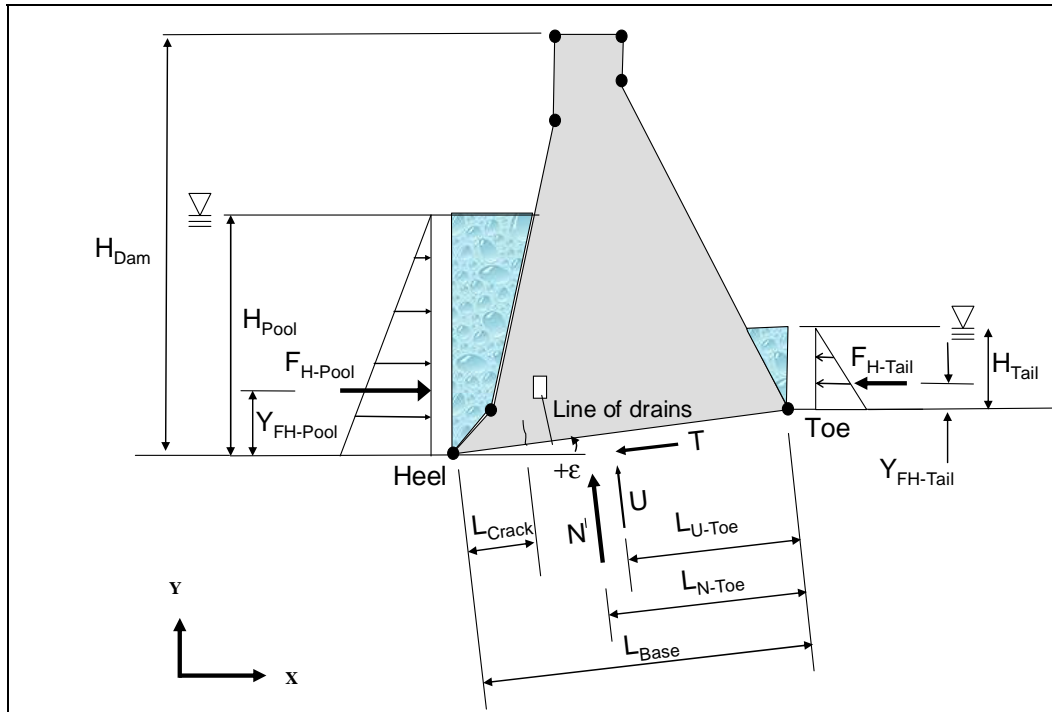
Figure B1. Diagram showing forces acting along the three imaginary boundaries and idealized cross section of a gravity dam with a line of drains – positive base slope ε.
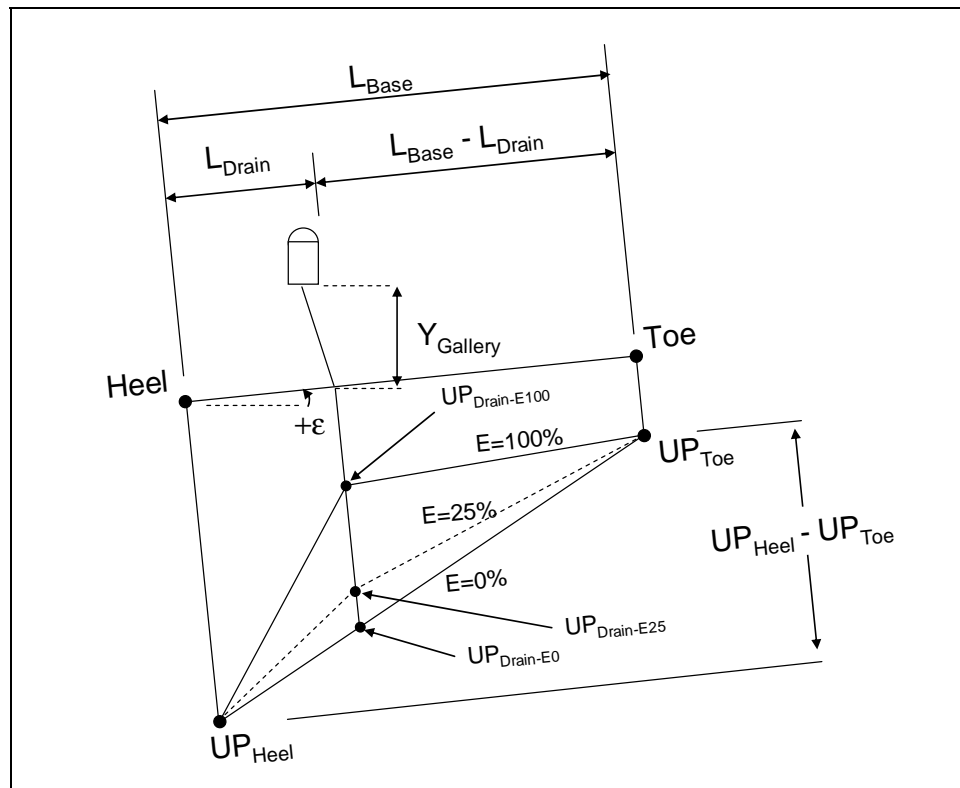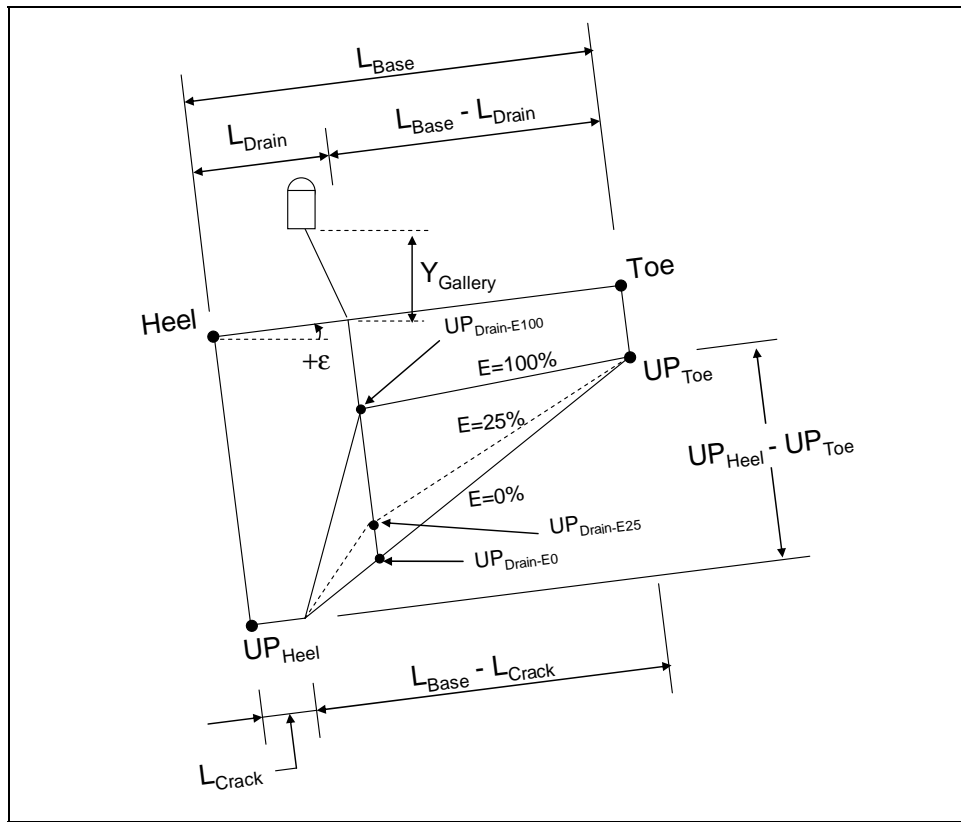

Figure B2. Uplift pressures along a sloping base for L_{Crack} = 0 and $UP_{Drain-E100}$ > UP_{Toe}.

Figure B3. Uplift pressures along a sloping base for $L_{Crack} > 0$ and $UP_{Drain\text{-}E100} > UP_{Toe}$.
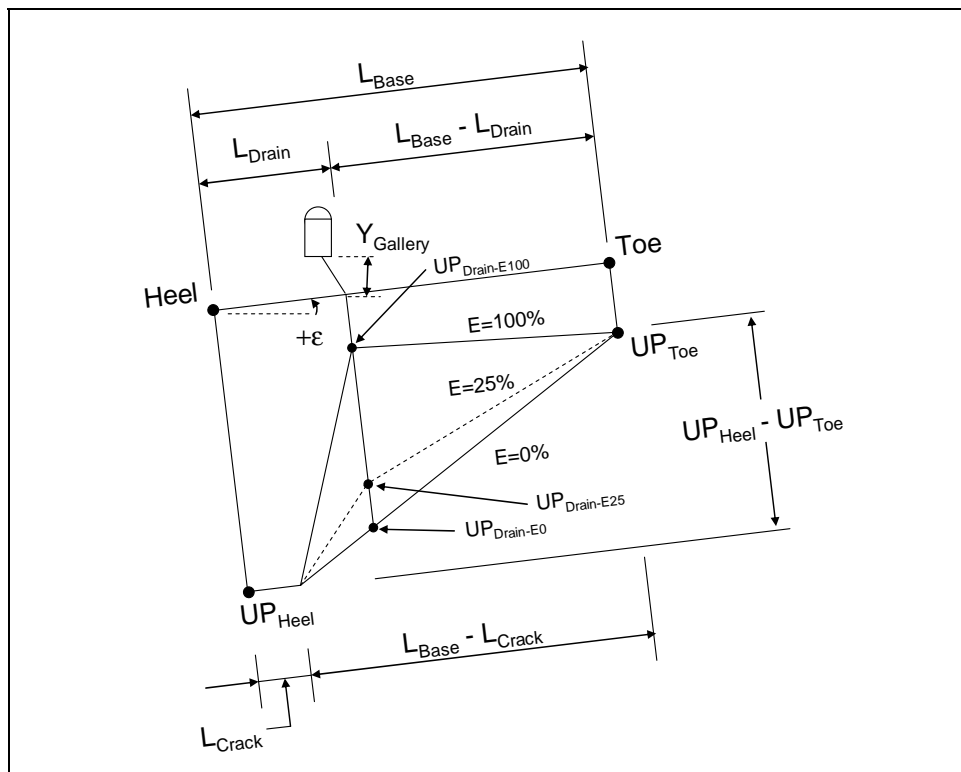

Figure B4. Uplift pressures along a sloping base for $L_{Crack} > 0$ and $UP_{Drain\text{-}E100} \leq UP_{Toe}$.

For a given value for drain effectiveness E, the uplift pressure distribution (dashed line) along the sloping base of a gravity-dam-to-foundation interface will lie between two limiting distributions (solid lines), as shown in Figure B2, for the case of no crack along the base of the dam (i.e., $L_{Crack} = 0$). One limiting uplift pressure distribution is based upon a fully or 100 percent effective drain. The uplift pressure at the drain when the drain is fully effective ($E = 1.0$) is calculated as

$$UP_{Drain-E100} = \gamma_w \bullet Y_{Gallery} \tag{B1}$$

$Y_{Gallery}$ is the vertical distance between the floor of the gallery and the point defined by the intersection of the line of drains and the sloping base for the gravity dam. The other limiting uplift pressure distribution is based upon an ineffective drain. With no crack, i.e., $L_{Crack} = 0$, the uplift pressure at the drain when the drain is clogged and ineffective ($E = 0$) is calculated as

$$UP_{Drain-E0} = UP_{Toe} + \frac{(L_{Base} - L_{Drain})}{L_{Base}} \bullet (UP_{Heel} - UP_{Toe}) \tag{B2}$$

where L_{Base} is the length of the base as measured from the points designated as heel and toe and L_{Drain} is the line of drains (Figure 1.1), with an uplift pressure at the heel of

$$UP_{Heel} = \gamma_w \bullet H_{Pool} \tag{B3}$$

where H_{Pool} is the specific height of pool, and at the toe of

$$UP_{Toe} = \gamma_w \bullet H_{Tail} \tag{B4}$$

The actual uplift pressure for the user-specified E value (expressed in decimal fraction) is given by

$$UP_{Drain-E} = UP_{Drain-E100} + (1 - E) \bullet (UP_{Drain-E0} - UP_{Drain-E100}) \tag{B5}$$

Figure B3 shows an example uplift distribution (dashed line) in the case of a crack extending a distance L_{Crack} from the heel of the dam to a point short of the line of drains (i.e., $L_{Crack} < L_{Drain}$), with $Y_{Gallery} > H_{Tail}$. Note that full hydrostatic water pressures ($= \gamma_w \bullet H_{Pool}$) are specified within the crack.

One limiting uplift pressure distribution is based upon a fully or 100 percent effective drain with $UP_{Drain\text{-}100}$ calculated using Equation B1. The other limiting uplift pressure distribution is based upon an ineffective drain. With $L_{Crack} > 0$ but with $L_{Crack} < L_{Drain}$, the uplift pressure at the drain when the drain is clogged and ineffective ($E = 0$) is calculated as

$$UP_{Drain-E0} = UP_{Toe} + \frac{\left(L_{Base} - L_{Drain}\right)}{\left(L_{Base} - L_{Crack}\right)} \bullet \left(UP_{Heel} - UP_{Toe}\right) \qquad \text{(B6)}$$

with an uplift pressure at the heel and at the toe computed using Equations B3 and B4, respectively. The actual uplift pressure for the user-specified E value (expressed in decimal fraction) is given by Equation B5.

Figure B4 shows an example uplift distribution (dashed line) in the case of a crack extending a distance L_{Crack} from the heel of the dam to a point short of the line of drains (i.e., $L_{Crack} < L_{Drain}$), for a closed drainage system for the gallery, and with $Y_{Gallery} < H_{Tail}$. Again, full hydrostatic water pressures (= $\gamma_w \bullet H_{Pool}$) are specified within the crack. For a discussion on open and closed drainage systems see Appendix A in Ebeling et al. (2000).

One limiting uplift pressure distribution is based upon a fully or 100 percent effective drain with $UP_{Drain\text{-}100}$ calculated using Equation B1. The other limiting uplift pressure distribution is based upon an ineffective drain. With $L_{Crack} > 0$ but with $L_{Crack} < L_{Drain}$, the uplift pressure at the drain when the drain is clogged and ineffective ($E = 0$) is calculated using Equation B6 with an uplift pressure at the heel and at the toe computed using Equations B3 and B4, respectively. The actual uplift pressure for the user-specified E value (expressed in decimal fraction) is given by Equation B5.

The uplift pressure distribution in the case of a crack extending along the sloping base and beyond the line of drains (i.e., $L_{Crack} \geq L_{Drain}$) is discussed in Section B.2.4.

B.2 Drain effectiveness

Four combinations of base cracking and drain effectiveness need to be considered in computing the uplift pressures:

- $L_{Crack} = 0$ and gallery pumped (closed system)
- $UP_{Drain-E} \geq UP_{Toe}$ and $L_{Crack} < L_{Drain}$
- $UP_{Drain-E} \leq UP_{Toe}$ and $L_{Crack} < L_{Drain}$
- $L_{Crack} \geq L_{Drain}$

For a discussion on open systems see Appendix A in Ebeling et al. (2000).

B.2.1 Case 1: L_{Crack} = 0 and gallery pumped (closed system)

Figure B5 shows an idealized cross section with these characteristics.

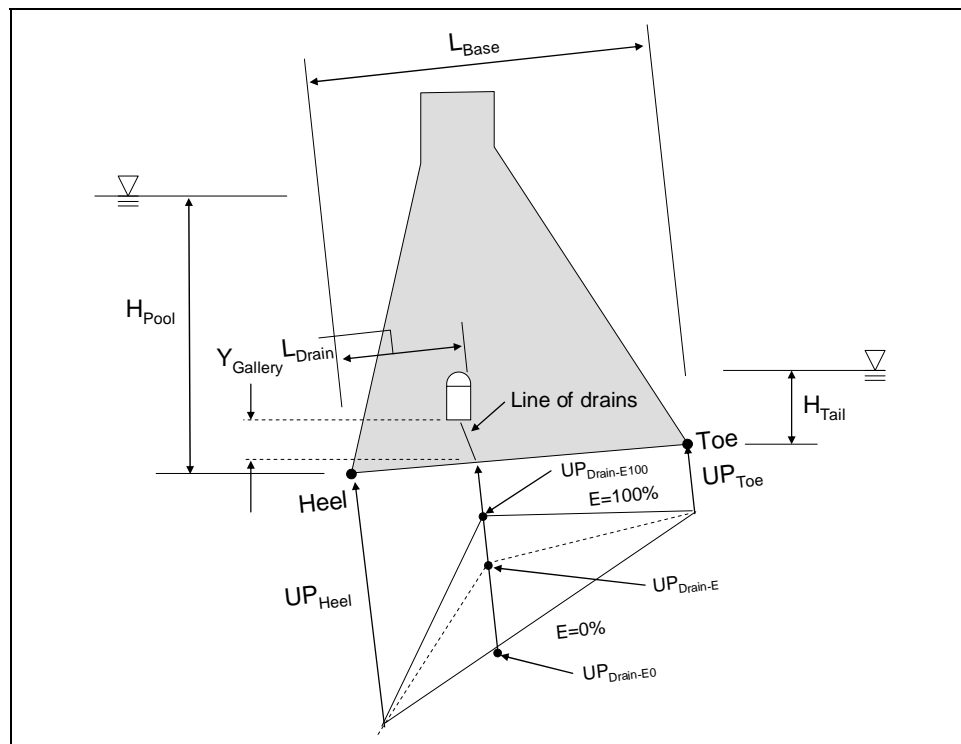Figure B5. Uplift pressures along a sloping base for L_{Crack} = 0 and gallery pumped (closed system).

The Figure B5 (no crack) uplift pressures at three key points along the base are computed as follows:

$$UP_{Drain-E0} = UP_{Toe} + \left(\frac{L_{Base} - L_{Drain}}{L_{Base}} \right) \bullet \left(UP_{Heel} - UP_{Toe} \right) \qquad \text{(bis B2)}$$

$$UP_{Drain-E100} = \gamma_w \bullet Y_{Gallery} \qquad \text{(bis B1)}$$

$$UP_{Drain-E} = UP_{Drain-E100} + (1-E) \bullet (UP_{Drain-E0} - UP_{Drain-E100}) \qquad \text{(bis B5)}$$

The resultant uplift force U and its point of application (refer to Figure B1) are computed using one of the two sets of equations given in Sections B.2.2 and B.2.3 with L_{Crack} set equal to zero. The equations in Section B.2.2 correspond to the case of $Y_{Gallery} > H_{Tail}$, and the equations in Section B.2.3 correspond to the case of $Y_{Gallery} \leq H_{Tail}$.

B.2.2 Case 2: $UP_{Drain-E} \geq UP_{Toe}$ and $L_{Crack} < L_{Drain}$

Figure B6 shows an idealized cross section with these characteristics.
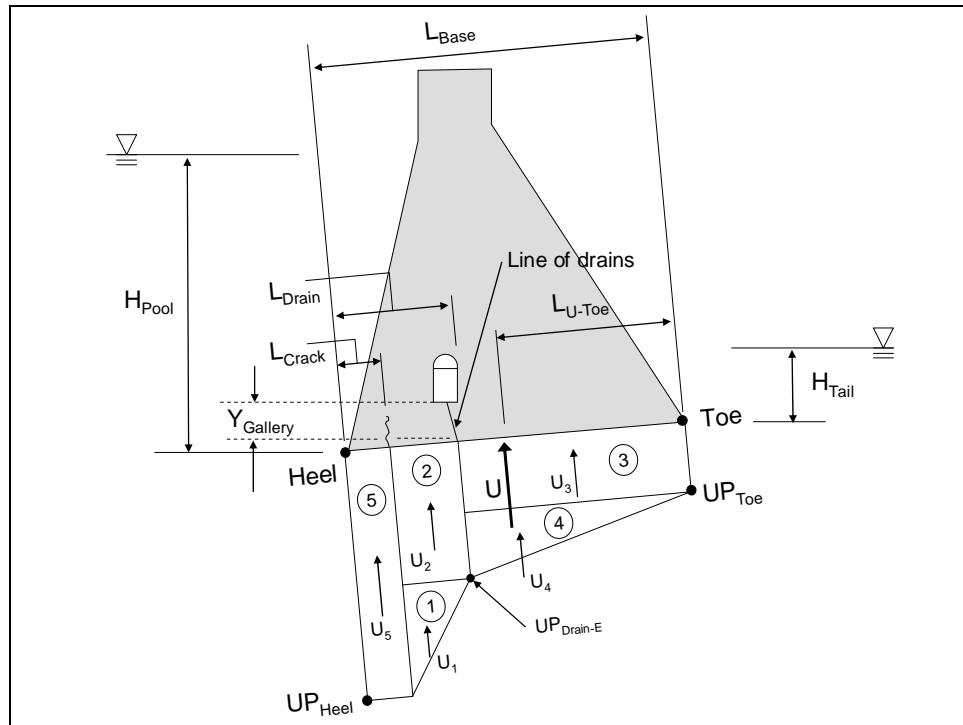
Figure B6. Uplift pressures along a sloping base for the condition
$UP_{Drain-E} \geq UP_{Toe}$ and $L_{Crack} < L_{Drain}$.

The Figure B6 ($L_{Crack} < L_{Drain}$) uplift pressures at three key points along the base are computed as follows:

$$UP_{Drain-E0} = UP_{Toe} + \frac{(L_{Base} - L_{Drain})}{(L_{Base} - L_{Crack})} \bullet (UP_{Heel} - UP_{Toe}) \qquad \text{(bis B6)}$$

$$UP_{Drain-E100} = \gamma_w \bullet Y_{Gallery} \qquad \text{(bis B1)}$$

$$UP_{Drain-E} = UP_{Drain-E100} + (1-E) \bullet (UP_{Drain-E0} - UP_{Drain-E100}) \quad \text{(bis B5)}$$

Referring to Figure B6, the five component uplift pressure resultant forces acting normal to the base with a crack of length L_{Crack} are computed as follows:

$$U_1 = \frac{1}{2} \bullet (L_{Drain} - L_{Crack}) \bullet (UP_{Heel} - UP_{Drain-E}) \quad \text{(B7)}$$

$$U_2 = (L_{Drain} - L_{Crack}) \bullet UP_{Drain-E} \quad \text{(B8)}$$

$$U_3 = (L_{Base} - L_{Drain}) \bullet UP_{Toe} \quad \text{(B9)}$$

$$U_4 = \frac{1}{2} \bullet (L_{Base} - L_{Drain}) \bullet (UP_{Drain-E} - UP_{Toe}) \quad \text{(B10)}$$

$$U_5 = L_{Crack} \bullet UP_{Heel} \quad \text{(B11)}$$

The resultant uplift force normal to the base is computed to be

$$U = [U_1 + U_2 + U_3 + U_4 + U_5] \quad \text{(B12)}$$

Figure B7 shows the position of the component forces U_1 through U_5 relative to the toe.

Referring to Figure B7, the resultant locations are computed as follows:

$$L_{U1} = (L_{Base} - L_{Drain}) + \frac{2}{3} \bullet (L_{Drain} - L_{Crack}) \quad \text{(B13)}$$

$$L_{U2} = (L_{Base} - L_{Drain}) + \frac{1}{2} \bullet (L_{Drain} - L_{Crack}) \quad \text{(B14)}$$

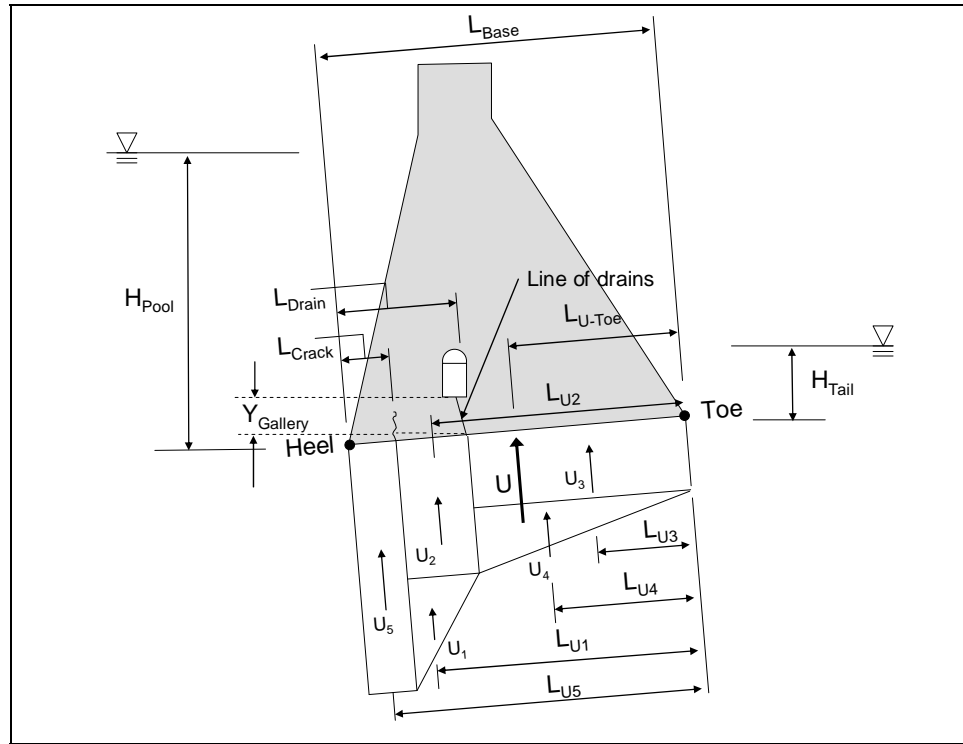$$L_{U3} = \frac{1}{2} \bullet (L_{Base} - L_{Drain}) \quad \text{(B15)}$$

Figure B7. Uplift pressures resultant locations along a sloping base for the condition $UP_{Drain-E} > UP_{Toe}$ and $L_{Crack} < L_{Drain}$.

$$L_{U4} = \frac{2}{3} \bullet \left(L_{Base} - L_{Drain} \right) \tag{B16}$$

$$L_{U5} = L_{Base} - \left(\frac{1}{2} \bullet L_{Crack} \right) \tag{B17}$$

The position of the resultant uplift force normal to the base, relative to the toe, is computed to be

$$L_{U-Toe} = \frac{\left(U_1 \bullet L_{U1} \right) + \left(U_2 \bullet L_{U2} \right) + \left(U_3 \bullet L_{U3} \right) + \left(U_4 \bullet L_{U4} \right) + \left(U_5 \bullet L_{U5} \right)}{U} \tag{B18}$$

B.2.3 Case 3: $UP_{Drain-E} \leq UP_{Toe}$ and $L_{Crack} < L_{Drain}$

Figure B8 shows an idealized cross section with these characteristics.

The Figure B8 ($L_{Crack} < L_{Drain}$) uplift pressures at three key points along the base are computed as follows:
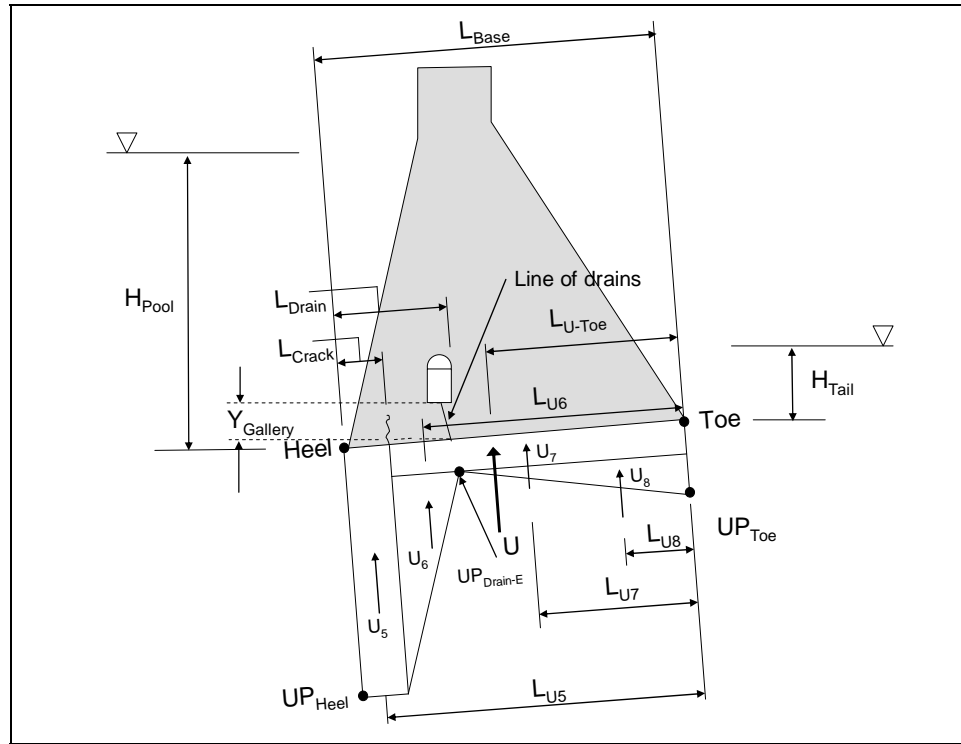
Figure B8. Uplift pressures and resultant locations along a sloping base for the condition $UP_{Drain-E} \leq UP_{Toe}$ and $L_{Crack} < L_{Drain}$.

$$UP_{Drain-E0} = UP_{Toe} + \frac{\left(L_{Base} - L_{Drain}\right)}{\left(L_{Base} - L_{Crack}\right)} \bullet \left(UP_{Heel} - UP_{Toe}\right) \qquad \text{(bis B6)}$$

$$UP_{Drain-E100} = \gamma_w \bullet Y_{Gallery} \qquad \text{(bis B1)}$$

$$UP_{Drain-E} = UP_{Drain-E100} + \left(1 - E\right) \bullet \left(UP_{Drain-E0} - UP_{Drain-E100}\right) \qquad \text{(bis B5)}$$

Referring to Figure B8, the uplift pressure resultant forces acting normal to the base with a crack of length L_{Crack} are computed as follows:

$$U_5 = L_{Crack} \bullet UP_{Heel} \qquad \text{(bis B11)}$$

$$U_6 = \frac{1}{2} \bullet \left(L_{Drain} - L_{Crack}\right) \bullet \left(UP_{Heel} - UP_{Drain-E}\right) \qquad \text{(B19)}$$

$$U_7 = \left(L_{Base} - L_{Crack}\right) \bullet UP_{Drain-E} \qquad \text{(B20)}$$

$$U_8 = \frac{1}{2} \bullet \left(L_{Base} - L_{Drain}\right) \bullet \left(UP_{Toe} - UP_{Drain-E}\right) \qquad \text{(B21)}$$

The resultant uplift pressure force is computed to be

$$U = \left[U_5 + U_6 + U_7 + U_8\right] \tag{B22}$$

The resultant locations are computed as follows:

$$L_{U5} = L_{Base} - \left(\frac{1}{2} \bullet L_{Crack}\right) \tag{bis B17}$$

$$L_{U6} = \left(L_{Base} - L_{Drain}\right) + \frac{2}{3} \bullet \left(L_{Drain} - L_{Crack}\right) \tag{B23}$$

$$L_{U7} = \frac{1}{2} \bullet \left(L_{Base} - L_{Crack}\right) \tag{B24}$$

$$L_{U8} = \frac{1}{3} \bullet \left(L_{Base} - L_{Drain}\right) \tag{B25}$$

The position of the resultant uplift force normal to the base, relative to the toe, is computed to be

$$L_{U-Toe} = \frac{\left(U_5 \bullet L_{U5}\right) + \left(U_6 \bullet L_{U6}\right) + \left(U_7 \bullet L_{U7}\right) + \left(U_8 \bullet L_{U8}\right)}{U} \tag{B26}$$

B.2.4 Case 4: $L_{Crack} \geq L_{Drain}$

Figure B9 shows an idealized cross section with these characteristics.

Referring to Figure B9, the uplift pressure resultant forces acting normal to the base with a crack of length L_{Crack} exceeding L_{Drain} are computed as follows:

$$U_9 = L_{Crack} \bullet UP_{Heel} \tag{B27}$$

$$U_{10} = \left(L_{Base} - L_{Crack}\right) \bullet UP_{Toe} \tag{B28}$$

$$U_{11} = \frac{1}{2} \bullet \left(L_{Base} - L_{Crack}\right) \bullet \left(UP_{Heel} - UP_{Toe}\right) \tag{B29}$$
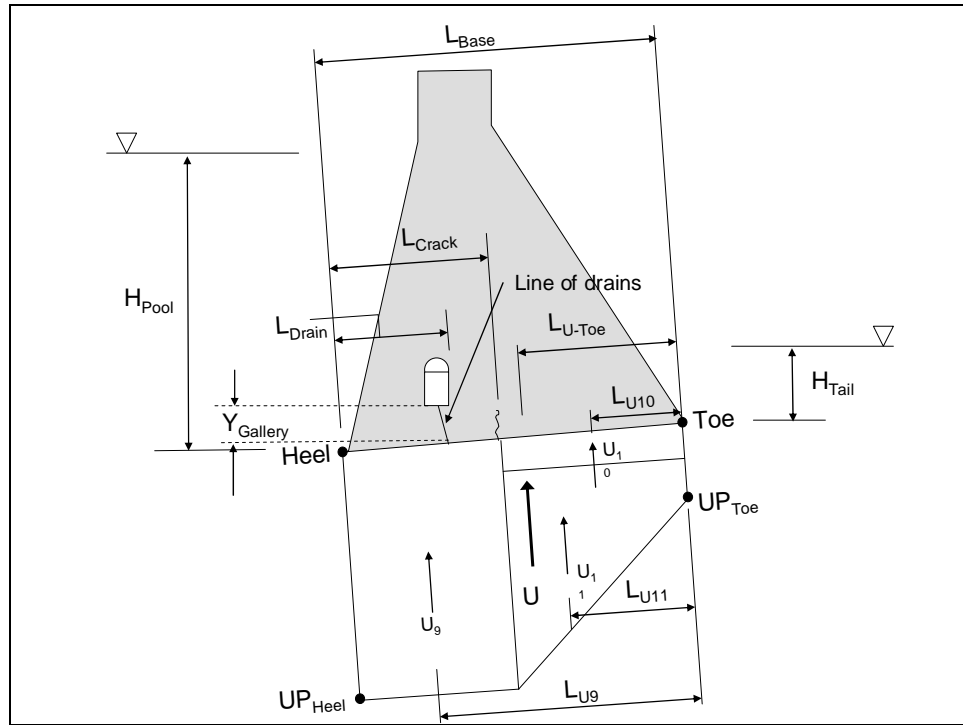
Figure B9. Uplift pressures and resultant locations along a sloping base for the condition $L_{Crack} \geq L_{Drain}$.

The resultant uplift pressure force normal to the base is computed to be

$$U = \left[U_9 + U_{10} + U_{11}\right] \tag{B30}$$

The resultant locations are computed as follows:

$$L_{U9} = L_{Base} - \left(\frac{1}{2} \bullet L_{Crack}\right) \tag{B31}$$

$$L_{U10} = \frac{1}{2} \bullet \left(L_{Base} - L_{Crack}\right) \tag{B32}$$

$$L_{U11} = \frac{2}{3} \bullet \left(L_{Base} - L_{Crack}\right) \tag{B33}$$

The position of the resultant uplift force normal to the base relative to the toe is computed to be

$$L_{U-Toe} = \frac{\left(U_9 \bullet L_{U9}\right) + \left(U_{10} \bullet L_{U10}\right) + \left(U_{11} \bullet L_{U11}\right)}{U} \tag{B34}$$

Appendix C: Listing and Description of the GDLAD_Sloping_Base ASCII Input Data File (GDLAD_Sloping_Base.in)

C.1 Introduction

This appendix lists and describes the contents of the ASCII input data file to the FORTRAN engineering computer program portion of GDLAD_Sloping_Base. This input data file, always designated as GDLAD_Sloping_Base.in, is created by the graphical user interface (GUI), the Visual Modeler portion of GDLAD_Sloping_Base.

The ASCII input data to GDLAD_Sloping_Base is provided in the following seven groups of data.

C.2 Group 1 - Geometry and Properties of a Concrete Gravity Dam

Num_Dam_Points

X_Dam (i), Y_Dam (i) (i = 1 to Num_Dam_Points; i = 1 corresponds to the heel and i = Num_Dam_Points corresponds to the toe)

L_Drain

GAMA_concrete, GAMA_water

Gconstant

with

Num_Dam_Points   = number of points identifying the structure of the concrete gravity dam. These points are specified in a clockwise orientation, from the heel to the toe

X_Dam = global x-coordinate of the points defining the dam geometry region

Y_Dam = global y-coordinate of the points defining the dam geometry region

L_Drain = distance along the base as measured from the heel to the intersection of the line of drains with the base of the gravity dam (refer to Figure 1.1)

GAMA_concrete = unit weight of concrete

GAMA_water = unit weight of water

Gconstant = the gravitational constant. The value for Gconstant identifies the units of length, density, force, and pressure being used according to the following tabulation.

Value for Gconstant	Units of Length	Units of Silt and Concrete Densities	Units of Force	Units of Pressure
32.174	feet	lb/ft^3	lb	lb/ft^2
386.086	inches	lb/in^3	lb	lb/in^2
9.80665	meters	kN/m^3	kN	kN/m^2 (=kPa)
980.665	centimeters	kN/cm^3	kN	kN/cm^2
9806.65	millimeters	kN/mm^3	kN	kN/mm^2

C.3 Group 2 - Characteristics of the Gallery

H_Gallery, B_Gallery, R_Gallery

X_W_Gallery, Y_B_Gallery, Y_Gallery

with
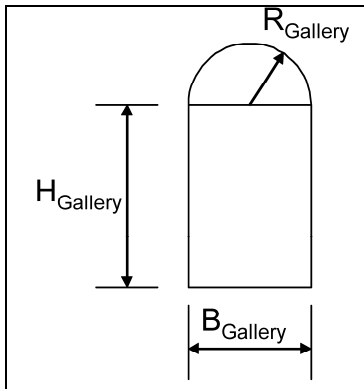
H_Gallery	=	height of rectangular portion of the gallery
B_Gallery	=	width of gallery
R_Gallery	=	radius of gallery ceiling
X_W_Gallery	=	distance to center of gallery from toe
Y_Gallery	=	distance to the bottom of gallery from Lbase

C.4 Group 3 - Characteristics of the Anchor Forces and Moment

Key_FA

MeanFA, Theta, StdDevFA

X_Anchors_Toe, Y_Anchors_Toe

with

Key_FA	= 0, anchor forces are not considered in this analysis
	= 1, generate resultant anchor force uncertainties
	= 2, deterministic analysis
MeanFA	= resultant anchor force
Theta	= angle between a horizontal line parallel to the axis at the toe and the line of anchors (degrees)
StdDevFA	= standard deviation of the resultant anchor force (for Key_A > 0)
	= 0 in a deterministic analysis
X_Anchors_Toe	= x-distance from anchors to toe
Y_Anchors_Toe	= y-distance from anchors to toe

C.5 Group 4 - Characteristics of Silt Parameters

Key_K0

Mean_K0, StdDevK0

H_Silt, Gamma_Moist, Gamma_Saturated

with

Key_K0	= 0, silt is not considered in this analysis = 1, generate at-rest lateral pressure coefficient uncertainties = 2, deterministic analysis
MeanK0	= mean value of pressure coefficient (for Key_K0 > 0)
StdDevK0	= standard deviation of pressure coefficient (for Key_K0 > 0)
H_Silt	= the depth of silt as measured from the heel
Gamma_Moist	= moist unit weight of silt (above the water)
Gamma_Saturated	= saturated unit weight of silt (below the water)

C.6 Group 5 – Simulations with Probabilistic and/or Deterministic Parameters

Key_Analysis[1]

NumberOfSimulations

Key_C_PHI

MeanC, StdDevC

MeanPHI, StdDevPHI

with

Key_Analysis[1]	= 1, probabilistic analysis = 2, deterministic analysis
NumberOfSimulations	= number of simulations (or samples) per pool elevation = 1, deterministic analysis
Key_C_PHI	= 1, generate C and PHI values = 2, generate only C values = 3, generate only PHI values = 4, deterministic analysis
MeanC	= mean value of the effective cohesion
StdDevC	= standard deviation of the effective cohesion = 0, deterministic analysis
MeanPHI	= mean value of the effective angle of internal friction
StdDevPHI	= standard deviation of the effective angle of internal friction = 0, in a deterministic analysis

[1] For a deterministic analysis, all standard deviation values will be set to zero. These zero values will be locked on the Excel user interface and cannot be modified until Key_Analysis is set back to one.

C.7 Group 6 – Calculations of Uplift Pressures

Key_JointFLOW[1]

MeanU[2], StdDevU[2], MeanLU[2], StdDevLU[2]

Key_E

MeanE[3], StdDevE[3]

with

Key_JointFLOW[1]	= 0, non-site-specific uplift pressures
	= 1, site-specific uplift pressures and locations using joint flow results
	= 2, generate only uplift pressures using joint flow results
	= 3, generate only location of uplift pressures using joint flow results
	= 4, deterministic analysis
MeanU[2]	= mean value of uplift force normal to the base of the structural wedge
StdDevU[2]	= standard deviation of uplift force normal to the base of the structural wedge
	= 0, deterministic analysis
MeanLU[2]	= mean value of uplift force resultant location as measured along the base and from the heel
StdDevLU[2]	= standard deviation of uplift force resultant location as measured along the base and from the heel
	= 0, deterministic analysis
Key_E	= 1, generate non-site-specific uplift pressure, E values
	= 2, deterministic analysis

MeanE[3] = mean value of the drain efficiency (for Key_E > 0)

StdDevE[3] = standard deviation of the drain efficiency (for Key_E > 0)
= 0 in a deterministic analysis

[1] For site-specific uplift pressures (Key_JointFLOW > 0), the analysis type of probabilistic or deterministic is considered for the entire analysis and not on a per pool/tailwater basis.

[2] Note: Values for these four parameters are specified when the site-specific pressure distribution (Key_JointFLOW = 1) is to be used in the analysis; otherwise, the values for these parameters are set to zero. These four parameters are computed for each pool and tailwater elevation pair and are specified within the ASCII file (JointFLOW.out), which is produced from the program JointFLOW, executed externally from GDLAD_Sloping_Base. When Key_JointFLOW = 0, values for these four variables are read but not used in the engineering computations.

[3] Note: Values for these two parameters are specified when the non-site-specific (Key_JointFLOW = 0) uplift pressure distribution as described in Appendix B is to be used in the analysis. Otherwise, site-specific data are specified. When site-specific data are used to specify the uplift pressure forces, values for these two parameters are set equal to zero.

C.8 Group 7 – Classification of Pool Elevations and the Event Tree

Num_Pools, NumberOfBranches

PoolArray (i), TailArray (i) (i = 1 to Num_Pools)

with

Num_Pools = number of pool elevations

NumberOfBranches = number of event tree branches (representing the PDF)

PoolArray = array of pool elevation values

TailArray = array of tailwater elevation values

REPORT DOCUMENTATION PAGE

1. REPORT DATE *(DD-MM-YYYY)*	2. REPORT TYPE	3. DATES COVERED *(From - To)*
November 2008	Final report	

4. TITLE AND SUBTITLE

Fragility Analysis of a Concrete Gravity Dam and Its System Response Curve Computed by the Analytical Program GDLAD_Sloping_Base

5a. CONTRACT NUMBER

5b. GRANT NUMBER

5c. PROGRAM ELEMENT NUMBER

6. AUTHOR(S)

Robert M. Ebeling, Moira T. Fong, Amos Chase, Sr., and Elias Arredondo

5d. PROJECT NUMBER

5e. TASK NUMBER

5f. WORK UNIT NUMBER
142082

7. PERFORMING ORGANIZATION NAME(S) AND ADDRESS(ES)

U.S. Army Engineer Research and Development Center
Information Technology Laboratory
3909 Halls Ferry Road, Vicksburg, MS 39180-6199;
Science Applications International Corporation
3532 Manor Drive, Suite 4, Vicksburg, MS 39180

8. PERFORMING ORGANIZATION REPORT NUMBER

ERDC/ITL TR-08-3

9. SPONSORING / MONITORING AGENCY NAME(S) AND ADDRESS(ES)

Headquarters, U.S. Army Corps of Engineers

Washington, DC 20314-1000

10. SPONSOR/MONITOR'S ACRONYM(S)

11. SPONSOR/MONITOR'S REPORT NUMBER(S)

12. DISTRIBUTION / AVAILABILITY STATEMENT

Approved for public release; distribution is unlimited.

13. SUPPLEMENTARY NOTES

14. ABSTRACT

This research report describes the engineering formulation and corresponding software developed for expressing the computed stability results for an idealized two-dimensional cross section of a rock-founded concrete gravity dam in terms of fragility curves for the potential modes of failure (e.g., sliding, overturning). Within the Corps the term *system response curve* is now being used to describe what is commonly referred to in the technical literature as the fragility curve; the term system response curve is used for the hydrologic fragility assessment of rock-founded concrete gravity dams. This report uses this new Corps terminology. Uncertainty in strength, uplift parameters, silt-induced earth pressure and post-tensioned anchor forces are accounted for in a multivariate probabilistic stability analysis resulting in the computation of a system response curve. The PC software GDLAD_Sloping_Base (Gravity Dam Layout and Design) is used in this research and development effort to perform the computations and construct the system response curve.

The resulting engineering methodology and corresponding software is applicable to a concrete gravity dam founded on rock with a level or sloping base. GDLAD_Sloping_Base is also capable of performing a deterministic (sliding and overturning) stability evaluation.

15. SUBJECT TERMS

Concrete dam	Rock-founded	Fragility analysis
Gravity dam	Multivariate probabilistic analysis	System response curve

16. SECURITY CLASSIFICATION OF:

a. REPORT	b. ABSTRACT	c. THIS PAGE	17. LIMITATION OF ABSTRACT	18. NUMBER OF PAGES	19a. NAME OF RESPONSIBLE PERSON
UNCLASSIFIED	UNCLASSIFIED	UNCLASSIFIED		99	19b. TELEPHONE NUMBER *(include area code)*